universität wien

DISSERTATION / DOCTORAL THESIS

Titel der Dissertation /Title of the Doctoral Thesis

„Human Gingival Fibroblasts - A Novel Cell Model Describing the Association between Bitter Taste Quality and Cellular Interleukin-6 Response“

verfasst von / submitted by

Johanna Tiroch BSc, MSc

angestrebter akademischer Grad / in partial fulfilment of the requirements for the degree of

Doktorin der Naturwissenschaften (Dr. rer. nat)

Wien, 2023 / Vienna 2023

Studienkennzahl lt. Studienblatt / degree programme code as it appears on the student record sheet:	A 796 605 419
Dissertationsgebiet lt. Studienblatt / field of study as it appears on the student record sheet:	Chemie/Chemistry
Betreut von / Supervisor:	Univ.-Prof. Mag. Dr. Veronika Somoza

„Was du lernst, kann dir niemand mehr nehmen,
und du lernst nur für dich"

~

Diese Worte leiteten mich nach wie vor,
Danke Oma!

Acknowledgments

The practical work of the dissertation was conducted from June 2017 until December 2021 at the Department of Physiological Chemistry under the chair of Professor Veronika Somoza.

I am very thankful that Professor Somoza gave me the opportunity to work and write my thesis at the Department of Physiological Chemistry. I also want to thank her for her supervision, help, expertise, patience as well as for the constructive discussions regarding the direction of the work.

I am grateful to Professor Mark Somoza for coordinating the micro array experiments, as well as Kathrin Hoelz and Erika Schaudy for their expertise and support during the lab work for the microarray experiments.

I would also like to thank Dr. Jakob Ley of the Symrise AG for the cooperation and stimulating discussions.

Many thanks to the Leibniz Institute for Food Systems Biology at the Technical University of Munich (LSB) for their cooperation. Especially I would like to thank Dr. Antonella Di Pizio for her supervision during my virtual visit, for providing an insight into molecular modeling. Thank you to Andreas Dunkel for supporting me with the data analysis, as well as also to Alessandro Nicoli and Mustafa Ghulam who helped me out with my software questions for modeling and visualisation.

From the Department of Physiological Chemistry, my gratitude to Professor Barbara Lieder and Professor Marc Pignitter who helped with their expertise during the lab work and for the constructive discussions.

My special thanks go to the other graduate students with whom I went through all ups and downs of a PhD. I appreciated the technical discussions and support during the lab work. Thank you for a great, fun, and hard-working time together.

I would like to thank my family and friends for their support, patience and encouragement. My deepest thanks go to Hans who supported me through all stages of the PhD.

Table of contents

List of figures

List of abbreviations

TAS2Rs	bitter taste receptors
IL-6	interleukin-6
IL- 8/ CXCL-8	interleukin-8
IL-1α	interleukin-1α
IL-1β	interleukin-1β
TNF-α	tumour necrosis factor α (TNF-α),
IL-6R	Interleukin-6 receptor
sIL-6R	soluble interleukin-6 receptor
GPCR	G protein-coupled receptors
HGT-1	human parietal cancer cell line
HEK 293 T	human embryonic kidney cells
HGF-1	human gingival fibroblasts
siRNA	small interfering RNA
LPS	lipopolysaccharides
Pg-LPS	*Porphyromonas gingivalis* lipopolysaccharides
2-AFC	two-alternative forced choice
3-AFC	three-alternative forced-choice method
TM1-7	seven transmembrane domains
ECL1-3	three extra cellular loops
GDP	guanosine diphosphate
GTP	guanosine triphosphate
IP3	inositol trisphosphate
PIP2	phosphatidylinositol biphosphate
TRPM5	transient receptor potential cation channel subfamily M member 5
FDI	world dental federation
PAMPs	pathogen-associated molecular patterns
TLR4	toll-like receptor-4
LBP	LPS binding protein
TIR	toll-interleukin-1 receptor
MyD88	myeloid differentiation primary response gene 88
TIRAP	TIR domain-containing adaptor protein
TRAM	TRIF-related adaptor molecule
NF-κB	nuclear factor kappa B
GCF	gingival crevicular fluid
PRRs	pattern recognition receptors

RSV	resveratrol
RA	rosmarinic acid
IPX	intracellular proton index
HED	homoeriodictyol
PCR	polymerase chain reaction
ELISA	enzyme-linked immunosorbent assay
DMFT-index	number of decayed, missing, and filled teeth in the permanent teeth
GNAI3	guanine nucleotide-binding protein G(I) subunit alpha
TRPM4	transient receptor potential cation channel, subfamily M, member 4
GNAT-3	G protein subunit alpha transducin 3
EGCG	epigallocatechin gallate
NAR	naringin
SNT	sinensetin
QHCl	quinine hydrochloride
CAB	carpinontriol B
DIOS	dioscin
IsoA	iso-alpha acids
IsoSNT	iso-sinensetin
L-Arg	L-arginine
THEO	theobromine

1 Introduction

The main objective of the dissertation was to investigate whether there is a functional role of chemoreceptors sensing bitter tasting compounds, named bitter taste receptors (TAS2Rs), in cellular immune responses. The research specifically aimed to examine whether and how bitter tasting compounds modulate the response of immune-competent human gingival fibroblasts to a pro-inflammatory stimulus via targeting TAS2Rs. Specifically, a functional role of TAS2Rs in reducing a stimulus-evoked release of the pro-inflammatory cytokine IL-6 in human gingival fibroblasts was hypothesized. Verification of this hypothesis could (1) lay grounds for a novel cell model suitable for the identification of bitter-tasting compounds, (2) provide knowledge regarding the functional roles of ectopically expressed TAS2Rs, and (3) open new avenues for therapeutic targets of cellular inflammatory processes.

The sensory perception of bitter is one of the five basic tastes that humans can detect, in addition to sweet, sour, salty, and umami. Bitter taste perception on the tongue is mediated by 25 bitter taste receptors (TAS2Rs), which are G protein-coupled (GPCR) receptors. [7,8] The evolutionary rational behind this amount of TAS2Rs is still unclear. One possibility is that the diversity of TAS2Rs enables humans to detect and avoid a wider range of potentially harmful bitter compounds, which are often associated with toxic substances found in nature.

Interestingly, TAS2Rs are not limited to the taste buds in the tongue, where they detect bitter compounds in foods. During the past decade, their ectopic expression of TAS2Rs has been reported in a variety of tissues throughout the body. [9–13] One of the first studies showing a functional role of ectopically expressed TAS2Rs was presented by Desphande et al. [11] , who demonstrated TAS2Rs agonists on airway smooth muscle to bronchodilate. This finding further highlights the potential of TAS2Rs as therapeutic targets in various pathological processes. [14] Building on this observation, the identification of TAS2R agonists could be facilitated through the exploration of cell-specific TAS2R-dependent responses, made possible by the ectopic expression of TAS2Rs in specialized cell types. Given the need to identify and predict bitter tasting and bitter taste modulating compounds for the development of palatable foods and drugs, such cell culture models would offer many advantages over human sensory trials. [15] Nevertheless, the wide range of chemical diversity among bitter tastants makes cell-based approaches for predicting bitterness a challenging endeavour.

The traditional approach for identifying taste qualities is through sensory studies. It should be noted that such studies may exhibit a large threshold variability [16] and require toxicological data before each tasting. Other methods to measure bitter taste qualities are *in silico* strategies. These approaches have led to the development of large databases, such as BitterDB [17] or

FSBI-DB [18], which contain hundreds of reported and *in silico*-tested bitter compounds. Also analytical gustatory tools are used like “electronic tongues”. [19,20] Given demands for methods to investigate the taste on a high throughput approach, *in vitro* methods might provide an alternative. The ideal cell system in this context might be human primary taste cell cultures and immortalised taste cell lines derived from human tongue tissue. However, these cell lines are so far neither available nor validated for high throughput screening approaches. [21,22] Instead, cell lines of non-taste tissues endogenously expressing TAS2Rs have been created to identify cellular responses to TAS2R activation. [15] Different cell models, (e.g. the human parietal cancer cell line (HGT-1) [23–25] or human embryonic kidney cells (HEK 293 T-Gα16gust44) [26,27]), have been established to identify bitter tasting and bitter taste modulating compounds. HEK 293 T-Gα16gust44 cells stably express the α chimeric G protein subunit Gα16gust44 [28], which activates TAS2Rs to induce a phospholipase C activity, resulting in the formation of inositol trisphosphate, finally leading to a mobilization of intracellular calcium. [26,27,29] HGT-1 cells respond to bitter tasting compounds via TAS2R-mediated proton secretion, and it has been shown that these data correlate well with sensory data. [24,25,30] In this cell system, involvement of individual TAS2Rs was validated by siRNA knock down and CRISPR-Cas9 knock out experiments. [25] However, both methods have limitations. For instance, substances with interfering fluorescence may produce false positive or false negative results. Additionally, the human embryonic kidney cells that are commonly used for TAS2R studies do not naturally express all the known TAS2Rs, known so far, and need to be transfected, making them a non-native cell line. Considering these limitations, it is important to explore new approaches that may overcome these challenges. Therefore, the search for a new, native cell line for TAS2R studies is warranted.

Human gingival fibroblast cells (HGF-1) could potentially serve as a novel cell line for investigating TAS2R functionality, provided that a correlation can be established between the cells' interleukin-6 response and bitter taste receptor activity. An increased production of the pro-inflammatory interleukins IL-6 and IL- 8 by HGF-1 cells exposed to *Porphyromonas gingivalis* (*Pg*)-LPS concentrations ranging from 1 to 100 ng/mL after 6 h has already been shown. [31] Furthermore, the function of TAS2Rs has been widely discussed in terms of immune defense functions of the airway smooth muscle [11], upper respiratory tract [32,33], skin [34] and bladder [35]. Therefore, it was proposed and investigated in the here presented dissertation whether bitter-tasting compounds may target TAS2Rs in producing anti-inflammatory effects in HGF-1 cells. At the time the here presented work started, it was not known if either HGF-1 cell express TAS2Rs nor whether they play a functional role in the cells’ IL-6 response. Further, the cellular signalling cascade through TAS2Rs and IL-6 was unclear. Only the potential of bitter-tasting substances for immune defense had been demonstrated in the existing literature to date. [36–38]

2 Sensory taste perception

The gustatory system, also known as the sense of taste, is responsible for the perception of taste. When a substance in the oral cavity chemically interacts with a taste receptor, it triggers the taste cell to release neurotransmitters, which in turn send a signal to the brain, ultimately resulting in the perception of taste.

2.1 The tongue and its taste buds

The embryonic tongue development is a complex process that begins at approximately four weeks of primary age [39], followed by the development of taste buds at the eighth week of gestation. Embryonic taste buds develop during the 9th to 11th week of gestation. [40] Differentiation into various cell types occurs around the 11th to 13th postovulatory week. [40] Basically, this underscores the intricate and sequential nature of the development of the taste system in humans. At the end of foetal development, the dorsal tongue surface is covered by the structure that contains taste buds, a stratified squamous epithelium, with numerous papillae: circumvallate papillae, fungiform papillae, filiform papillae, and foliate papillae (Figure 1). [1,40,41]

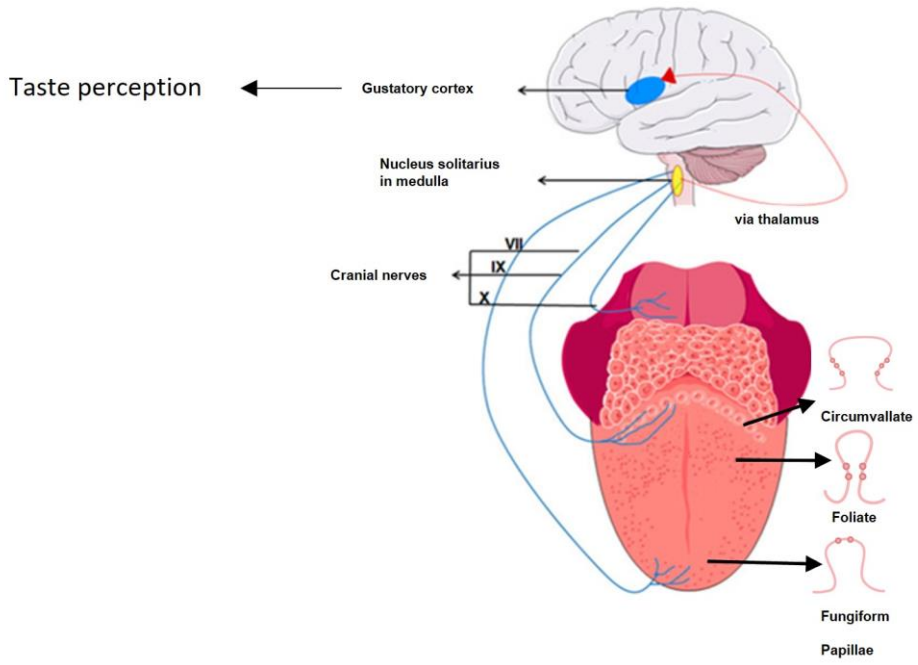

Figure 1. The tongue's architecture of numerous papillae which connected to the brain by nerves that transduce the taste signal. Three cranial nerves are innervating the taste buds: VII facial nerve, IX glossopharyngeal nerve and X vagus nerve. Figure adapted and created with BioRender.com from Ahmad and Dalziel et al 2020. [1]

Taste cells are located within the taste buds and are classified into four types. [39] Type I cells have glia like functions. The two main classes are Type II and Type III cells, which account for one-third and 2-20 % of the cells in the taste bud, respectively. [42] Type II cells are G-Protein coupled receptor cells, which are stimulated by sweet, umami and bitter tasting compounds. [39] Type III cells are stimulated by salty substances. [42] Located at the base of the taste buds are Type IV cells, which are termed basal cells. [39] It has been shown that several cell-to-cell communication systems exists in the taste buds and are involved in signal processing. [42]

The signal transduction from the taste buds to the brain starts with by the initiated signal of taste receptors by synaptic association with sensory neurons. [1,43,44] Three cranial nerves innervate the taste buds: VII facial nerve, IX glossopharyngeal nerve and X vagus nerve.
Apart from the physiological activity of these cell types and the resulting signal transduction, genetic variations of taste receptor proteins and specific settings of sensory tests must be considered when a taste quality is described. [1,16,45]

2.2 Sensory tests to evaluate the perception of bitter taste

Amerine et al. (1965) [46] provided a definition of flavor as the collective sensations arising from the activation of the sensory receptors situated at the opening of the digestive and respiratory tracts. In sensory science, flavor is typically described as the overall impression perceived through the chemical senses of a product in the mouth (Caul, 1957) [47].

The perception of flavor, like bitterness, can be best evaluated by means of human sensory trials. Ideally, the sensory panelists are voluntary human participants, who are trained to distinguish the main taste qualities – sweet, bitter, sour, salty and umami. According to the ISO [48] the basic taste quality training is conducted for the basic taste modalities (1) sweet by administration of 10 ppm sucrose, (2) bitter by administration of 0.3 ppm caffeine, (3) salty by administration of 2 ppm sodium chloride and (4) umami by administrations of 0.6 ppm monosodium glutamate. [48] To evaluate a taste sensitivity of a compound, ascending concentrations of, e.g., the bitter tasting caffeine, are presented to and evaluated by either trained or non-trained panelists. [49,50] Additionally, panelists are also asked to rank at least four concentrations of the test compound, e.g. caffeine or the bitter substance of relevance, according to their taste intensity. [50] For compounds with multiple sensory qualities, e.g. acesulfame k or saccharin, a sensory characterization might involve testing for sweet and bitter taste descriptors. [51]

The sensory taste threshold test is a widely used method for assessing the taste quality of taste active compounds. This test determines the minimum concentration of a compound that can be detected by a panelist. [52] In the 19th century, the term “taste threshold” was first introduced by psychophysicists as a measure of the minimum concentration at which a substance can be sensed by a panelist. As per the ISO [49] definition, the stimulus threshold refers to the concentration of a test substance that elicits a sensory impression distinguishable from water, regardless of the specific taste being recognized. In contrast, the recognition threshold represents the concentration of a test substance at which the taste panelists can correctly identify and assign the sensory impression to the corresponding taste. [50]

The most fundamental way to characterize a perceptual system is to determine its ability to detect a minimum signal strength, known as the detection threshold. Typically, this is assessed by having a subject indicate the presence or absence of a signal to a stimulus as a function of fractional concentration measurements of a substance. [53,54] Alternatively, forced-choice tasks can be employed, in which the subject must identify which of several alternative stimuli elicits the signal. This approach produces an estimate of the detection threshold that is unbiased by a decision criterion. In practice, forced choice tasks are the most usually used psychophysical procedures. Although independent of the decision criterion, forced-choice tasks may suffer from response, temporal or position bias, which are considered negligible in most cases. [55] The ideal setup for forced-choice testing requires long experimental durations and motivated panelists who are willing and capable of time-intensive sensory test sessions. The two-alternative forced choice (2-AFC) methods can decrease the number of trials, while maintaining good precision. As the number of alternatives increases, the stability of the threshold estimates is found to improve. [53,56]

The ascending forced-choice method is a sensory evaluation technique that employs the method of limits to determine the concentration at which a substance becomes detectable to human senses. The concentration is gradually increased in predetermined steps until the substance is perceived by the subject. In addition to the method of limits, a forced-choice paradigm is employed, in which the substance to be detected is presented among a set of two blanks with no test compound concentration. This results in a three-alternative forced-choice method (3-AFC), in which the subject is required to identify the one different sample from a set of three. In case of uncertainty, the panelist has to make a guess. [52]

According to the ISO 13301:2018(E) [57], the 3-AFC procedure is used in two modes: (I) investigation of the sensitivity of subjects to specific stimuli; (II) investigation of the ability of a chemical substance to stimulate the chemoreceptive senses. In detail, the 3-AFC procedure is described as follows [57]: “The test is of discrimination in which the panelist is presented with three samples,

one of which is a test sample containing a selected stimulus familiar to the assessor, the other two being references, and where the assessor is instructed to identify the test sample."
Another method for sensory evaluation of a flavor quality that includes the onset and lingering is a time intensity (TI) study, which allows panelists to scale their perceived sensations over time. [58] The onset refers to the duration between the initial appearance of a taste sensation and its first peak intensity, while lingering refers to the length of time a taste persists in the mouth before gradually fading away. Therefor it can acquire from each panelist and sample the following information: "the maximum intensity perceived, the time to maximum intensity, the rate and shape of the increase in intensity to the maximum point, the rate and shape of the decrease in intensity to half maximal intensity and to the extinction point, and the total duration of the sensation. " [58]

Sensory studies may encounter limitations in terms of threshold variability [16] and require toxicological data prior to each tasting. Also analytical tools like "electronic tongues" are used. [19,20] Other methods for the identification of bitter tasting substances are *in silico* strategies. [17]

2.3 Human cell-based assays to evaluate the bitterness

In response to the need for efficient methods to identify taste active and taste modulating compounds in a high throughput manner, in vitro approaches could serve as a potential alternative to sensory trials. Human primary taste cell cultures and immortalized taste cell lines derived from human tongue tissue might be the ideal cell systems in this regard. However, it should be noted that these cell lines are currently unavailable and have not yet been validated for high throughput screening purposes. [21,22] Therefore, several cell lines of non-taste tissues endogenously expressing TAS2Rs have been established to identify cellular response of TAS2R activation. [15] These cell models e.g. are the human parietal cancer cell line (HGT-1) [23–25] and the human embryonic kidney cells (HEK 293 T-Gα16gust44) [26,27]). The activation of TAS2Rs in HGT-1 cells is mechanistically linked to a secretion of protons. [24,59] This process is measured by determining the intracellular proton concentration using a pH-sensitive fluorescence dye known as SNARF-1 AM. This dye enables the investigation and assessment of the intracellular proton index. [24,59] The HEK 293 T-Gα16gust44 stable express the α chimeric G protein subunit Ga16gust44 [28] which is involved in a signals cascade which finally is leading to a intracellular calcium mobilization and can be measured with a fluorescence radiometric dye.

Both cell models have limitations, like interfering fluorescence of substances, which may lead to false positive or false negative results. Additionally, also pH sensitive substances are a chal-

lenge for the measurement. [60] It has been demonstrated that phloretin [24], in addition, has the potential to suppress the fluorescence of the membrane-bound probe [61]. On the one hand, results from the HGT-1 cells are hardly not in line with sensory trials. [24] The human embryonic kidney cell line [28], on the other hand, does not naturally possess all the currently known TAS2Rs and requires transfection, thus making it a non-native cell line.

Given these limitations, it becomes crucial to investigate new approaches that can address these challenges. Therefore, the quest for a new, high-throughput native cell lines specifically for TAS2R studies is justified.

2.4 Bitter substances and the chemical bitter space

Sensory data, such as bitter taste thresholds, along with information on chemical properties, structures, and pharmacological activities of compounds, are available in the BitterDB. As of 2019, the database contains information regarding 1041 bitter compounds [17,62], although not all bitter substances are included due to ongoing research. The effective concentration, as well as the EC_{50}, the half maximal concentration to require 50 % of the maximal response, at which a substance activates a TAS2R receptor is also listed in the database. [17,62] It is shown that some TAS2Rs can be activated by structurally diverse compounds at a wide range of concentrations (so-called broadly tuned TAS2Rs), whereas other TAS2Rs are activated by a narrow range of compounds (called narrowly-tunes). [27,63] The diversity of chemical compounds that elicit a bitter taste sensation is illustrated in a 2-dimensional t-SNE plot as the bitter chemical space (Figure 2). [2]

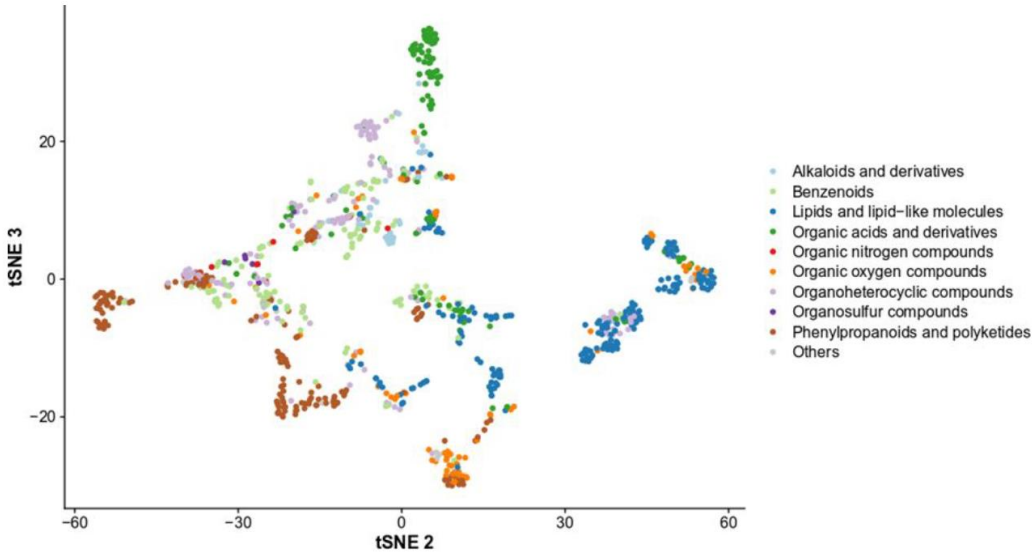

Figure 2. 2-D t-SNE plot of the bitter chemical space, showing the chemical superclasses colored according to ClassyFire (t-SNE 2 and 3) from Dunkel et al 2020. [2]

This plot is created on a fingerprint-basis via a machine learning algorithm. [2,64] The chemical space is very complex and encompasses a wide variety of chemical superclasses like: alkaloids and derivates, benzenoid, lipids and lipid-like molecules, organic acids and derivates, organic nitrogen compounds, organic oxygen compounds, organoheterocyclic compounds, organosulfur compounds, phenylpropanoids and polyketides as well as other chemicals. [2] This so called chemoinformatic view studies the structural similarities between sensory-evaluated bitter tasting substances and their TAS2R molecular docking properties. [2,65]

The motivation for exploring the bitter chemical space is to gain a better understanding of the molecular basis of bitter taste perception, as well as to identify and predict structural requirements for bitter tasting compounds that could be used in food formulations and medical therapeutic approaches.

3 Non-gustatory expressed bitter taste receptors and their role in inflammation

Non-gustatory TAS2Rs are expressed, for example, in the gastrointestinal tract, where their activation results, e.g., in gastric acid secretion [9,25] or the release of satiety hormones from enteroendocrine cells [66,67]. It is also shown that TAS2Rs are stimulated for immune defence functions, in the upper airway, TAS2R38 mediates the beat frequency of ciliated cells from the nasal epithelium in response to quorum sensing acetyl–homoserine lactones (AHLs) from gram negative bacteria. [32,33,38] In the lung, the airway smooth muscle contractility, which is of interest for

the treatment of asthma, has been shown to be mediated by activation of TAS2Rs. [11,68] As some studies already reported TAS2Rs to play a role in the innate immunity, it is not surprising that also immune cells express TAS2Rs, like primary lung macrophages [69] and leucocytes [70,71].

Substances that counteract inflammation or combat invaders, such as zinc, accompany inflammation and immune cells hand in hand. Zinc is well known for its anti-inflammatory properties [72] and its activation of TAS2R7. [73] Furthermore, drugs like antibiotics (chloramphenicol, erythromycin, and ofloxacin), anti-malaria drugs (quinine and chloroquine), analgesics (acetamonifen) and, thyrostatic agents (metimazole and propylthiouracil) are bitter active substances. [4,74]

In a cellular level, TAS2R activation or inhibition by TAS2R agonists or antagonists, respectively, results in a modulation of a signalling cascade (Figure 3) (for review see [3,4]).

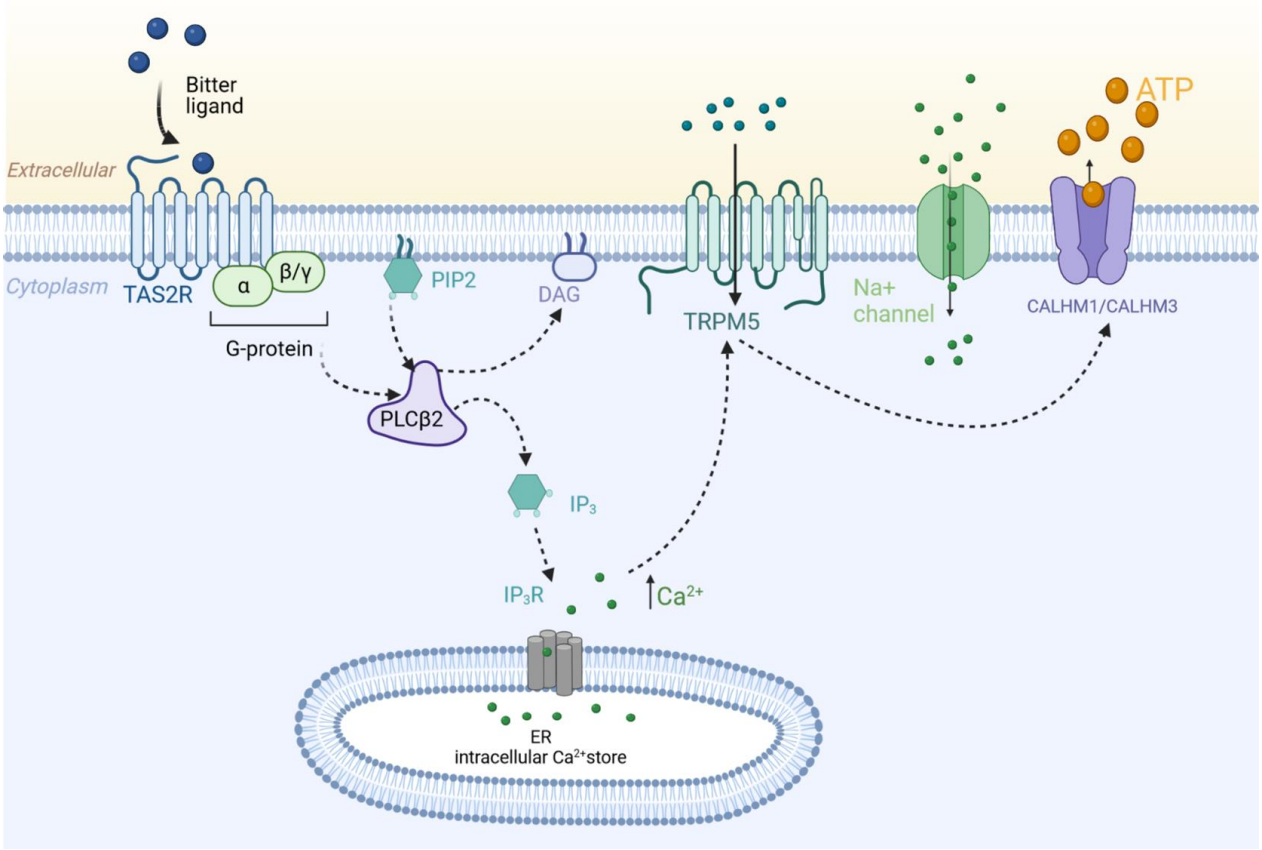

Figure 3. Pathway of bitter taste receptors and their involvement in intracellular calcium mobile-zation, adapted and created with BioRender.com, for review see [3,4] .

When a bitter tasting compound (which may also taste sweet at the same time, such as acesulfame k, saccharin) [51] binds to a TAS2R, it activates the chemoreceptor consisting of seven transmembrane domains (TM1-7) and three extra cellular loops (ECL1-3). [4,75] This activation leads to a guanosine diphosphate (GDP) to guanosine triphosphate (GTP) exchange, which dissociates into the α- subunit and the βγ-heterodimer. [4] This step subsequently activates the enzyme phospholipase Cβ2, which, in turn, generates inositol trisphosphate (IP3) from the precursor phosphatidylinositol biphosphate PIP2. [4]As a result, calcium is released intracellularly, leading to the opening of the Transient Receptor Potential Cation Channel Subfamily M Member 5 (TRPM5). [4] Opening of this cation-channel allows the influx of sodium ions and promotes cellular depolarization. [76] Although this signalling cascade has been described for many non-gustatory cells, e.g. human gastric parietal cells [25] and airway smooth muscle [11], human gingival fibroblasts have not been characterised accordingly. Moreover, no functional role of TAS2Rs in cellular mechanisms involved in responses to pro-inflammatory stimuli by immune-competent HGF-1 cells have been reported. Therefore, it is necessary to investigate and establish HGF-1 cells as an in vitro cell model for identifying bitter-tasting compounds. Consequently, improving our understanding of the functional role of TAS2Rs in anti-inflammatory responses becomes crucial to advance medical therapeutic strategies aimed at maintaining oral health.

3.1 Mechanisms of immune response human gingival fibroblasts located in the oral cavity

The world dental federation (FDI) defines oral health as the health of the mouth, associated with the ability to speak, smile, smell, taste, touch, chew, swallow, as well as the ability to give facial expressions of emotions with confidence and without experiencing pain in the craniofacial complex. [77,78] According to the Global Burden of Disease Study 2019 [79], around 3.5 billion people suffer from oral diseases, with the consumption of a high sugar diet as well as the use of tobacco and alcohol being major risk factors. Furthermore, the oral hygiene is a key factor, along with hereditary impacts and environmental (e.g. dietary) impacts on the dental-plaque derived growth of bacterial communities, which are chiefly responsible for oral health. [77] According to 16S rRNA sequencing, dental plaque comprises more than 500 distinct species, with *Actinobacteria, Bacteroidetes, Firmicutes, Fusobacteria, Proteobacteria,* and *Spirochaetes* being the most prevalent phyla. [80] The oral microbiota that live in a symbiotic relationship with the host play a vital role in preventing opportunistic pathogens from colonizing the oral cavity. This phenomenon is known as colonization resistance, which is due to the limited available space for pathogen colonization. *Streptococcus salivarius* strain K12 is a beneficial bacterium associated with

good oral health that produces bacteriocin, a protein that has the ability to inhibit the growth of gram-negative bacteria that are commonly associated with periodontitis. [80]

There are also other critical factors for oral health, like the accumulation of dental plaque and the overgrowth of gram-negative bacteria, such as *Porphyromonas gingivalis* (*Pg*), *Tannerella forsythia*, and *Treponema denticola*, in periodontal pockets. These bacteria can trigger an over-reaction of the immune system in the gum tissue, resulting in inflammation and the progression of chronic periodontitis. [81–83] As one of these bacteria, *Porphyromonas gingivalis*, an immotile obligate anaerobe bacterium, is equipped with virulence factors such as fimbriae, proteases, capsules, and lipopolysaccharides (LPS), which are endotoxins localized in their outer membrane. At the beginning of the investigation of the here presented thesis, there was no available information in the literature regarding the relationship between LPS and the cellular chemosensory signalling of TAS2Rs in humans.

LPS triggers inflammatory responses that can exert both beneficial and harmful effects on tissues. While inflammation processes help tissue protection and healing, chronic inflammation can lead to tissue damage. This is seen in gingivitis, which can progress to periodontitis and ultimately result in tooth loss. [79,84,85] Although periodontal diseases can reach an irreversible stage, they can still be stopped. Hence, it is crucial to investigate the impact of anti-inflammatory substances, their potential pathways, and their identification. The host immune system responds to an inflammatory infiltrate by activating monocytes, macrophages, neutrophils, dendritic cells, and fibroblasts. [81,86]

However, microbial invasion in general activates innate and adaptive immune responses. The adaptive immune response activates a highly specific reaction. The response involves the recognition and elimination of specific pathogens by B and T lymphocytes. B cells produce antibodies against specific pathogens, which can neutralize and eliminate them. T cells, on the other hand, can directly kill infected cells or help B cells produce antibodies. Both B and T cells can also develop immunological memory, which allows for a more rapid and efficient response to subsequent infections. [87]

The innate immune response in the oral cavity involves physical barriers such as saliva, mucosa, and gingival crevicular fluid. These barriers contain antimicrobial peptides and enzymes that can directly eliminate invading microorganisms. Additionally, resident immune cells such as neutrophils, macrophages, and dendritic cells play an important role in phagocytosing and presenting antigens to the adaptive immune system. Furthermore, the innate response reacts instantly to pathogen-associated molecular patterns (PAMPs) such as lipopolysaccharides (LPS) which are present in the outer cell membrane of gram-negative bacteria, such as *Porphyromo-*

nas gingivalis (*Pg*). [88] The lipid A molecule is the active centre of *Pg*-LPS, and has been demonstrated to be responsible for endotoxic activation. It acts as an agonist for toll-like receptor-4 (TLR4) expressed in immune-competent cells, such as gingival fibroblasts. [5,89,90] The LPS binding protein (LBP), functions as soluble shuttle protein and directly binds to LPS. Furthermore, it enhance the binding between LPS and CD14. [91,92]

CD14, a glycosylphosphatidylinositol-anchored protein, then transfers LPS to TLR4. The downstream pathway activation of the TLR-4 activation is shown in Fig. 4, adapted from Lu et *al*., 2008. [5] When LPS binds to TLR-4, it triggers the intracellular process of the translocation of the NF – κB protein from the cytoplasm into the cell nucleolus. Upon recognition of LPS, TLR4 undergoes oligomerization and downstream activation via Toll-interleukin-1 receptor (TIR) domains. There are five TIR domain-containing adaptor proteins namely: myeloid differentiation primary response gene 88 (MyD88), TIR domain-containing adaptor protein, also known as Mal, MyD88-adapter-like (TIRAP), TIR domain-containing adaptor inducing IFN-β (TRIF), TRIF-related adaptor molecule (TRAM), and sterile α and HEAT-Armadillo motifs-containing protein (SARM). [93] Thereafter TLR4 signalling is divided into MyD88 and TRIF dependent pathways. [5]

NF-κB also plays an important role in the transcription of cytokine genes, including pro-inflammatory cytokines such as IL-1β, IL-6, and TNF-α. [94]

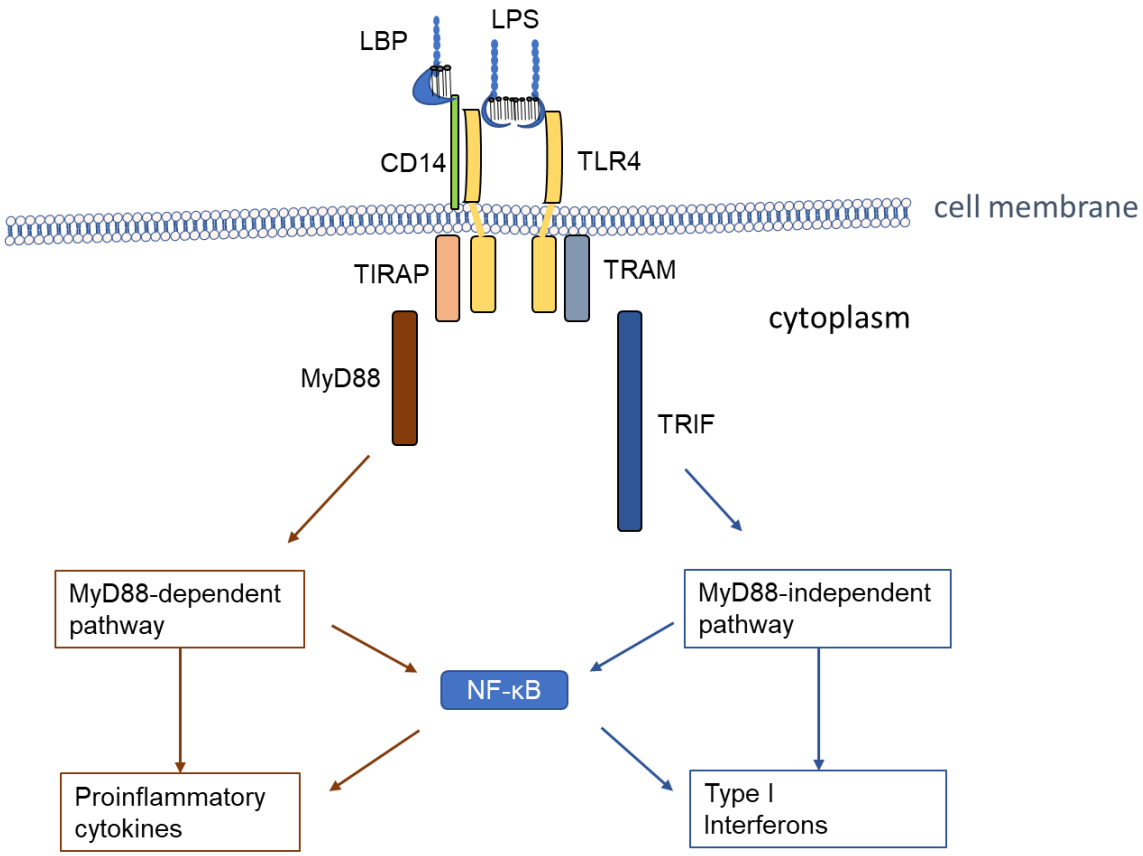

Figure 4. Overview of LPS/TLR4 signalling. TLR4 signalling can lead to two pathways: the MyD88-depent and the MyD88-independent pathway. Adapted from the Lu et al. 2008 [5].

The production of the pro-inflammatory cytokine IL-6 is attributed to various cells including B-Lymphocytes, monocytes, macrophages, keratinocytes, endothelial cells, and fibroblasts. [95] The first description of IL-6 dates back to the 1970s, when it was identified as B cell stimulatory factor 2 (BSF-2) in the supernatant of T-Lymphocyte culture. Initially, it was found to be crucial for stimulating B cells to generate antibodies. [96] In fibroblasts, IFN-β2 and a 26 - kD protein, which were shown to be identical to BSF-2, cytokine IL-6 was detected in 1986. [97,98] IL-6 exhibits a four helical bundle structure, using a homodimer of the β-receptor glycoprotein 130 kDa (gp130) and an α – receptor subunit (IL-6R). [99,100] In addition to the membrane-bound IL-6R, there also exists a trans-signaling pathway through a soluble form of IL-6 called sIL-6R. [101] This soluble form of the receptor can bind to IL-6 and activate cells that do not express the membrane-bound receptor.

IL-6 can exhibit a dual role in immune response. In acute inflammation, it acts as a defense mechanism and plays a vital role in host defense by stimulating immune cells such as T and B lymphocytes. However, in chronic inflammation, IL-6 can promote a pro-inflammatory environ-

ment, contributing to the pathogenesis of various diseases. IL-6 is capable of inducing the soluble receptor antagonist of IL-1 and TNF-α and inhibiting the production of IL-1 and TNF-α. [102] High levels of IL-6 have been associated with several inflammatory disorders, including rheumatoid arthritis, multiple sclerosis, and periodontal disease. Therefore, IL-6 has been suggested as a potential therapeutic target for treating chronic inflammatory diseases. Additionally, IL-6 has been proposed as a marker for periodontal diseases. [102]

Under physiological conditions, IL-6 in human serum typically shows a concentration range of 1-5 pg/mL. [103] A study by Kurtis et al. in 1999 evaluated gingival crevicular fluid (GCF) levels of IL-6 and found that adult periodontitis patients had levels of 1.31 ± 0.92 ng/mL, while healthy subjects demonstrated levels of 0.62 ± ng/mL. [104] It is important to note that the adult periodontitis patients in this study had significant loss of teeth attachment, pocket depth greater than 3mm, and alveolar bone resorption. [104]

The cell model studied here, namely the human gingival fibroblast cell model, was chosen because it is a well-proven cell model for the study of inflammatory processes in the oral cavity. [31,105–108] Moreover, this particular cell line exhibited anti-inflammatory activity when exposed to various substances listed in BitterDB [17], including but not limited to hesperetin [107,108], neohesperidine [108], resveratrol [108], camphor [105] and naringenin, [107]

Fibroblasts originate from mesenchymal cells and are present in all tissues where they synthesize connective tissue. Their shape varies. They can be spindle-shaped, flattened, or elongated depending on their location. Fibroblast cells have a variety of functions, ranging from the production of collagen and elastin fibres to the regulation of the extracellular matrix and contractility. [109] They also play essential roles in wound healing and providing structural support. [109] Fibroblasts are often described in the literature as sentinels due to their ability to respond to microbial pathogens. [110]

More specifically, human gingival fibroblasts (HGF-1 cells) are the predominant cells in the gingival connective tissue (as shown in Figure 5). [111]

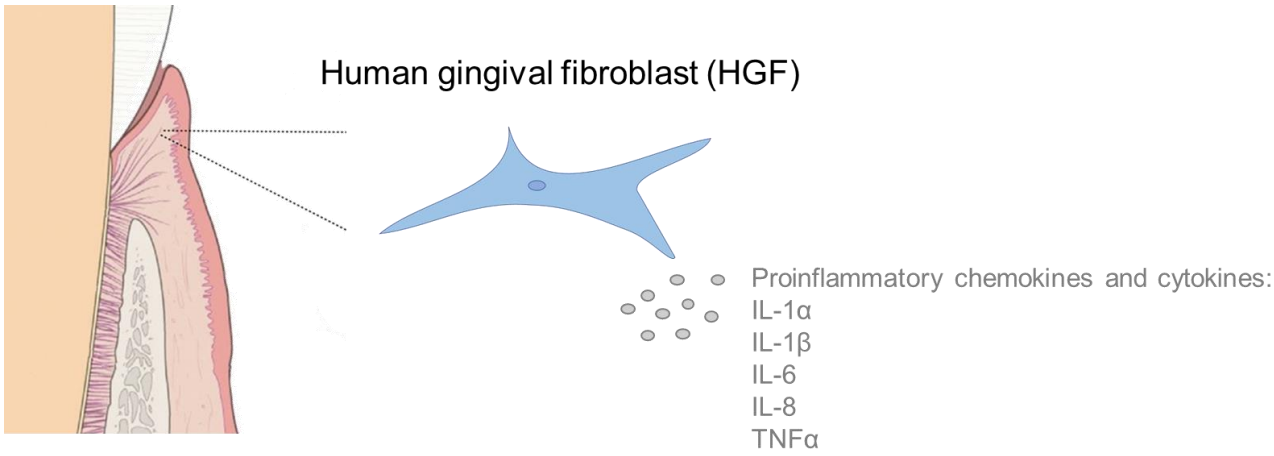

Figure 5. Localization of the human gingival fibroblast and types of pro-inflammatory cytokines adapted from Soto-Barreras et al 2017 [6].

The tissues surrounding and supporting teeth can be affected by periodontitis, a chronic inflammatory disease. In this pathogenesis, pro-inflammatory cytokines like IL-1α, IL-6, and TNF-α play a crucial role, produced by various cells in the periodontal tissues upon exposure to bacterial attack. They include macrophages, neutrophils, and gingival fibroblasts. The relationship of pro-inflammatory cytokines, like IL-1α, IL-6 and TNF-α with periodontitis is shown in various reports. [112–114] These cytokines have been demonstrated to stimulate the activity of osteoclasts, which break down bone tissue and result in bone resorption. They also facilitate the migration and activation of immune cells to the infected site, leading to the destruction of periodontal tissues. Furthermore, they contribute to the degradation of extracellular matrix components, such as collagen and proteoglycans, causing a loss of attachment of connective tissue to the tooth. As the immune system responds to the pro-inflammatory stimulation via monocytes, neutrophils and macrophages [115], the inflamed tissue is than attacked by host defence mechanisms via matrix metalloproteinases [116]. IL-8 act as chemotactic agents for neutrophils, which are identified as a key player in periodontitis, causing tissue destruction. [117,118]

Human gingival fibroblasts (HGF -1) cells are the predominant cell type of the alveolar bone-lining mucosa, and they interact constantly with the oral microbiome and its molecules. These cells express pattern recognition receptors (PRRs) and respond to molecular patterns. During bacterial virulence factors they react via TLR-4 with cytokines and chemokine production. [119] This further leads to a recruitment of macrophages to attack bacteria. The use of *Pg*-LPS stimulated HGF-1 cells to study anti-inflammatory compounds is well known. [31,106,107] Moreover, it has been shown experimentally that the production of IL-6 and IL-8 increases with exposure to *Pg*-LPS (1 – 100 ng/mL) for 6 h. [31] So, upon stimulation with various physical and pathophysiologi-

cal factors, HGF-1 cells can release cytokines and chemical mediators, including proinflammatory chemokines and cytokines such as IL-1α, IL-1β, IL-6, IL-8, and TNF-α. [31,105,112,119–122] Therefore, it was proposed that investigating the HGF-1 cell model may help identify a potential link between bitter-tasting substances and the IL-6 response.

4 Objectives

The here presented work was aimed at investigating whether bitter-tasting compounds can induce anti-inflammatory effects in human gingival fibroblasts (HGF-1 cells) via targeting TAS2Rs. The underlying hypothesis was that HGF-1 cells functionally express TAS2Rs and regulate their anti-inflammatory response via TAS2R signaling. Proof of this hypothesis could (1) lay grounds for the HGF-1 cell line being established as *in vitro* cell model for the identification of bitter-tasting compounds, and (2) improve our understanding of the functional role of TAS2Rs in anti-inflammatory responses with relevance for medical therapeutic approaches in maintaining oral health.

The first step of the here presented work was to investigate whether TAS2Rs are expressed in HGF-1 cells and whether they play a functional role in the anti-inflammatory effects of bitter-tasting compounds in *Pg*-LPS treated HGF-1 cells. After evaluation of the bitterness of two food constituents for which a bitterness had been reported in the literature, the more bitter tasting compound was selected for a mechanistic study using HGF-1 cells. In this study, HGF-1 cells were exposed to *Pg*-LPS as pro-inflammatory stimulus, which resulted in the release of pro-inflammatory cytokine IL-6 and changes in TAS2R gene expression. Co-treatment of the bitter compound selected and *Pg*-LPS revealed a functional role of one of the TAS2Rs, as evidenced by results from a comprehensive molecular biology approach including TAS2R50 siRNA knock-down experiments.

The second step was to test whether the modulation of *Pg*-LPS stimulated IL-6 release demonstrated for a TAS2R50 agonist was receptor- and/or compound-specific, or whether an association between any compound's bitterness perceived and its effect on the *Pg*-LPS evoked IL-6 release can be established. This research question was tested using a selection of various bitter-tasting compounds from the bitter chemical space. Whereas receptor-specificity was tested by means of molecular docking experiments, compound-specificity of the cell model was studied by means of a molecular biology approach of which the results were correlated with the test compounds' bitter taste threshold data available from the literature. Results from this correlation were taken to evaluate the established cell model for its suitability to identify bitter tasting compounds.

5 Results

5.1 "Bitter Sensing TAS2R50 Mediates the trans-Resveratrol-Induced Anti-inflammatory Effect on Interleukin 6 Release in HGF-1 Cells in Culture"

Johanna Tiroch[1], Sonja Sterneder[1], Antonella Di Pizio[2], Barbara Lieder[1], Kathrin Hoelz[3], Ann-Katrin Holik[1], Marc Pignitter[1], Maik Behrens[2], Mark Somoza[2,3,4], Jakob P. Ley[5], Veronika Somoza[1,2,6]

[1] Department of Physiological Chemistry, Faculty of Chemistry, University of Vienna, Vienna, Austria.

[2] Leibniz Institute of Food Systems Biology at the Technical University of Munich, Freising, Germany.

[3] Department of Inorganic Chemistry, Faculty of Chemistry, University of Vienna, Vienna, Austria.

[4] Chair of Food Chemistry and Molecular Sensory Science, Technical University Munich, Freising, Germany.

[5] Symrise AG, Holzminden, Germany

[6] Chair for Nutritional Systems Biology, Technical University Munich, Freising, Germany

Published in *Journal of Agricultural and Food Chemistry* **2021** *69* (45), 13339-13349
DOI: 10.1021/acs.jafc.0c07058

This study investigated the anti-inflammatory properties of the bitter-tasting substances resveratrol and rosmarinic acid and whether their bitter taste could be reduced by the antagonistic compound homoeriodictyol which targets TAS2R20, TAS2R31, TAS2R43, TAS2R50 in HGF-1 cells. Furthermore, it sought to clarifying the involvement of TAS2R50 as a key player during the anti-inflammatory activity of resveratrol. This was conducted via ELISA, PCR and knock-down experiments and validated with molecular modeling. Additionally, the molecular interaction of *Pg*-LPS with resveratrol and homoeriodictyol was examined via LC-MS/MS analysis. A DAVID Cluster Analysis following a cDNA microarray approach was performed on HGF-1 cells to determine changes in individual gene expression.

I participated in the experimental design of the sensory study and subsequent analysis of the results. Additionally, I planned and analysed the *in vitro* experiments in HGF-1 cells to measure their mRNA expression and IL-6 release, as well I conducted the siRNA knock-down experiment in HGF-1 cells for TAS2R50. Additionally, I performed and analysed the molecular interaction

analysis of *Pg*-LPS with resveratrol and homoeriodictyol via LC-MS/MS. The DNA microarray synthesis was done by Kathrin Hoelz. I performed the cDNA preparation of the HGF-1 cells and analysed both the microarray results and the DAVID cluster analyses. The *in vitro* experiments in human gastric parietal tumour cells (HGT-1 cells) were conducted and analysed by Sonja Sterneder. The molecular modeling was performed by Dr. Antonella di Pizio. Furthermore, I did the statistical data analysis and prepared the draft of the manuscript.

JOURNAL OF AGRICULTURAL AND FOOD CHEMISTRY

pubs.acs.org/JAFC Article

Bitter Sensing *TAS2R50* Mediates the *trans*-Resveratrol-Induced Anti-inflammatory Effect on Interleukin 6 Release in HGF-1 Cells in Culture

Johanna Tiroch, Sonja Sterneder, Antonella Di Pizio, Barbara Lieder, Kathrin Hoelz, Ann-Katrin Holik, Marc Pignitter, Maik Behrens, Mark Somoza, Jakob P. Ley, and Veronika Somoza*

Cite This: *J. Agric. Food Chem.* 2021, 69, 13339−13349 Read Online

ACCESS | Metrics & More | Article Recommendations | Supporting Information

ABSTRACT: Recent data have shown anti-inflammatory effects for *trans*-resveratrol (RSV) and rosmarinic acid (RA) in various immune-competent cell models through reduction of lipopolysaccharide (LPS)-induced interleukin 6 (IL-6) release. Because both compounds have been reported to taste bitter, we hypothesized an involvement of human bitter taste sensing receptors (TAS2Rs) on IL-6 release in LPS-treated human gingival fibroblasts (HGF-1). First, the bitter taste intensity of RSV and RA was compared in a sensory trial with 10 untrained panelists, of whom 90% rated a 50 ppm of RSV in water solution more bitter than 50 ppm of RA. A mean 19 ± 6% reduction of the RSV-induced bitter taste intensity was achieved by co-administration of 50 ppm of the bitter-masking, TAS2R43 antagonist homoeriodictyol (HED). Mechanistic experiments in a stably CRISPR-Cas9-edited *TAS2R43ko* gastric cell model revealed involvement of TAS2R43 in the HED-evoked effect on RSV-induced proton secretion, whereas the cellular response to RSV did not depend upon *TAS2R43*. Next, the IL-6 modulatory effect of 100 μM RSV was studied in LPS-treated immune-competent HGF-1 cells. After 6 h of treatment, RSV reduced the LPS-induced IL-6 gene expression and protein release by −46.2 ± 12.7 and −73.9 ± 2.99%, respectively. This RSV-evoked effect was abolished by co-administration of HED. Because real-time quantitative polymerase chain reaction analyses revealed a regulation of *TAS2R50* in RSV with or without HED-treated HGF-1 cells, an siRNA knockdown approach of *TAS2R50* was applied to verify *TAS2R50* involvement in the RSV-induced reduction of the LPS-evoked IL-6 release in HGT-1 cells.

KEYWORDS: *human gingival fibroblasts (HGF-1), resveratrol, homoeriodictyol, human bitter taste receptors, interleukin 6, lipopolysaccharide*

1. INTRODUCTION

Bitter taste receptors (TAS2Rs) belong to the taste 2 receptor family and are G-protein-coupled receptors, which respond to a variety of bitter substances. While some of the 25 TAS2Rs identified thus far[1−3] are activated by a narrow range of bitter compounds, some members of the TAS2R family are generalists, stimulated by a large variety of bitter-tasting food constituents.[4] TAS2Rs were first discovered on the tongue[5] but have since then been identified in various other organ systems, including the upper airway,[6−8] thyroid,[9] lung,[10] and gastrointestinal tract.[11,12] The role of extra-oral TAS2Rs is currently under intense investigation, but it has widely been accepted that TAS2Rs are involved in various local chemosensory functions beyond bitter taste perception.[13]

Involvement of TAS2Rs in anti-inflammatory processes has been shown in immune defense functions of the airway smooth muscle,[10] heart tissue,[14] bladder,[15] upper respiratory tract,[6,8] and skin.[16] Particularly high expression levels of the TAS2R encoding genes *TAS2R31*, *TAS2R43*, and *TAS2R38*[17,18] have been detected in immune-competent blood cells, such as leukocytes.[17,19] Recently, primary human lung macrophages were not only demonstrated to express mRNA of 16 TAS2Rs (*TAS2R3/4/5/7/8/9/10/14/19/20/31/38/39/43/45* and *46*) but also showed an upregulation of *TAS2R7* and *TAS2R38* after a 24 h treatment with 10 ng of lipopolysaccharide (LPS)/mL of cell culture medium.[20] Application of the highly bitter tasting, broadly activating TAS2R agonist denatonium benzoate, targeting TAS2R4/8/10/13/39/43/46 and 47, prior to LPS treatment reduced the LPS-induced release of the pro-inflammatory proteins tumour necrosis factor α (TNF-α), C−C motif chemokine ligand 3 (CCL3), and interleukin 8 (IL-8). The authors hypothesized TAS2Rs as novel drug targets in inflammatory lung disease. Although a role of TAS2R agonists as drug-like effectors for the treatment of metabolic diseases has been proposed recently,[21] a pivotal, sensory-linked function of TAS2Rs in other peripheral immune-competent cells has not yet been elucidated.

Another key player in the immune system is fibroblasts, with several functions ranging from structural roles and tissue repair via the extracellular matrix (ECM) to processes regulating

Special Issue: Highlights of AGFD program at 259th ACS Virtual National Meeting

Received: November 12, 2020
Revised: December 23, 2020
Accepted: January 7, 2021
Published: January 18, 2021

https://dx.doi.org/10.1021/acs.jafc.0c07058
J. Agric. Food Chem. 2021, 69, 13339−13349

acute inflammation and adaptive immunity.[22−24] One well-established fibroblast cell model to study anti-inflammatory effects is human gingival fibroblast cells (HGF-1).[25−28] Inflammatory processes in the oral cavity have two sides: they help tissue heal and protect it against further damage, but on the other hand, if the inflammatory state persists, the chronic inflammation can lead to tissue damage, which could range from gingivitis to periodontitis. According to the FDI World Dental Federation, 50% of the global population has periodontal (gum) diseases and 30% at the age of 65−75 years old suffer from a complete loss of teeth.[29] In gingival cells, pro- or anti-inflammatory responses, such as, e.g., the release of cytokines, can be achieved via stimulation with LPS isolated from the Gram-negative bacterium *Porphyromonas gingivalis* (*Pg*-LPS),[27] which has been associated with gingivitis.[30] Experimentally, we previously demonstrated an increased production of the pro-inflammatory interleukins IL-6 and IL-8 by HGF-1 cells exposed to *Pg*-LPS concentrations ranging from 1 to 100 ng/mL for 6 h.[27]

Two bitter tasting food constituents for which anti-inflammatory properties have been demonstrated *in vitro* are rosmarinic acid (RA), an ester of caffeic acid and 3,4-dihydroxyphenyllactic acid,[31] and *trans*-resveratrol (RSV), a 3,5,4′-trihydroxystilbene.[32] Both compounds have been shown to reduce a LPS-induced release of TNF-α and IL-6 by immune-competent cells.[28,33−37] However, a potential involvement of TAS2Rs in the anti-inflammatory effect of RSV and RA is unknown, even though RSV has been shown to activate TAS2R1,[38] TAS2R14,[38,39] and TAS2R39,[39] whereas potential target TAS2Rs for RA remain unknown.

Thus, the present study hypothesized an involvement of TAS2Rs in anti-inflammatory effects, mediated by bitter-tasting compounds, in HGF-1 cells. RSV and RA were selected as bitter-tasting test compounds as a result of (i) the vast evidence of anti-inflammatory properties[28,34−36,40,41] and (ii) their reported bitter taste.[31,32] However, taste detection thresholds for these compounds reported in the literature differ substantially, with values from 17 to 390 ppm for RSV[32] and mean data of 37 ± 1.25 ppm for RA.[31] To directly compare the bitterness of RSV and RA, a sensory study was conducted with untrained volunteers, who were asked, first, to evaluate the best estimated threshold for RSV. Afterward, the bitter intensity of 50 ppm in water solution of RSV and RA was evaluated by means of a two-alternative forced choice (2-AFC) test. Because these results revealed RSV to be more bitter than RA, the effect of the bitter-masking TAS2R antagonist homoeriodictyol (HED) on the RSV-induced bitter perception was tested. HED is a bitter-masking flavanone (3′-methoxy-4′,5,7-trihydroxyflavanone) extracted from yerba santa (*Eriodictyon californicum*),[42,43] which targets several TAS2Rs as antagonist, e.g., TAS2R14,[39] TAS2R39, and TAS2R43.[12] Next, we aimed to verify the involvement of TAS2Rs in the bitter-masking effect demonstrated for HED on the bitterness perceived for RSV by means of an *in vitro* approach. For these experiments, human gastric tumor cells (HGT-1), a well-established cell model for the identification of bitter-tasting and bitter-taste-modulating compounds,[12,44] were chosen to quantitate TAS2R-dependent proton secretion in the presence of RSV with or without HED. Because involvement of a TAS2R in proton secretion of HGT-1 cells was demonstrated by means of stably CRISPR-Cas9-edited TAS2R knockout cells,[12] the final proof of our hypothesis was given in immune-competent human gingival (HGF-1) cells in culture. After the effect of RSV and RA on *Pg*-LPS-stimulated IL-6 release in HGF-1 cells was shown, we verified the TAS2R50 dependency of the RSV-evoked anti-inflammatory effect in TAS2R50 siRNA-edited HGF-1 cells. More broadly, we demonstrate that TAS2Rs bitter sensing is involved in gingival inflammation processes and might be used to identify anti-inflammatory compounds promoting oral health.

2. MATERIALS AND METHODS

2.1. Materials. *trans*-Resveratrol (RSV, 98% purity) was purchased from Breko GmbH, and rosmarinic acid (RA, 98% purity) was purchased from Carbolution Chemicals GmbH. The sodium salt of homoeriodictyol (3′-methoxy-4′,5,7-trihydroxyflavanone, HED, 94% purity) was kindly provided by Symrise AG. All other chemicals were obtained from Sigma-Aldrich (Merck KGaA, Darmstadt, Germany), unless indicated otherwise. Compounds with limited solubility in water were pre-dissolved in 98% ethanol (EtOH), of which a 0.1% (v/v) final concentration for cell culture incubations and 1% (v/v) final concentration for the sensory study were reached. Lipopolysaccharides of *P. gingivalis* (*Pg*-LPS) were obtained from InvivoGen and reconstituted to a concentration of 1 mg/mL. The final concentration applied to cells was 10 μg/mL.

2.2. Sensory Study. A total of 15 sensorially untrained volunteers, 10 females and 5 males (22−40 years old), participated in the sensory study. Prior to performing the sensory test, the panelists signed a written informed consent. None of the participants reported any taste disorders, which was validated in a preliminary test for bitterness and sweetness perception evoked by caffeine (0.03%, w/v) and sucrose (0.6%, w/v). At 2 h prior to the sensory test, panelists were asked to abstain from food or beverages, except for water. All tests were conducted 2−3 times on different days with at least 3 days in between. The sample cups were filled with 20 mL of test substance and labeled with a randomized three-digit code, which was generated using the software Research Randomizer (version 4.0). All solutions were prepared with distilled water to avoid ions and other trace minerals. To neutralize between samples, the panelists rinsed their mouth with water and were provided with yogurt (10% fat) in case further neutralization was required.

2.2.1. Threshold Determination. To determine the best estimate threshold (BET) and the individual threshold for RSV, a triangular forced choice test with ascending concentration series, conforming to the Society of Sensory Professionals and ASTM International[45] standards, was conducted. Seven RSV concentrations (0.1, 0.5, 1, 5, 10, 50, and 100 ppm) with a final concentration of 1% EtOH (v/v) were tested in triplicate and compared to distilled water containing 1% EtOH (v/v). Taste thresholds were calculated using the geometric mean of the highest not identified concentration and the next higher concentration.[45] Five panelists were excluded because they did not reach their individual threshold in the seven concentration levels of RSV.

2.2.2. Comparison of trans-Resveratrol and Rosmarinic Acid. Additionally, the bitter taste intensity of RSV (50 ppm) and RA (50 ppm) was compared in a sensory trial with the 10 panelists by means of a 2-AFC test, conforming to the methodology described in the *Practical Handbook of Sensory for Product Development and Quality Assurance*.[46] Panelists had to choose the more bitter-tasting substance of the two samples.

2.2.3. Bitter-Masking Effect of Homoeriodictyol. Furthermore, the bitter-masking effect of co-administration of HED (50 ppm) and RSV (50 ppm) was assessed by eight panelists on 3 different days (24 individual tastings), also applying the 2-AFC method. In addition, panelists were asked to rank the bitter intensity of RSV with or without HED on a 10 cm scale ranging from no bitter taste (0 cm) to very strong bitter taste perception (10 cm). Prior to this test, the panelists were trained with four different concentrations of RSV (0, 5, 10, 50, and 70 ppm). Mean bitterness ratings were calculated on the basis of the 10 cm scale and expressed as a percent of the RSV rating.

2.3. Cell Culture. Human gingival fibroblasts (HGF-1; passage number 16) were obtained from the American Type Culture

https://dx.doi.org/10.1021/acs.jafc.0c07058
J. Agric. Food Chem. 2021, 69, 13339−13349

Table 1. Sequence of All Primer Pairs[12,33] Used in the RT-qPCR Experiments[a]

target	amplicon size (bp)	5′ → 3′ sequence
PPIA	144	FW: CCA CCA GAT CAT TCC TTC TGT AGC
		RV: CTG CAA TCC AGC TAG GCA TGG
GAPDH	95	FW: AGG TCG GAG TCA ACG GAT TTG
		RV: GGG GTC ATT GAT GGC AAC AAT A
IL-6R	141	FW: CCA CCC CCA TGC AGG CAC TTA
		RV: CCA GGC TCC CTC CAG CAA CCA
IL-6	73	FW: AAA CAA CCTGAA CCT TCC AAA GA
		RV: GCA AGT CTC CTC ATT GAA TCC A
TAS2R14	128	FW: CCA GGT GAT GGG AAT GGC TTA
		RV: AGG GCT CCC CAT CTT TGA AC
TAS2R20	183	FW: ATT TGG GGG AAC AAG ACG CT
		RV: ACTA CGG AAA AAC TTG TGG GAA
TAS2R31	218	FW: TTG AGG AGT GCA GTG TAC CTT TC
		RV: ACG GCA CAT AAC AAG AGG AAA A
TAS2R39	207	FW: TTC TGT GGC TGT CCG TGT TTA
		RV: GGG TGG CTG TCA GGA TGA AC
TAS2R43	148	FW: ATA TCT GGG CAG TGA TCA ACC
		RV: CCC AAC AAC ATC ACC AGA ATG AC
TAS2R50	151	FW: CGC AAG ATC TCA GCA CCA AGG TC
		RV: GCC TTG CTA ACC ATG ACA ACC GGG

[a]Primer pairs were synthesized by Sigma-Aldrich (Austria), except for *IL-6*, *IL-6R*, and *TAS2R50*, which were synthesized by VBC Biotech (Austria).

Collection (ATCC 2014), and human gastric cells (HGT-1; passage number 56) were obtained from Dr. C. Laboisse (Laboratory of Pathological Anatomy, Nantes, France). Both were cultured in Dulbecco's modified Eagle's medium (DMEM) high glucose (4.5 g/L D-glucose), GlutaMAX (ThermoFisher) supplemented with 10% fetal bovine serum (FBS, Invitrogen, Vienna, Austria), 100 units mL^{-1} penicillin, and 0.1 mg mL^{-1} streptomycin (Sigma-Aldrich, Merck KGaA, Darmstadt, Germany) at standard conditions (37 °C, 5% CO_2, and a humidified atmosphere).

2.4. Cell Viability. To exclude cytotoxic effects of the test substances in concentrations applied during the 1 and 6 h incubations, the metabolic cell activity of HGF-1 and HGT-1 cells was determined via the 3-(4,5-dimethylthiazolyl-2)-2,5-diphenyltetrazolium bromide (MTT) assay, for which cells were cultivated in 96-well plates. Whereas HGF-1 cells were seeded at a density of 5000 cells per well 72 h prior to the experiment, a total of 100 000 HGT-1 cells per well were seeded 24 h prior the viability test. After the incubation, the absorbance of the formazan salt was measured at 570 nm, with a reference wavelength of 630 nm using a Tecan Infinite M200 PRO plate reader (Tecan, Switzerland).

2.5. Determination of Proton Secretion in HGT-1 Cells. Determination of the proton secretion in HGT-1 cells was investigated using the pH-sensitive fluorescent dye SNARF-1 AM, as described before.[44,47] In brief, HGT-1 cells were cultivated in 96-well plates with 100 000 cells per well 24 h prior to the measurement. As a first step, the cells were washed twice with 100 μL of Krebs-Ringer HEPES buffer [KRHB; 10 mM 4-(2-hydroxyethyl)-1-piperazineethanesulfonic acid (HEPES), 11.7 mM D-glucose, 4.7 mM KCl, 130 mM NaCl, 1.3 mM $CaCl_2$, 1.2 mM $MgSO_4$, and 1.2 mM KH_2PO_4], brought to a pH of 7.4 with 5 M KOH. Afterward, the cells were stained with 3 μM SNARF-1 AM in KRHB (Invitrogen) for 35 min at standard conditions. Next, the cells were treated with histamine (positive control, 1 mM) and 100 μL of RSV or RA (50 + 100 μM) for 10 min, with or without the addition of HED (50 + 100 μM). An additional washing step with KRHB was performed to remove residual compounds before the fluorescence was measured at emission wavelengths of 580 and 640 nm after excitation at 488 nm using an Infinite 200 PRO plate reader (Tecan, Männderdorf, Switzerland) with 100 μL/well KRHB. The ratio of 580/640 nm was then used to calculate the intracellular proton index (IPX) as $\log_2$ of the ratio between the intracellular H^+ concentration of treated and untreated cells by means of an external pH calibration curve (pH 7.0, 7.2, 7.4, 7.6, 7.8, and 8.0).

2.6. Determination of Cellular IL-6 Release. The IL-6 concentration in the cellular supernatant as a marker for IL-6 release of HGF-1 cells was measured by a sandwich enzyme-linked immune sorbent assay [ELISA, Sigma-Aldrich/Merck KGaA, Darmstadt, Germany; limit of detection (LOD), 3 pg/mL, intra-assay reproducibility coefficient of variation (CV), <10%; interassay reproducibility CV, <12%], following the protocol of the manufacturer. HGF-1 cells were seeded in 48 well plates at a density of 9700 cells/well 72 h before the experiment. Prior to the addition of 10 μg/mL *Pg*-LPS, the cells were pretreated for 1 h with 100 μM of either RSV or RA, with or without HED (1, 10, and 100 μM), and harvested for further analysis after an incubation time of 6 h.

2.7. DAVID Cluster Analyses Following a cDNA Microarray Approach Performed in HGF-1 Cells. The effects of RA, RSV, and HED on G-protein-coupled receptors in HGF-1 cells were investigated by applying customized cDNA microarrays as described before.[48,49] Whole genome cDNA microarrays, including 4−15 60-mer oligonucleotide probes of genes predominantly associated with G-protein-coupled receptors, were synthesized on glass slides using the method of maskless array synthesis.[50,51] The HGF-1 cells were seeded in 10 cm dishes at a density of 8.3×10^5 cells 72 h prior to the experiment and incubated after phosphate-buffered saline (PBS) washing with 100 μM RSV, RA, and HED for 3 h. RNA isolation was performed by the RNeasy Mini Kit (Qiagen, Hilden, Germany), according to the protocol of the manufacturer. Labeling was accomplished during transcription of the corresponding cDNA using Cy-3-labeled random nonamer primers (Tebu Bio, Offenbach, Germany).[52] Hybridization of labeled cDNA with the microarrays was carried out for 20 h at 42 °C. A GenePix 4400A microarray scanner (Molecular Devices, Sunnyvale, CA, U.S.A.) was used for the array scanning. Afterward, the scanned images were evaluated by the NimbleScan 2.1 software (NimbleGen, Madison, WI, U.S.A.). For the normalization, a robust multichip analysis was performed. The calculated fold changes of the regulated genes were analyzed using pathway analysis software Database for Annotation, Visualization and Integrated Discovery (DAVID; http://david.abcc.ncifcrf.gov) after extracting fold changes below 0.83 or above 1.2 to identify and select genes showing potential regulation by the test compounds.

https://dx.doi.org/10.1021/acs.jafc.0c07058
J. Agric. Food Chem. 2021, 69, 13339−13349

2.8. Gene Expression Analysis of *IL-6*, *IL-6R*, and *TAS2Rs*. For the gene expression analysis of human *IL-6*, *IL6R*, *PPIA*, *GAPDH*, and selected *TAS2Rs* (*TAS2R14*, *TAS2R20*, *TAS2R31*, *TAS2R39*, *TAS2R43*, and *TAS2R50*), HGF-1 cells were seeded in 6 cm dishes at a density of 5.5×10^5 cells 72 h prior to the experiment. After washing with PBS, the pre-incubation with 100 μM RSV with or without the co-application of 100 μM HED was started. After the 1 h pre-incubation, *Pg*-LPS was added to a final concentration of 10 μg/mL for another 6 h. Subsequently, the cells were washed with ice-cold PBS and lysed for the RNA isolation, which was performed with the MasterPure Complete DNA and RNA Purification Kit (Lucigen) following the protocol of the manufacturer. Purity and yield of the RNA were determined spectrophotometrically by the ratios of A_{260}/A_{280} and A_{260}/A_{230}. To transcribe 1 μg of RNA into cDNA, the high capacity cDNA kit (Applied Biosystems, Austria) was used according to the protocol of the manufacturer. Real-time quantitative polymerase chain reaction (RT-qPCR) was performed in triplicates with the previously transcribed cDNA, amplified with Fast SYBR Green Master Mix (Applied Biosystems, Austria) on a StepOne Plus PCR device (Applied Biosystems, Austria). The specific sequences of the used primers are shown in Table 1. The primer pairs were synthesized by Sigma-Aldrich (Austria) or VBC Biotech (Austria). The qPCR was composed of an initial denaturation step at 95 °C for 20 s and 40 amplification cycles consisting of denaturation at 95 °C for 3 s, annealing at 60 °C for 30 s, and elongation with a fluorescence measurement at 67 °C for 15 s. RT-qPCR data were analyzed with LinRegPCR (version 2018.0) to determine the respective hypothetical mRNA starting concentrations (N_0 value) based on the C_T values under consideration of PCR efficiency. The geometric mean of the two reference genes *GAPDH* and *PPIA* was used to normalize the N_0 values of the target genes.

2.9. Knockdown of TAS2R50 with Small Interfering RNA (siRNA). *TAS2R50* expression levels were knocked down in HGF-1 cells using siRNA. The siRNA sequence (FW, 5′-GAAUACAGUACAUCUUUCA-3′; RV, 5′-UGAAAGAUGUACUGUAUUC-3′) was based on Rosetta Predictions and obtained from Sigma-Aldrich (Merck KGaA, Darmstadt, Germany). Using the fast-forward protocol, 2.88×10^4 cells were seeded in a 24-well plate followed by transfection with the HiPerFect Transfection Reagent (QIAGEN, Austria) and 30 nM[53] of the gene-specific siRNA targeting *TAS2R50* following the protocol of the manufacturer. Every performed knockdown was validated using a positive control, *MAPK1* siRNA (Qiagen), a negative control (Allstars Negative Control siRNA, Qiagen), and a mock transfection (no siRNA added). Toxicity of the HiPerFect Reagent was excluded by MTT tests, as described above. After 48 h, the knockdown efficacy was analyzed via RT-qPCR. The subsequent incubation with the test substances was performed for each biological replicate with the wild-type and knockdown cells.

2.10. Chemical Interaction Analysis of *Pg*-LPS with RSV and HED via Liquid Chromatography−Tandem Mass Spectrometry (LC−MS/MS). To analyze the potential interactions between *Pg*-LPS and RSV or HED, a LC−MS/MS analysis was carried out using Shimadzu 8040 LC−MS/MS with a Synergi 4 μm Fusion-RP 80 A column (150 × 2 mm, Phenomenex). RSV and HED were incubated with *Pg*-LPS in medium under the same conditions as those applied to cell culture samples. As a control, RSV and HED were incubated without *Pg*-LPS. Ice-cold 98% (v/v) EtOH was added to precipitate the proteins. The supernatant was collected, dried using a SpeedVac concentrator (Eppendorf), and reconstituted with LC−MS-grade water. A total volume of 10 μL of sample was injected, and a valve was used for only allowing effluent between 9 and 15 min of the run time to enter MS. The MS interface settings were as follows: nebulizing gas flow, 3 L min^{-1}; desolvation line (DL) temperature, 150 °C; heat block temperature, 350 °C; and drying gas flow, 15 L min^{-1}. The flow rate was set to 0.5 mL min^{-1}. Gradient component A was LC/MS-grade water, and gradient B was acetonitrile supplemented with 0.1% formic acid. The transition from m/z 227.05 to 143 and 185 was used in the quantification of RSV. For HED, the transition from m/z 301 to 163.80 and 150 was used in the quantification. The following HPLC conditions were used: 0−12 min, 100% A; 13−22 min, 20% A; and 23−30 min, 100% A.

2.11. Molecular Modeling. The three-dimensional (3D) structure model of TAS2R50 was downloaded from the 2019 release of BitterDB[54] and prepared for the following simulations with the Protein Preparation Wizard tool in the Schrödinger Small-Molecule Drug Discovery Suite 2019-4 (Schrödinger, LLC, New York). The structure of RSV was built using the Builder tool and prepared for docking through the generation of stereoisomers and protonation states at pH 7 ± 0.5 with LigPrep, as implemented in the Schrödinger Small-Molecule Drug Discovery Suite 2019-4 (Schrödinger, LLC, New York). The Schrödinger induced fit extended sampling docking protocol (Schrödinger Suite 2019-4 induced fit docking protocol; Glide, Schrödinger, LLC, New York; Prime, Schrödinger, LLC, New York)[55] was then used to investigate the binding mode of RSV into the canonical binding site of TAS2R50, as previously defined.[56]

2.12. Statistical Analysis and Nomenclature. Data are presented as the mean ± standard error of the mean (SEM) calculated from 3−6 biological replicates, which were received from 2−3 technical replicates, unless indicated otherwise. Outliers were identified by means of Nalimov's test and removed from the final analysis. The results were analyzed with SigmaPlot 13.0 (Systat). Each data set was tested for normal distribution by means of a Shapiro−Wilk test, and in the case of no normal distribution, non-parametrical tests were performed. Significant differences were tested by either Student's t test/Mann−Whitney U test or one-way analysis of variance (ANOVA)/one-way ANOVA on ranks followed by the post hoc test of Holm−Šidák, according to the respective hypothesis and data distribution. Treated values over control values are expressed as T/C or T/*Pg*-LPS and shown as a percent (%). The cutoff for statistically significant differences was set at p values of <0.05.

We followed the nomenclature rules according to HUGO, which designate the symbol of the bitter taste receptor gene as *TAS2Rx* and the corresponding protein as TAS2Rx.[57]

3. RESULTS

3.1. Sensory Study. The sensory study was conducted to compare the bitter taste perception induced by RSV and RA. Furthermore, we investigated whether the bitterness of RSV can be reduced by the bitter-masking compound HED. For these experiments, only panelists who were able to recognize the bitter and sweet taste of caffeine (0.03% solution in water) and sucrose (0.6% solution in water), respectively, were recruited.

The BET for RSV of 29 tastings by 10 panelists ranged between 0.1 and 22.36 ppm. From 15 respondents, five were excluded because they did not reach their individual threshold in the seven concentration levels of RSV. However, as a result of the limited solubility of RSV in water, higher concentrations could not be applied. Next, the bitterness of 50 ppm of RSV and 50 ppm of RA was compared via a 2-AFC test, and RSV was rated to be more bitter than RA by 90% of 29 individual tastings. The RSV-induced bitter taste intensity was reduced by 19 ± 6%, when 50 ppm of the bitter-masking compound HED was co-administered (Table 2). No bitter reduction with HED was tested for RA.

3.2. Cell Viability. None of the test compounds applied under the experimental conditions showed an effect on the viability of HGF-1 and HGT-1 cells (Table S1 of the Supporting Information).

3.3. Determination of Proton Secretion in HGT-1 Cells. RA, RSV, and HED were tested for their effects on proton secretion in human gastric cancer cells (HGT-1 cells) in culture. Proton secretion in this cell model has been demonstrated to be associated with cellular activation of bitter taste receptors[12] and, in general, correlates well with sensory

https://dx.doi.org/10.1021/acs.jafc.0c07058
J. Agric. Food Chem. 2021, 69, 13339−13349

Table 2. Comparison of Bitter Perception between 50 ppm of RA and 50 ppm of RSV Using a 2-AFC Test and the Bitter Reduction of 50 ppm of RSV by 50 ppm of HED[a]

	RA	RSV	RSV + HED
bitter comparison (2-AFC) (%)	10	90	
bitter reduction (2-AFC) (%)			19 ± 6
N (individual tastings)	29	29	24

[a]Number of individual tastings per each sensory trial.

data on bitter perception.[44] Therefore, HGT-1 cells have been validated as tools for the identification of bitter tastants and bitter-taste-modulating compounds.[12,44] Figure 1 shows the impact of RA (Figure 1A) and RSV (Figure 1B) on proton secretion in HGT-1 cells. Whereas treatment of the cells with RSV increased the proton secretion, indicated by a reduced intracellular proton concentration (IPX of −0.34 ± 0.04 at 50 μM and −0.41 ± 0.05 at 100 μM compared to controls set to zero), RA induced a reduction thereof. Because sensory data revealed a bitter-masking effect of the *TAS2R43*,[12] *TAS2R14*,[39] and *TAS2R39*[39] antagonist HED on the bitterness perceived for RSV (Table 2), involvement of the bitter-taste-sensing receptor TAS2R43 was verified by means of a homozygote *TAS2R43ko*. In HGT-1 wild-type cells, 50 μM HED reduced the 50 μM RSV-induced proton secretion by −12.76 ± 12.33% ($p < 0.01$), whereas the level of statistical significance was not reached in HGT-1 TAS2R43ko cells (−23.70 ± 14.57%; $p > 0.05$). For 100 μM RSV, however, the IPX response was the same in both cell lines, indicating a *TAS2R43*-independent mechanism on proton secretion (panels C and D of Figure 1).

3.4. IL-6 Release in HGF-1 Cells. To quantitate the effect on IL-6 protein release in HGF-1 cells induced by RSV and RA, the cell culture supernatant post-treatment was subjected to an ELISA. The effects of 100 μM RSV and 100 μM RA on IL-6 release after 6 h co-incubation with 10 μg/mL *Pg*-LPS showed inhibition of −73.9 ± 2.99 and −41.7 ± 2.09%, respectively, which were significantly different from each other (Mann−Whitney *U* test; $p < 0.001$; Figure 2). The effect evoked by RSV was reduced by co-administration of 100 μM HED, resulting in a mean reduction of −56.8 ± 2.90%, corresponding to a mean reduction of 17 ± 2.15% of the RSV-induced effect on the IL-6 release in HGF-1 cells. The concentration of 100 μM HED was chosen from dose−response experiments (Figure S1 of the Supporting Information). Moreover, the RA-induced effect was not affected by the addition of HED.

3.5. Determination of Gene Cluster in HGF-1 Cells Following cDNA Microarray Analyses. The impact of the selected bitter and bitter-modulating compounds RA, RSV, and HED in a concentration of 100 μM on gene expression in HGF-1 cells was analyzed using a customized cDNA microarray.[48,49] To determine changes in individual gene expression, an enrichment analysis of gene expression data was performed by applying the functional annotation clustering software DAVID using genes with fold changes under 0.83 or over 1.2 as thresholds. The cluster with the highest enrichment score of 6.67, 2.88, and 4.34 (RA, RSV, and HED) was found to involve genes associated with the G-protein-coupled receptor signaling pathway. In the annotation cluster, RA showed the following: e.g., G-protein-coupled serotonin receptor activity (Benjamini, 1.4×10^{-9}), phospholipase-C-

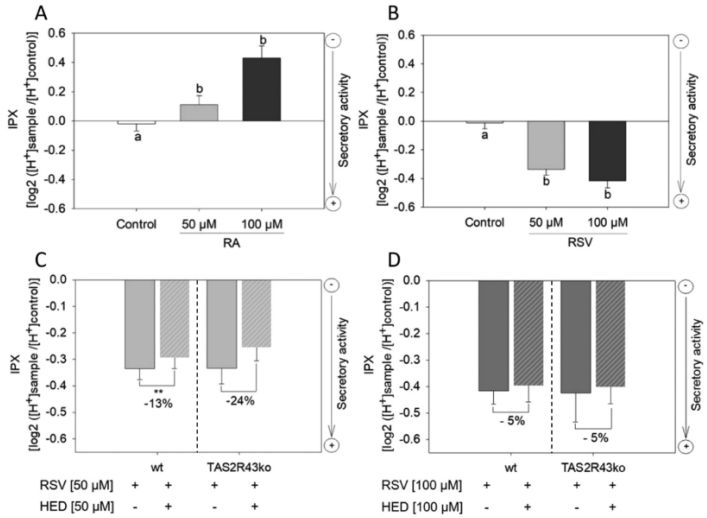

Figure 1. IPX of HGT-1 wild-type cells treated with (A) RA for 10 min compared to the control (KRHB) and (B) RSV for 10 min compared to the control [KRHB + 0.1% dimethyl sulfoxide (DMSO)]. Statistics: (A) One-way ANOVA on ranks with post hoc Dunn's method, with different letters indicating significance ($p < 0.05$). (B) One-way ANOVA with post hoc Holm−Šidák test, with different letters indicating significance ($p < 0.05$). IPX in HGT-1 wild-type cells and HGT-1 cells with homozygous TAS2R43ko treated with RSV with or without HED (C, 50 μM) and (D, 100 μM) for 10 min (h)compared to the solvent control [KRHB + DMSO (0.1%)]. IPX data are shown as the mean ± SEM ($n = 3$; technical replicates = 3−6). Statistics: (C and D) Student's *t* test for RSV versus HED treatment; (**) $p < 0.01$.

https://dx.doi.org/10.1021/acs.jafc.0c07058
J. Agric. Food Chem. 2021, 69, 13339−13349

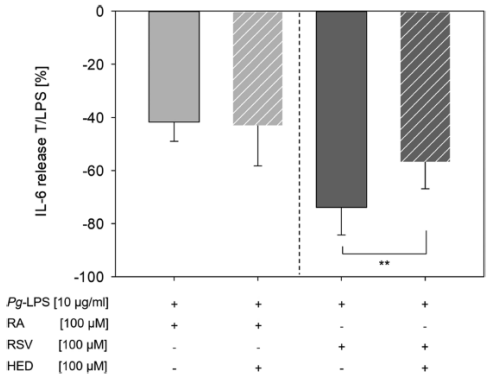

Figure 2. IL-6 release of HGF-1 cells treated with *trans*-resveratrol and rosmarinic acid 1 h of pre-incubation and 6 h of incubation with *Pg*-LPS with or without HED. Data are calculated as treatment over the control in percent, with the effect of *Pg*-LPS set to zero (T/LPS, %; LPS = 0%). Data are shown as the mean ± SEM (n = 6; technical replicates = 2). Statistics: Mann−Whitney U test; (**) $p < 0.01$. Statistics: Mann−Whitney U test for RSV with *Pg*-LPS versus RA with *Pg*-LPS ($p < 0.001$).

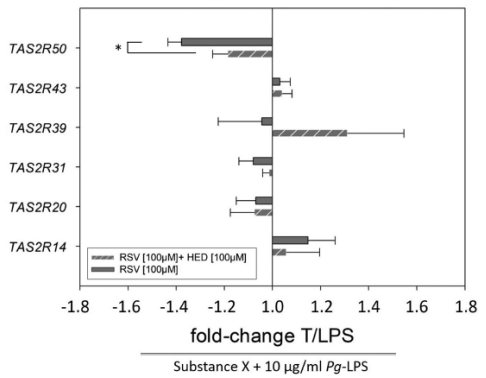

Figure 3. Determination of involved *TAS2Rs* in HGF-1 cells as a result of a mRNA expression screening of known resveratrol and homoeriodictyol targets (*TAS2R14*, *TAS2R20*, *TAS2R31*, *TAS2R43*, and *TAS2R50*), at 1 h of pre-incubation of the substance with or without HED and 6 h of co-incubation with *Pg*-LPS. Data are indicated as the mean ± SEM in comparison to *Pg*-LPS (set to 1). Calculations were made from at least three biological replicates, and values of *trans*-resveratrol with or without homoeriodictyol were compared to each other (technical replicates = 2−3). Statistics: Mann−Whitney U test; (*) $p \leq 0.05$. Statistics: Mann−Whitney U test for *Pg*-LPS versus RSV with *Pg*-LPS ($p < 0.001$).

activating G-protein-coupled receptor signaling pathway (Benjamini, 1.2×10^{-3}), and adenylate cyclase-inhibiting G-protein-coupled receptor signaling pathway (Benjamini, 6.0×10^{-5}). Furthermore, RSV showed, e.g., G-protein-coupled serotonin receptor activity (Benjamini, 2.9×10^{-5}) and G-protein-coupled receptor signaling pathway, coupled to cyclic nucleotide second messenger (Benjamini, 4.8×10^{-2}). HED showed, e.g., G-protein-coupled serotonin receptor activity (Benjamini, 1.4×10^{-5}), phospholipase-C-activating G-protein-coupled receptor signaling pathway (Benjamini, 1.0×10^{-3}), adenylate-cyclase-inhibiting G-protein-coupled receptor signaling pathway (Benjamini, 2.6×10^{-2}), and G-protein-coupled receptor signaling pathway, coupled to cyclic nucleotide second messenger (Benjamini, 8.2×10^{-5}). For validation of the involvement of specific G-protein-coupled receptors, namely, TAS2Rs, a more sensitive RT-qPCR analysis was conducted.

3.6. *IL-6* and *TAS2R* Gene Expression Screening of Known RSV and HED Targets in HGF-1 Cells. To elucidate a TAS2R-dependent mechanism of IL-6 secretion in HGF-1 cells, gene expression levels of IL-6 as well as known targets of RSV and HED were studied in experiments applying 100 μM equimolar concentrations for 1 h, followed by a 6 h co-incubation step with *Pg*-LPS in HGF-1 cells. In comparison to cells treated with *Pg*-LPS, IL-6 gene expression levels were reduced by −46.2 ± 12.7% ($p < 0.001$) and −26.0 ± 16.6% ($p < 0.001$) after co-incubation with RSV and RSV + HED, respectively, showing a statistically relevant difference for both treatments ($p < 0.05$). Moreover, gene expression levels of described target TAS2Rs for HED[12] and RSV[39] were investigated (Figure 3). Whereas genes encoding for *TAS2R14*, *TAS2R20*, *TAS2R31*, *TAS2R39*, *TAS2R43* were expressed in HGF-1 cells but showed no significant changes after RSV with or without HED application versus *Pg*-LPS treatment solely (set to 1), relative to *TAS2R50* expression levels decreased after treatment with RSV (−1.38 ± 0.06; $p < 0.05$). This RSV-evoked effect was ameliorated by co-application of RSV + HED (−1.19 ± 0.06; $p < 0.05$).

3.7. Impact of *TAS2R50* siRNA on the RSV-Evoked IL-6 Gene Expression and Protein Release in *Pg*-LPS-Treated HGF-1 Cells. To verify the involvement of *TAS2R50* in the RSV-induced effect on *Pg*-LPS-stimulated IL-6 gene expression and protein release in HGF-1 cells, a siRNA knockdown experiment was performed. Knockdown efficacy of the positive control MAPK1 was 59 ± 4%, whereas *TAS2R50* was downregulated by 37 ± 7% compared to non-targeted control cells (Figure S2 of the Supporting Information). Treatment with scrambled siRNA as the negative control as well as mock transfection had no effect.

Whereas application of RSV solely and treatment of the cells with RSV + HED prior to *Pg*-LPS resulted in a reduced, different *TAS2R50* expression of −64.9 ± 5.62 and −37.4 ± 10.38% ($p < 0.05$) compared to *Pg*-LPS treated HGF-1 wild-type cells (Figure 4A), respectively, no difference for these treatments was demonstrated in *TAS2R50* kd cells, with reduced gene expression levels of −21.2 ± 7.91 and −23.3 ± 8.76% for RSV and RSV + HED, respectively (Figure 4B). Notably, effect sizes for RSV and RSV + HED treatments were lower in HGF-1 *TAS2R50* kd compared to HGF-1 wild-type cells ($p < 0.05$).

Pg-LPS-induced IL-6 release (panels C and D of Figure 4) in HGF-1 wild-type cells was reduced more potently by RSV (−65.6 ± 1.7%) than by RSV + HED (−21.4 ± 6.2%; $p < 0.05$), whereas no such difference was demonstrated in *TAS2R50* kd cells, showing percentage reductions of the *Pg*-LPS-induced IL-6 release of −42.6 ± 3.9 and −47.4 ± 5.0% for RSV and RSV + HED treatments ($p > 0.05$).

3.8. Molecular Interaction Analysis of *Pg*-LPS with RSV and HED. To exclude chemical interactions of RSV and HED with the pro-inflammatory stimulus *Pg*-LPS, concen-

https://dx.doi.org/10.1021/acs.jafc.0c07058
J. Agric. Food Chem. 2021, 69, 13339−13349

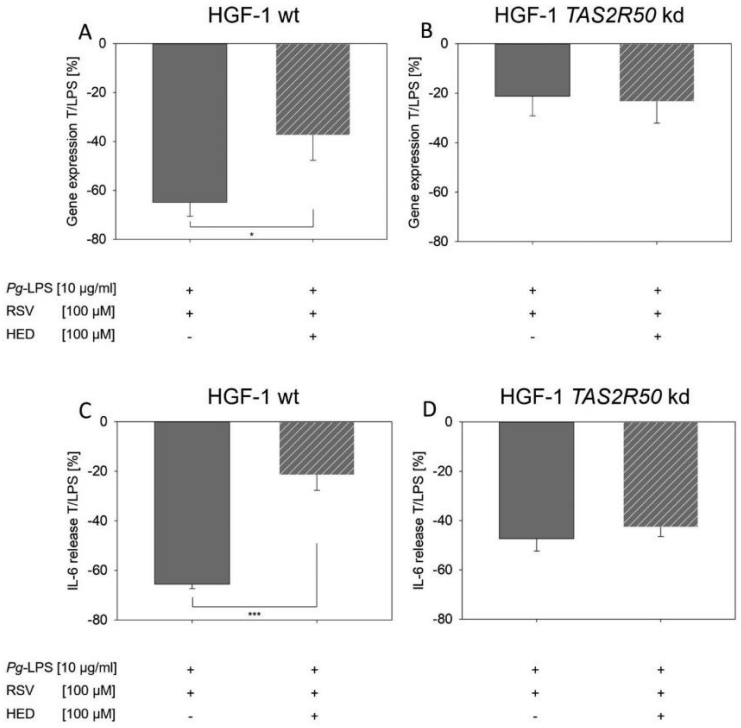

Figure 4. Effect of RSV with or without HED in (A) HGF-1 wild-type cells and (B) HGF-1 cells with *TAS2R50* knocked down (*TAS2R50* kd) on the mRNA expression level as well for the IL-6 release via IL-6 ELISA in (C) wild-type and (D) *TAS2R50* kd cells, at 1 h of pre-incubation of the substance with or without HED and 6 h of co-incubation with *Pg*-LPS. Data are calculated as the treatment over the control in percent, with the effect of *Pg*-LPS set to zero (T/LPS, %; LPS = 0%). Data are shown as the mean ± SEM (n = 3−4; technical replicates = 2−3). RSV with or without HED (panels A and B and panels C and D) were compared to each other to clarify the involvement of *TAS2R50*. Statistics: Mann−Whitney U test; (∗) $p \leq 0.05$ and (∗∗∗) $p \leq 0.001$.

trations of free RSV and HED were quantitated in cell-free experiments for which RSV and HED were incubated with *Pg*-LPS in cell culture medium under the same conditions as applied in cell culture experiments. Under none of the applied conditions did the presence of *Pg*-LPS affect the concentrations of free RSV and HED (Figure 3 of the Supporting Information).

3.9. Putative Binding Mode of RSV in TAS2R50. To provide insights into the potential mode of interactions of RSV with TAS2R50, an induced fit docking simulation was performed, which takes into account the flexibility of both ligand and binding site residues. The best predicted docking pose (docking score of −9.73 kcal/mol) locates RSV within transmembranes (TMs) of 3, 4, 5, and 6: the ligand establishes a $\pi-\pi$ stacking interaction with Trp88 and hydrogen bonds with Asn92 and Ser248 (Figure 5A), and it is accommodated in a highly hydrophobic pocket (Figure 5B).

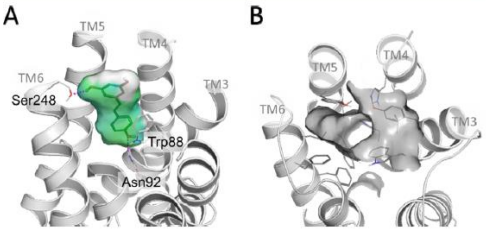

Figure 5. (A) 3D representation of the binding mode of RSV (shown as green sticks with the surface) within the TAS2R50 binding pocket. Ligand-interacting residues are shown as gray sticks, and hydrogen bonds as magenta dashed lines. (B) TAS2R50 binding site. Aromatic residues shaping the TAS2R50 binding site (Trp88, His142, Tyr176, Val179, Trp183, Phe241, Phe244, and Tyr285) are shown as sticks.

4. DISCUSSION

RSV and RA are reported as anti-inflammatory and bitter-tasting compounds, although the question of whether their anti-inflammatory potential is linked to activation of extra-oral TAS2Rs has not been addressed thus far.

As a first step for answering this research question, a sensory study with untrained panelists was conducted, aiming to identify the individual BET to allow for comparable compound concentrations for a subsequent comparison of RSV and RA administered above individual BET. For RSV, a broad BET

https://dx.doi.org/10.1021/acs.jafc.0c07058
J. Agric. Food Chem. 2021, 69, 13339−13349

range of 0.1−22.36 ppm was revealed versus a previously described large range of 17−390 ppm.[32] In our study, concentrations exceeding 100 ppm of RSV were not tested as a result of the limited solubility of RSV in water. With that said, we cannot exclude higher individual BET values in the presence of organic solvents, which would allow for sensory tests of water-based solutions containing RSV concentrations above 100 ppm. In general, broad individual BET ranges might be explained by genetic variations because large individual variations of bitter taste perception are known to be linked to the allelic diversity of TAS2R receptors,[58,59] e.g., TAS2R38.[60] However, whether the bitter taste perception of RSV is linked to genetic variations of TAS2Rs, namely, TAS2R1,[38] TAS2R14,[38,39] and TAS2R39,[39] or any other TAS2R has not yet been elucidated.

On the basis of the BET range evaluated in this study, a concentration of 50 ppm of RSV in water was administered in a 2-AFC to compare its bitter taste perception with 50 ppm of RA. In this setting, RSV was evaluated as the more bitter-tasting compound by 90% of the panelists, who also reported a mean 19 ± 6% reduction of the perceived bitterness when RSV was administered together with the bitter-masking TAS2R antagonist HED.[42,43]

Because RSV was described to be more bitter than RA, the highest concentration of the individual BET for RSV (22.36 ppm, corresponding to approximately 100 μM RSV) was used for the subsequent cell culture experiments, which were intended to identify whether TAS2Rs are involved in RSV-evoked anti-inflammatory processes.

To confirm that extra-oral TAS2Rs play a functional role in cellular processes associated with the bitter perception of our test compounds, we used an *in vitro* model of human gastric cells (HGT-1). This human cell model is known to functionally express *TAS2Rs*[12] and has been validated for the identification of bitter-tasting and bitter-taste-modulating compounds by means of TAS2R-dependent proton secretion.[12,44] Results of the proton secretion assay in our study not only confirmed our findings from the sensory trial by proving RSV more bitter than RA and the RSV-evoked effect being ameliorated by HED, they also showed involvement of *TAS2R43* in the HED-induced response. However, *TAS2R43* could not be verified as a target of RSV.

Next, we investigated the ability of RSV and RA to reduce a *Pg*-LPS-induced release of the pro-inflammatory cytokine IL-6 in human gingival fibroblasts (HGF-1 cells) depending upon TAS2R activation. Fibroblasts are well-established for studies on the complex pathways of IL-6 release and have helped to show that an overexpression of IL-6 is a driving force in many chronic inflammatory diseases.[61−64] Experimental settings, namely, a concentration of 10 μg/mL *Pg*-LPS and an incubation time of 6 h, were applied according to previous studies targeted to the identification of anti-inflammatory plant constituents.[26,27] In comparison to RA, RSV more potently reduced the *Pg*-LPS-induced release of IL-6, and moreover, its effect was reduced in co-incubation experiments with HED. IL-6 gene expression analysis also demonstrated that HED reduces the RSV-evoked effect. HED has been verified to reduce not only the bitterness of caffeine in trained panelists by up to 43%[43] but also a TAS2R-dependent gastric acid secretion, induced by caffeine, by 49%.[12] In the study presented here, results of the sensory test with untrained panelists demonstrated HED to reduce the perceived bitterness of RSV by 19 ± 6%. In experiments with HGT-1 cells, HED reduced the RSV-evoked effect on proton secretion by a mean value of 13%, and 17 and 20% reductions were shown for IL-6 release and IL-6 gene expression in HGF-1 cells, respectively. Whereas involvement of TAS2R43 in the HED-mediated effect on proton secretion in HGT-1 cells was verified by means of a CRISPR-Cas9 knockout approach not only in this but also in one of our previous works,[12] the functional role of TAS2Rs on the IL-6 release in HGF-1 cells was investigated by a RT-qPCR screening of specific *TAS2Rs* known to be targeted by HED, RSV, and LPS. Prior to these experiments, a cDNA microarray approach combined with DAVID pathway analysis revealed G-protein-coupled receptors as potential targets of HED and RSV. For RT-qPCR screening, *TAS2R14* and *TAS2R39* were selected on the basis of results published in transiently transfected HEK293 cells by Roland et al.,[39] who reported a dose-dependent activation of TAS2R14 and TAS2R39 by RSV, with EC_{50} values of 30 and 109 μM, respectively.[39] *TAS2R20* and *TAS2R31* were targeted on the basis of recent results obtained from LPS-treated macrophages.[20] On the basis of the results of transfected HEK-293T and Ca^{2+} mobilization, showing that HED is an antagonist for TAS2R50,[12] gene expression of *TAS2R50* was included in the analysis as well. In our study, we demonstrated for the first time that HGF-1 cells express *TAS2R14*, *TAS2R20*, *TAS2R31*, *TAS2R39*, *TAS2R43*, and *TAS2R50* on mRNA level. Among these genes, only expression of *TAS2R50* was regulated by RSV when compared to treatment of HGF-1 cells with *Pg*-LPS solely ($p < 0.001$). Co-treatment of *Pg*-LPS stimulated cells with RSV and HED again reduced the RSV-evoked effect. The functional role of *TAS2R50* in these findings was validated by means of a knockdown experiment applying *TAS2R50*-specific siRNA. Moreover, molecular modeling analyses have highlighted a potential interaction between RSV and TAS2R50.

Our results point to a functional role of *TAS2Rs* in anti-inflammatory response pathways, although further research needs to clarify the underlying mechanisms. Thus far, it is not clear whether the bitter-masking compound HED, which antagonizes TAS2R43, TAS2R20, TAS2R31, and TAS2R50,[12] but is described as an agonist for TAS2R14[39] and TAS2R39,[39] blocks access to the respective bitter taste receptor or whether it interacts with the bitter receptor by altering the protein structure, which prevents RSV and other potential ligands from binding. Cellular effects as a result of a chemical interaction between RSV, HED, and *Pg*-LPS can be excluded on the basis of the results of our cell-free LC−MS/MS analysis.

In conclusion, we demonstrate involvement of TAS2R50 in an anti-inflammatory, IL-6 targeting pathway induced by RSV in *Pg*-LPS-treated human gingival cells in culture. The specificity of RSV on TAS2R50 has to be elucidated in future kinetic binding studies. In addition, whether the overall anti-inflammatory defense of gingival cells is linked to sensory bitter perception has to be elucidated in future studies. Another open question is whether bitter sensory tests might useful to identify anti-inflammatory compounds promoting oral health.

■ ASSOCIATED CONTENT

Supporting Information

The Supporting Information is available free of charge at https://pubs.acs.org/doi/10.1021/acs.jafc.0c07058.

HGT-1 and HGF-1 cells administered with the test compounds in concentrations of 100 μM (Table S1), IL-6 release of HGF-1 cells treated with RSV at 1 h of pre-

https://dx.doi.org/10.1021/acs.jafc.0c07058
J. Agric. Food Chem. 2021, 69, 13339−13349

incubation and 6 h of incubation with *Pg*-LPS with or without HED (Figure S1), gene expression of *MAPK1* in HGF-1 cells, which were transfected with the transfection reagent (Mock) or combined with either positive control Hs/Mm_MAPK1 siRNA (PC) or Allstars Negative Control siRNA (NC) for 48 h (Figure S2), and molecular interaction analysis of *Pg*-LPS with HED and RSV by means of LC−MS/MS (Figure S3) (PDF)

AUTHOR INFORMATION

Corresponding Author

Veronika Somoza − *Department of Physiological Chemistry, Faculty of Chemistry, University of Vienna, 1090 Vienna, Austria; Leibniz-Institute of Food Systems Biology at the Technical University of Munich, 85354 Freising, Germany; Chair for Nutritional Systems Biology, Technical University of Munich, 85354 Freising, Germany;* orcid.org/0000-0003-2456-9245; Email: v.somoza.leibniz-lsb@tum.de

Authors

Johanna Tiroch − *Department of Physiological Chemistry, Faculty of Chemistry, University of Vienna, 1090 Vienna, Austria*

Sonja Sterneder − *Department of Physiological Chemistry, Faculty of Chemistry, University of Vienna, 1090 Vienna, Austria*

Antonella Di Pizio − *Leibniz-Institute of Food Systems Biology at the Technical University of Munich, 85354 Freising, Germany;* orcid.org/0000-0002-8520-5165

Barbara Lieder − *Department of Physiological Chemistry, Faculty of Chemistry, University of Vienna, 1090 Vienna, Austria;* orcid.org/0000-0002-0527-8330

Kathrin Hoelz − *Department of Inorganic Chemistry, Faculty of Chemistry, University of Vienna, 1090 Vienna, Austria*

Ann-Katrin Holik − *Department of Physiological Chemistry, Faculty of Chemistry, University of Vienna, 1090 Vienna, Austria*

Marc Pignitter − *Department of Physiological Chemistry, Faculty of Chemistry, University of Vienna, 1090 Vienna, Austria;* orcid.org/0000-0002-5793-8572

Maik Behrens − *Leibniz-Institute of Food Systems Biology at the Technical University of Munich, 85354 Freising, Germany;* orcid.org/0000-0003-2082-8860

Mark Somoza − *Leibniz-Institute of Food Systems Biology at the Technical University of Munich, 85354 Freising, Germany; Department of Inorganic Chemistry, Faculty of Chemistry, University of Vienna, 1090 Vienna, Austria; Chair of Food Chemistry and Molecular Sensory Science, Technical University of Munich, 85354 Freising, Germany;* orcid.org/0000-0002-8039-1341

Jakob P. Ley − *Symrise AG, 37603 Holzminden, Germany;* orcid.org/0000-0001-9388-4260

Complete contact information is available at: https://pubs.acs.org/10.1021/acs.jafc.0c07058

Notes

The authors declare no competing financial interest.

REFERENCES

(1) Matsunami, H.; Montmayeur, J. P.; Buck, L. B. A Family of Candidate Taste Receptors in Human and Mouse. *Nature* **2000**, *404* (6778), 601−604.

(2) Chandrashekar, J.; Mueller, K. L.; Hoon, M. A.; Adler, E.; Feng, L.; Guo, W.; Zuker, C. S.; Ryba, N. J. P. T2Rs Function as Bitter Taste Receptors. *Cell* **2000**, *100* (6), 703−711.

(3) Adler, E.; Hoon, M. A.; Mueller, K. L.; Chandrashekar, J.; Ryba, N. J. P.; Zuker, C. S. A Novel Family of Mammalian Taste Receptors. *Cell* **2000**, *100* (6), 693−702.

(4) Meyerhof, W.; Batram, C.; Kuhn, C.; Brockhoff, A.; Chudoba, E.; Bufe, B.; Appendino, G.; Behrens, M. The Molecular Receptive Ranges of Human TAS2R Bitter Taste Receptors. *Chem. Senses* **2010**, *35* (2), 157−170.

(5) Margolskee, R. F. Molecular Mechanisms of Bitter and Sweet Taste Transduction. *J. Biol. Chem.* **2002**, *277* (1), 1−4.

(6) Workman, A. D.; Palmer, J. N.; Adappa, N. D.; Cohen, N. A. The Role of Bitter and Sweet Taste Receptors in Upper Airway Immunity. *Curr. Allergy Asthma Rep.* **2015**, *15* (12), 72.

(7) Gil, S.; Coldwell, S.; Drury, J. L.; Arroyo, F.; Phi, T.; Saadat, S.; Kwong, D.; Chung, W. O. Genotype-Specific Regulation of Oral Innate Immunity by T2R38 Taste Receptor. *Mol. Immunol.* **2015**, *68* (2), 663−670.

(8) Patel, N. N.; Workman, A. D.; Cohen, N. A. Role of Taste Receptors as Sentinels of Innate Immunity in the Upper Airway. *J. Pathog.* **2018**, *2018*, 1−8.

(9) Clark, A. A.; Dotson, C. D.; Elson, A. E. T.; Voigt, A.; Boehm, U.; Meyerhof, W.; Steinle, N. I.; Munger, S. D. TAS2R Bitter Taste Receptors Regulate Thyroid Function. *FASEB J.* **2015**, *29* (1), 164−172.

(10) Deshpande, D. A.; Wang, W. C. H.; McIlmoyle, E. L.; Robinett, K. S.; Schillinger, R. M.; An, S. S.; Sham, J. S. K.; Liggett, S. B. Bitter Taste Receptors on Airway Smooth Muscle Bronchodilate by Localized Calcium Signaling and Reverse Obstruction. *Nat. Med.* **2010**, *16* (11), 1299−1304.

(11) Wu, S. V.; Rozengurt, N.; Yang, M.; Young, S. H.; Sinnett-Smith, J.; Rozengurt, E. Expression of Bitter Taste Receptors of the T2R Family in the Gastrointestinal Tract and Enteroendocrine STC-1 Cells. *Proc. Natl. Acad. Sci. U. S. A.* **2002**, *99* (4), 2392−2397.

(12) Liszt, K. I.; Ley, J. P.; Lieder, B.; Behrens, M.; Stöger, V.; Reiner, A.; Hochkogler, C. M.; Köck, E.; Marchiori, A.; Hans, J.; Widder, S.; Krammer, G.; Sanger, G. J.; Somoza, M. M.; Meyerhof, W.; Somoza, V. Caffeine Induces Gastric Acid Secretion via Bitter Taste Signaling in Gastric Parietal Cells. *Proc. Natl. Acad. Sci. U. S. A.* **2017**, *114* (30), E6260−E6269.

(13) Di Pizio, A.; Behrens, M.; Krautwurst, D. Beyond the Flavour: The Potential Druggability of Chemosensory G Protein-Coupled Receptors. *Int. J. Mol. Sci.* **2019**, *20* (6), 1402.

(14) Foster, S. R.; Blank, K.; See Hoe, L. E.; Behrens, M.; Meyerhof, W.; Peart, J. N.; Thomas, W. G. Bitter Taste Receptor Agonists Elicit G-Protein-Dependent Negative Inotropy in the Murine Heart. *FASEB J.* **2014**, *28* (10), 4497−4508.

(15) Deckmann, K.; Filipski, K.; Krasteva-Christ, G.; Fronius, M.; Althaus, M.; Rafiq, A.; Papadakis, T.; Renno, L.; Jurastow, I.; Wessels, L.; Wolff, M.; Schütz, B.; Weihe, E.; Chubanov, V.; Gudermann, T.; Klein, J.; Bschleipfer, T.; Kummer, W. Bitter Triggers Acetylcholine Release from Polymodal Urethral Chemosensory Cells and Bladder Reflexes. *Proc. Natl. Acad. Sci. U. S. A.* **2014**, *111* (22), 8287−8292.

(16) Shaw, L.; Mansfield, C.; Colquitt, L.; Lin, C.; Ferreira, J.; Emmetsberger, J.; Reed, D. R. Personalized Expression of Bitter 'Taste' Receptors in Human Skin. *PLoS One* **2018**, *13* (10), e0205322.

(17) Malki, A.; Fiedler, J.; Fricke, K.; Ballweg, I.; Pfaffl, M. W.; Krautwurst, D. Class I Odorant Receptors, TAS1R and TAS2R Taste Receptors, Are Markers for Subpopulations of Circulating Leukocytes. *J. Leukocyte Biol.* **2015**, *97* (3), 533−545.

(18) Gaida, M. M.; Dapunt, U.; Hänsch, G. M. Sensing Developing Biofilms: The Bitter Receptor T2R38 on Myeloid Cells. *Pathog. Dis.* **2016**, *74* (3), ftw004.

(19) Tran, H. T. T. T.; Herz, C.; Ruf, P.; Stetter, R.; Lamy, E. Human T2R38 Bitter Taste Receptor Expression in Resting and Activated Lymphocytes. *Front. Immunol.* **2018**, *9*, 2949.

(20) Grassin-Delyle, S.; Salvator, H.; Mantov, N.; Abrial, C.; Brollo, M.; Faisy, C.; Naline, E.; Couderc, L. J.; Devillier, P. Bitter Taste Receptors (TAS2Rs) in Human Lung Macrophages: Receptor Expression and Inhibitory Effects of TAS2R Agonists. *Front. Physiol.* **2019**, *10*, 1267.
(21) Behrens, M.; Somoza, V. Gastrointestinal Taste Receptors: Could Tastants Become Drugs? *Curr. Opin. Endocrinol., Diabetes Obes.* **2020**, *27* (2), 110−114.
(22) Brewer, D. B. The Fibroblast. *Proc. R. Soc. Med.* **1967**, *60*, 778−782.
(23) Komuro, T. Re-Evaluation of Fibroblasts and Fibroblast-like Cells. *Anat. Embryol.* **1990**, *182*, 103−112.
(24) Vaday, G. G.; Lider, O. Extracellular Matrix Moieties, Cytokines, and Enzymes: Dynamic Effects on Immune Cell Behavior and Inflammation. *J. Leukocyte Biol.* **2000**, *67* (2), 149−159.
(25) Josino Soares, D.; Walker, J.; Pignitter, M.; Walker, J. M.; Imboeck, J. M.; Ehrnhoefer-Ressler, M. M.; Montenegro Brasil, I.; Somoza, V. Pitanga (Eugenia Uniflora L.) Fruit Juice and Two Major Constituents Thereof Exhibit Anti-Inflammatory Properties in Human Gingival and Oral Gum Epithelial Cells. *Food Funct.* **2014**, *5* (11), 2981−2988.
(26) Walker, J.; Reichelt, K. V.; Obst, K.; Widder, S.; Hans, J.; Krammer, G. E.; Ley, J. P.; Somoza, V. Identification of an Anti-Inflammatory Potential of: Eriodictyon Angustifolium Compounds in Human Gingival Fibroblasts. *Food Funct.* **2016**, *7* (7), 3046−3055.
(27) Walker, J. M.; Maitra, A.; Walker, J.; Ehrnhoefer-Ressler, M. M.; Inui, T.; Somoza, V. Identification of Magnolia Officinalis L. Bark Extract as the Most Potent Anti-Inflammatory of Four Plant Extracts. *Am. J. Chin. Med.* **2013**, *41* (03), 531−544.
(28) Ehrnhöfer-Ressler, M. M.; Fricke, K.; Pignitter, M.; Walker, J. M.; Walker, J.; Rychlik, M.; Somoza, V. Identification of 1,8-Cineole, Borneol, Camphor, and Thujone as Anti-inflammatory Compounds in a *Salvia officinalis* L. Infusion Using Human Gingival Fibroblasts. *J. Agric. Food Chem.* **2013**, *61* (14), 3451−3459.
(29) FDI World Dental Federation. The Challenge of Oral Disease—A Call for Global Action. *The Oral Health Atlas*, 2nd ed.; FDI World Dental Federation: Geneva, Switzerland, 2015.
(30) Yang, N. Y.; Zhang, Q.; Li, J. L.; Yang, S. H.; Shi, Q. Progression of Periodontal Inflammation in Adolescents Is Associated with Increased Number of Porphyromonas Gingivalis, Prevotella Intermedia, Tannerella Forsythensis, and Fusobacterium Nucleatum. *Int. J. Paediatr. Dent.* **2014**, *24* (3), 226−233.
(31) García, J. M.; Prieto, L. J.; Guevara, A.; Malagon, D.; Osorio, C. Chemical Studies of Yellow Tamarillo (*Solanum betaceum* Cav.) Fruit Flavor by Using a Molecular Sensory Approach. *Molecules* **2016**, *21* (12), 1729.
(32) Koga, C. C.; Becraft, A. R.; Lee, Y.; Lee, S.-Y. Taste Detection Thresholds of Resveratrol. *J. Food Sci.* **2015**, *80* (9), S2064−S2070.
(33) Walker, J.; Schueller, K.; Schaefer, L. M.; Pignitter, M.; Esefelder, L.; Somoza, V. Resveratrol and Its Metabolites Inhibit Pro-Inflammatory Effects of Lipopolysaccharides in U-937 Macrophages in Plasma-Representative Concentrations. *Food Funct.* **2014**, *5* (1), 74−84.
(34) Soleas, G. J.; Diamandis, E. P.; Goldberg, D. M. Resveratrol: A Molecule Whose Time Has Come? And Gone? *Clin. Biochem.* **1997**, *30* (2), 91−113.
(35) Zdařilová, A.; Svobodová, A.; Šimánek, V.; Ulrichová, J. Prunella Vulgaris Extract and Rosmarinic Acid Suppress Lipopolysaccharide-Induced Alteration in Human Gingival Fibroblasts. *Toxicol. In Vitro* **2009**, *23* (3), 386−392.
(36) Rocha, J.; Eduardo-Figueira, M.; Barateiro, A.; Fernandes, A.; Brites, D.; Bronze, R.; Duarte, C. M.; Serra, A. T.; Pinto, R.; Freitas, M.; Fernandes, E.; Silva-Lima, B.; Mota-Filipe, H.; Sepodes, B. Anti-Inflammatory Effect of Rosmarinic Acid and an Extract of Rosmarinus Officinalis in Rat Models of Local and Systemic Inflammation. *Basic Clin. Pharmacol. Toxicol.* **2015**, *116* (5), 398−413.
(37) Zong, Y.; Sun, L.; Liu, B.; Deng, Y.-S.; Zhan, D.; Chen, Y.-L.; He, Y.; Liu, J.; Zhang, Z.-J.; Sun, J.; Lu, D. Resveratrol Inhibits LPS-Induced MAPKs Activation via Activation of the Phosphatidylinositol 3-Kinase Pathway in Murine RAW 264. 7 Macrophage Cells. *PLoS One* **2012**, *7* (8), e44107.
(38) Lossow, K.; Hübner, S.; Roudnitzky, N.; Slack, J. P.; Pollastro, F.; Behrens, M.; Meyerhof, W. Comprehensive Analysis of Mouse Bitter Taste Receptors Reveals Different Molecular Receptive Ranges for Orthologous Receptors in Mice and Humans. *J. Biol. Chem.* **2016**, *291* (29), 15358−15377.
(39) Roland, W. S. U.; Van Buren, L.; Gruppen, H.; Driesse, M.; Gouka, R. J.; Smit, G.; Vincken, J. P. Bitter Taste Receptor Activation by Flavonoids and Isoflavonoids: Modeled Structural Requirements for Activation of HTAS2R14 and HTAS2R39. *J. Agric. Food Chem.* **2013**, *61* (44), 10454−10466.
(40) de Sá Coutinho, D.; Pacheco, M.; Frozza, R.; Bernardi, A. Anti-Inflammatory Effects of Resveratrol: Mechanistic Insights. *Int. J. Mol. Sci.* **2018**, *19* (6), 1812.
(41) Leiro, J.; Arranz, J. A.; Fraiz, N.; Sanmartín, M. L.; Quezada, E.; Orallo, F. Effect of *Cis*-Resveratrol on Genes Involved in Nuclear Factor Kappa B Signaling. *Int. Immunopharmacol.* **2005**, *5* (2), 393−406.
(42) Ley, J. P.; Krammer, G.; Reinders, G.; Gatfield, I. L.; Bertram, H. J. Evaluation of Bitter Masking Flavanones from Herba Santa (*Eriodictyon californicum* (H. & A.) Torr., Hydrophyllaceae). *J. Agric. Food Chem.* **2005**, *53* (15), 6061−6066.
(43) Ley, J. P.; Dessoy, M.; Paetz, S.; Blings, M.; Hoffmann-Lücke, P.; Reichelt, K. V.; Krammer, G. E.; Pienkny, S.; Brandt, W.; Wessjohann, L. Identification of Enterodiol as a Masker for Caffeine Bitterness by Using a Pharmacophore Model Based on Structural Analogues of Homoeriodictyol. *J. Agric. Food Chem.* **2012**, *60* (25), 6303−6311.
(44) Liszt, K. I.; Hans, J.; Ley, J. P.; Köck, E.; Somoza, V. Characterization of Bitter Compounds via Modulation of Proton Secretion in Human Gastric Parietal Cells in Culture. *J. Agric. Food Chem.* **2018**, *66* (10), 2295−2300.
(45) ASTM International. *ASTM E-679-04, Standard Practice for Determining Odor and Taste Thresholds by a Forced-Choice Ascending Concentration Series Method of Limits*; ASTM International: West Conshohocken, PA, 2008.
(46) Busch-Stockfisch, M. *Praxishandbuch Sensorik in der Produktentwicklung und Qualitätssicherung (Practical Handbook of Sensory for Product Development and Quality Assurance)*; Behr's Verlag GmbH & Co. KG: Hamburg, Germany, 2015; pp 663.
(47) Weiss, C.; Rubach, M.; Lang, R.; Seebach, E.; Blumberg, S.; Frank, O.; Hofmann, T.; Somoza, V. Measurement of the Intracellular pH in Human Stomach Cells: A Novel Approach to Evaluate the Gastric Acid Secretory Potential of Coffee Beverages. *J. Agric. Food Chem.* **2010**, *58* (3), 1976−1985.
(48) Sack, M.; Hölz, K.; Holik, A. K.; Kretschy, N.; Somoza, V.; Stengele, K. P.; Somoza, M. M. Express Photolithographic DNA Microarray Synthesis with Optimized Chemistry and High-Efficiency Photolabile Groups. *J. Nanobiotechnol.* **2016**, *14* (1), 1−13.
(49) Rohm, B.; Holik, A. K.; Somoza, M. M.; Pignitter, M.; Zaunschirm, M.; Ley, J. P.; Krammer, G. E.; Somoza, V. Nonivamide, a Capsaicin Analog, Increases Dopamine and Serotonin Release in SH-SY5Y Cells via a TRPV1-Independent Pathway. *Mol. Nutr. Food Res.* **2013**, *57* (11), 2008−2018.
(50) Holik, A. K.; Rohm, B.; Somoza, M. M.; Somoza, V. Ne-Carboxymethyllysine (CML), a Maillard Reaction Product, Stimulates Serotonin Release and Activates the Receptor for Advanced Glycation End Products (RAGE) in SH-SY5Y Cells. *Food Funct.* **2013**, *4* (7), 1111−1120.
(51) Kretschy, N.; Holik, A.; Somoza, V.; Stengele, K.; Somoza, M. M. Next-Generation *o*-Nitrobenzyl Photolabile Groups for Light-Directed Chemistry and Microarray Synthesis. *Angew. Chem., Int. Ed.* **2015**, *54* (29), 8555−8559.
(52) Ouellet, M.; Adams, P. D.; Keasling, J. D.; Mukhopadhyay, A. A Rapid and Inexpensive Labeling Method for Microarray Gene Expression Analysis. *BMC Biotechnol.* **2009**, *9*, 97.
(53) Morandini, A. C. F.; Chaves Souza, P. P.; Ramos-Junior, E. S.; Brozoski, D. T.; Sipert, C. R.; Souza Costa, C. A.; Santos, C. F. Toll-

https://dx.doi.org/10.1021/acs.jafc.0c07058
J. Agric. Food Chem. 2021, 69, 13339−13349

Like Receptor 2 Knockdown (SDF-1/CXCL12) in Human Periodontal but Not Stromal Derived Factor-1 Modulates Interleukin (IL)-6 and IL-8 Ligament and Gingival Fibroblasts. *J. Periodontol.* **2013**, *84* (4), 535−544.
(54) Dagan-Wiener, A.; Di Pizio, A.; Nissim, I.; Bahia, M. S.; Dubovski, N.; Margulis, E.; Niv, M. Y. Bitterdb: Taste Ligands and Receptors Database in 2019. *Nucleic Acids Res.* **2019**, *47* (D1), D1179−D1185.
(55) Sherman, W.; Day, T.; Jacobson, M. P.; Friesner, R. A.; Farid, R. Novel Procedure for Modeling Ligand/Receptor Induced Fit Effects. *J. Med. Chem.* **2006**, *49* (2), 534−553.
(56) Di Pizio, A.; Niv, M. Y. Promiscuity and Selectivity of Bitter Molecules and Their Receptors. *Bioorg. Med. Chem.* **2015**, *23* (14), 4082−4091.
(57) Bruford, E. A.; Braschi, B.; Denny, P.; Jones, T. E. M.; Seal, R. L.; Tweedie, S. Guidelines for Human Gene Nomenclature. *Nat. Genet.* **2020**, *52*, 754−758.
(58) Reed, D. R.; Zhu, G.; Breslin, P. A. S.; Duke, F. F.; Henders, A. K.; Campbell, M. J.; Montgomery, G. W.; Medland, S. E.; Martin, N. G.; Wright, M. J. The Perception of Quinine Taste Intensity Is Associated with Common Genetic Variants in a Bitter Receptor Cluster on Chromosome 12. *Hum. Mol. Genet.* **2010**, *19* (21), 4278−4285.
(59) Hayes, J. E.; Wallace, M. R.; Knopik, V. S.; Herbstman, D. M.; Bartoshuk, L. M.; Duffy, V. B. Allelic Variation in TAS2R Bitter Receptor Genes Associates with Variation in Sensations from and Ingestive Behaviors toward Common Bitter Beverages in Adults. *Chem. Senses* **2011**, *36* (3), 311−319.
(60) Behrens, M.; Gunn, H. C.; Ramos, P. C. M.; Meyerhof, W.; Wooding, S. P. Genetic, Functional, and Phenotypic Diversity in TAS2R38-Mediated Bitter Taste Perception. *Chem. Senses* **2013**, *38* (6), 475−484.
(61) Woo, P.; Humphries, S. E. IL-6 Polymorphisms: A Useful Genetic Tool for Inflammation Research? *J. Clin. Invest.* **2013**, *123* (4), 1413−1414.
(62) Sundararaj, K. P.; Samuvel, D. J.; Li, Y.; Sanders, J. J.; Lopes-Virella, M. F.; Huang, Y. Interleukin-6 Released from Fibroblasts Is Essential for up-Regulation of Matrix Metalloproteinase-1 Expression by U937 Macrophages in Coculture: Cross-Talking between Fibroblasts and U937 Macrophages Exposed to High Glucose. *J. Biol. Chem.* **2009**, *284* (20), 13714−13724.
(63) Scheller, J.; Chalaris, A.; Schmidt-Arras, D.; Rose-John, S. The Pro- and Anti-Inflammatory Properties of the Cytokine Interleukin-6. *Biochim. Biophys. Acta, Mol. Cell Res.* **2011**, *1813* (5), 878−888.
(64) Tanaka, T.; Narazaki, M.; Kishimoto, T. IL-6 in Inflammation, Immunity, and Disease. *Cold Spring Harbor Perspect. Biol.* **2014**, *6* (10), a016295−a016295.

https://dx.doi.org/10.1021/acs.jafc.0c07058
J. Agric. Food Chem. 2021, 69, 13339−13349

Supplemental material to

Bitter sensing *TAS2R50* mediates the trans-resveratrol induced anti-inflammatory effect on IL-6 release in HGF-1 cells in culture

Johanna Tiroch[1], Sonja Sterneder[1], Antonella Di Pizio[2], Barbara Lieder[1], Kathrin Hoelz[3], Ann-Katrin Holik[1], Marc Pignitter[1], Maik Behrens[2], Mark Somoza[2,3,4], Jakob P. Ley[5], Veronika Somoza[1,2,6]

[1] Department of Physiological Chemistry, Faculty of Chemistry, University of Vienna, Vienna, Austria.
[2] Leibniz Institute of Food Systems Biology at the Technical University of Munich, Freising, Germany.
[3] Department of Inorganic Chemistry, Faculty of Chemistry, University of Vienna, Vienna, Austria.
[4] Chair of Food Chemistry and Molecular Sensory Science, Technical University Munich, Freising, Germany.
[5] Symrise AG, Holzminden, Germany
[6] Chair for Nutritional Systems Biology, Technical University Munich, Freising, Germany.

Supplemental Material

Table S1. HGT-1 and HGF-1 cells were administered with the test compounds (RA – rosmarinic acid, RSV – trans-resveratrol, HED – homoeriodictyol) in concentrations of 100 µM. HGF-1 cells were treated in combination with 10 µg/mL Pg-LPS for 6 h, whereas incubation time of HGT-1 cells with the test compounds solely was 1 h. Data are based on three biological replicates with 3-4 technical replicates, calculated as treatment over control (Ctrl: medium only-treated cells, set to 100 %), and indicated as mean ± SEM. Statistics: One-way ANOVA with post-hoc Holm-Sidak test, vs. control.

[%]	Ctrl	RA	RSV	RA + HED	RSV + HED	p-value
HGT-1						
wt	100 ± 1.7	101 ± 1.5	105 ± 1.6	n.a.	97 ± 1.7	p > 0.05
TAS2R43 ko	100 ± 1.6	103 ± 2.3	96 ± 2.0	n.a.	105 ± 2.6	p > 0.05
HGF-1						
wt	100 ± 2.1	102 ± 1.9	105 ± 2.3	105 ± 1.8	100 ± 2.7	p > 0.05
TAS2R50 kd	102 ± 2.3	n.a.	99 ± 2.8	n.a.	103 ± 4.5	p > 0.05

Figure captions

Figure S1. IL-6 release of HGF-1 cells treated with trans-resveratrol (RSV) one-hour pre-incubation and six-hour incubation with *Pg*–LPS w/o homoeriodictyol (HED) (1-10µM). Data are calculated as treatment over control in percent, with the effect of *Pg*-LPS set to zero (T/LPS, %; LPS=0 %). Data are shown as mean ± SEM n=3 t.r.=2. Statistics: One-Way ANOVA on Ranks ($p > 0.05$).

Figure S2. Gene expression of *MAPK1* in HGF-1 cells, which were transfected with the transfection reagent (Mock), combined either with positive control Hs/Mm_MAPK1 siRNA (PC), or all-stars negative control siRNA (NC) for 48 h. The transfection efficiencies were analyzed by means of qRT-PCR. Data are calculated as treatment over non-treated cells (C) (T/C, %; C =100 %) ± SEM, n = 4; t.r.=2-3. PC showed a 59 % reduction compared to C. Statistics: one-way ANOVA on Ranks with post-hoc Dunn's method; significant differences are shown with letters; $p \leq 0.05$.

Figure S3. Molecular interaction analysis of *Pg*-LPS with homoeriodictyol (HED) and trans-resveratrol (RSV) by means of LC-MS/MS. In a cell-free approach, RSV and HED were incubated with *Pg*-LPS dissolved in cell culture in medium with FBS and analyzed for respective peak areas measured after t_0 and 6 hours. Results are shown as means of AUC. Data are calculated as treatment over control whereby *control* refers to the AUC of HED or RSV at $t_{0\ hours}$, and treatment to the AUC of of HED or RSV at $t_{6\ hours}$ of incubation (T/C, %; C = 100 % and indicated as dashed line) ± SEM, n = 3; t.r.=2. Statistics: one-way ANOVA HED/RSV t_0 compared to HED/RSV and HED/RSV + *Pg*-LPS after 6 h; $p > 0.05$.

Figure S1.

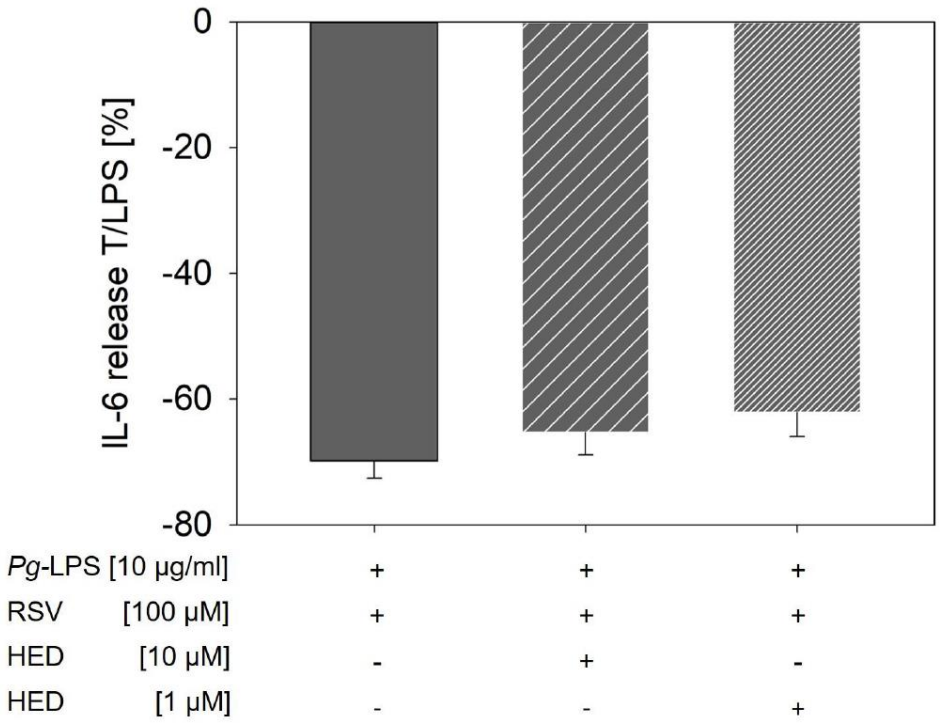
0
-20
-40
-60
-80
IL-6 release T/LPS [%]
Pg-LPS [10 µg/ml] + + +
RSV [100 µM] + + +
HED [10 µM] - + -
HED [1 µM] - - +

Figure S2.

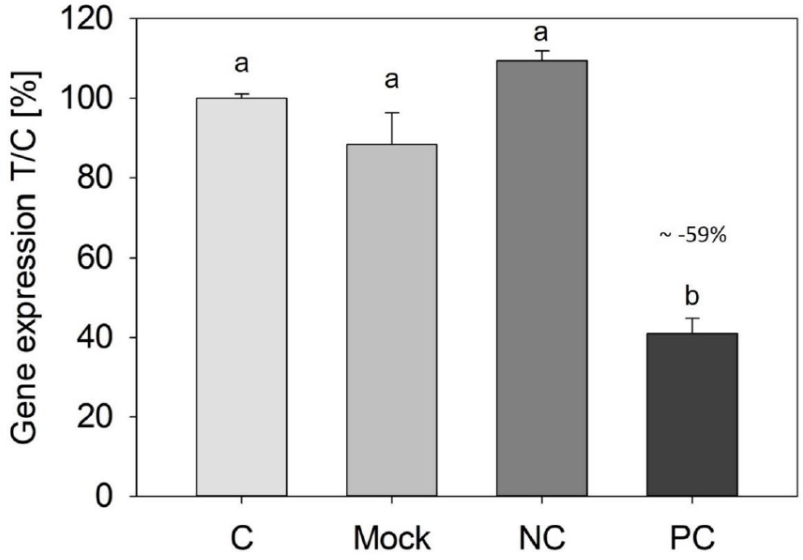

5

Figure S3.

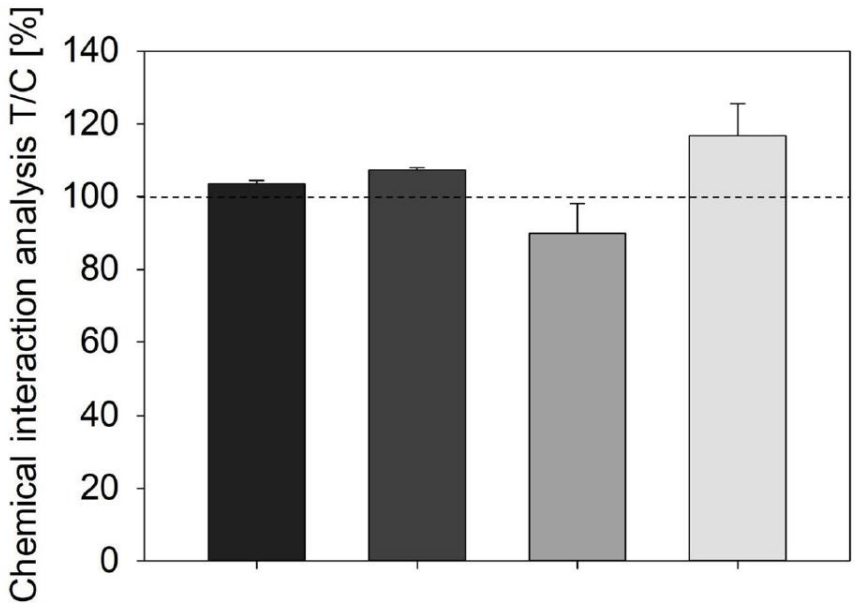
Chemical interaction analysis T/C [%]
140
120
100
80
60
40
20
0
Pg-LPS [10 µg/ml] + +
HED [100 µM] + +
RSV [100 µM] + +

6

5.2 "Human Gingival Fibroblasts as a Novel Cell Model Describing the Association between Bitter Taste Thresholds and Interleukin-6 Release"

Johanna Tiroch[1,2], Andreas Dunkel[3], Antonella Di Pizio[3], Jakob P. Ley[4], Barbara Lieder[1], Veronika Somoza[1,3,5]

[1] Department of Physiological Chemistry, Faculty of Chemistry, University of Vienna, Vienna, Austria.
[2] Vienna Doctoral School in Chemistry (DoSChem), University of Vienna, Austria.
[3] Leibniz Institute for Food Systems Biology at the Technical University of Munich, Freising, Germany.
[4] Symrise AG, Holzminden, Germany
[5] Chair for Nutritional Systems Biology, Technical University Munich, Freising, Germany.

Published in *Journal of Agricultural and Food Chemistry* ***2023*** *71 (13), 5314-5325*
DOI: 10.1021/acs.jafc.2c06979

This study investigated whether HGF-1 can give rise to a suitable cell model for the identification of bitter tasting substances. The first step was to investigate whether the association between IL-6 release and TAS2R50 in HGF-1 cells was selective to resveratrol. For this purpose, four different substances (epigallocatechin gallate, quinine HCl, naringin and sinensetin) were selected from the chemical bitter space to test their anti-inflammatory activity in *Pg*-LPS treated HGF-1 cells measured via IL-6 release reduction compared to their potential binding in TAS2R50 via molecular binding studies. Further, co-incubation experiments using bitter tasting compounds and the bitter masking compounds homoeriodictyol and matairesinol were performed to evaluate the possible involvement of other TAS2Rs beside TAS2R50. Moreover, additional compounds from the chemical space were selected to test their anti-inflammatory activity in the *Pg*-LPS evoked IL-6 release by HGF-1 cells. Together with literature-based bitter taste threshold data for the tested compounds, results were subjected to a correlation analysis in order to test the model's suitability to identify potentially bitter tasting compounds.

The computational pathway analysis of the link between TAS2R50 and IL-6 release was led by Andreas Dunkel. I supported this analysis via literature research. I planned, developed, and analysed the verification of these results *in vitro* via immunofluorescence staining of HGF-1 cells for GNAI3. Furthermore, I studied the role of TAS2R50 for the potential binding of four different substances (epigallocatechin gallate, quinine HCl, naringin and sinensetin) from the chemical

bitter space via molecular binding under the supervision of Antonella di Pizio. I also carried out the IL-6 ELISA experiments of which the results were normalized and statistically analysed by Andreas Dunkel. Analysis of the intracellular proton index of human gastric parietal tumor cells (HGT-1 cells) were conducted by Sonja Sterneder and Sofie Zehentner. Furthermore, I prepared the draft of the manuscript.

JOURNAL OF AGRICULTURAL AND FOOD CHEMISTRY

pubs.acs.org/JAFC

Article

Human Gingival Fibroblasts as a Novel Cell Model Describing the Association between Bitter Taste Thresholds and Interleukin-6 Release

Johanna Tiroch, Andreas Dunkel, Sonja Sterneder, Sofie Zehentner, Maik Behrens, Antonella Di Pizio, Jakob P. Ley, Barbara Lieder, and Veronika Somoza*

Cite This: *J. Agric. Food Chem.* 2023, 71, 5314−5325

Read Online

ACCESS | Metrics & More | Article Recommendations | Supporting Information

ABSTRACT: Human gingival fibroblast cells (HGF-1 cells) present an important cell model to investigate the gingiva's response to inflammatory stimuli such as lipopolysaccharides from *Porphyromonas gingivalis* (*Pg*-LPS). Recently, we demonstrated *trans*-resveratrol to repress the *Pg*-LPS evoked release of the pro-inflammatory cytokine interleukin−6 (IL-6) via involvement of bitter taste sensing receptor TAS2R50 in HGF-1 cells. Since HGF-1 cells express most of the known 25 TAS2Rs, we hypothesized an association between a compound's bitter taste threshold and its repressing effect on the *Pg*-LPS evoked IL-6 release by HGF-1 cells. To verify our hypothesis, 11 compounds were selected from the chemical bitter space and subjected to the HGF-1 cell assay, spanning a concentration range between 0.1 μM and 50 mM. In the first set of experiments, the specific role of TAS2R50 was excluded by results from structurally diverse TAS2R agonists and antagonists and by means of a molecular docking approach. In the second set of experiments, the HGF-1 cell response was used to establish a linear association between a compound's effective concentration to repress the *Pg*-LPS evoked IL-6 release by 25% and its bitter taste threshold concentration published in the literature. The Pearson correlation coefficient revealed for this linear association was $R^2 = 0.60$ ($p < 0.01$), exceeding respective data for the test compounds from a well-established native cell model, the HGT-1 cells, with $R^2 = 0.153$ ($p = 0.263$). In conclusion, we provide a predictive model for bitter tasting compounds with a potential to act as anti-inflammatory substances.

KEYWORDS: *human gingival cells (HGF-1), bitter taste threshold, bitter taste receptors, bitter taste modulators, interleukin-6*

INTRODUCTION

Fibroblasts are located in connective tissues and represent an important key player in the inflammatory responses to external stimuli.[1] They are involved in processes of tissue repair via the extra cellular matrix as well as regulating processes during acute and adaptive immunity.[2−4] Human gingival fibroblasts of the HGF-1 cell line are well established for the identification of anti-inflammatory plant components by reducing the release of the pro-inflammatory proteins tumor necrosis factor α (TNF-α), interleukin-8 (IL-8), and interleukin-6 (IL-6)[5−9] after exposure to lipopolysaccharides (LPS).[6] Expression of human bitter taste receptors (TAS2Rs) and their involvement in inflammatory processes in HGF-1 cells has been demonstrated by the following two very recent studies: Zhou et al. demonstrated HGF-1 cells (i) to express TAS2Rs and downstream signaling proteins, and (ii) the activation of TAS2R16 signaling by salicin to inhibit the release of LPS-induced pro-inflammatory cytokine IL-8 by repressing LPS-induced intracellular cAMP elevation and NF-κB p65 nuclear translocation.[10] In one of our own previous studies, TAS2R50 showed an involvement in the *trans*-resveratrol-mediated IL-6 response of HGF-1 cells to a 6 h treatment with LPS isolated from the Gram-negative bacterium *Porphyromonas gingivalis* (*Pg*-LPS).[9] In the study presented here, we aimed at elucidating whether the impact on the *Pg*-LPS-induced IL-6 release by HGF-1 cells is associated with the bitter taste threshold of taste active food compounds.

The perception of bitter taste is initiated by agonist−receptor interactions of orally ingested compounds and TAS2Rs, which are expressed in taste buds of the oral cavity.[11,12] In humans, the 25 TAS2Rs are G protein-coupled receptors (GPCRs).[13] Analytical methods for the identification of bitter tasting compounds targeting TAS2Rs traditionally comprise sensory procedures,[14] for which safety data and amounts in the milligram range are required. Sensory studies are limited by the sensory fatigue of panelists, with a relatively low number of compounds that can be tested per day, which makes sensory testing a relatively slow and low throughput method. Sensory methods targeted to identify compounds with a lower recognition threshold might not capture bitter tasting compounds with high threshold concentrations. Therefore, the entire chemical space of bitter tasting compounds might not have been deciphered yet. This presents a major limitation not only for the understanding but also for modulation of bitter tastes of foods and food formulations.

Received: October 8, 2022
Revised: February 19, 2023
Accepted: February 21, 2023
Published: March 21, 2023

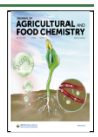

https://doi.org/10.1021/acs.jafc.2c06979
J. Agric. Food Chem. 2023, 71, 5314−5325

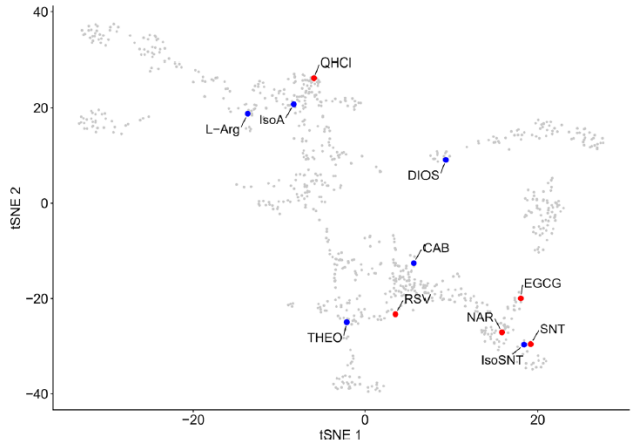

Figure 1. Selected substances (red, first selection; blue, second selection) and their mapped localization in the 2D t-SNE plot of the bitter chemical space[32] (gray).

The discovery of TAS2Rs has initiated various *in silico* and *in vitro* approaches for the identification of bitter tasting compounds. *In silico* strategies build on structural similarities between in vitro and sensory-evaluated bitter tastants and their TAS2R molecular interaction properties, as already compiled in several databases, e.g., BitterDB[15] or FSBI-DB.[16] One of the most recent works by Bayer et al.[17] presented a systematic chemoinformatic analysis of the patterns of identified TAS2R agonists,[18,19] providing a detailed characterization of associations between the chemical properties of bitter tastants in foods and TAS2Rs and a framework for chemoinformatic work on the growing number of food bitter compounds.

Although *in silico* approaches benefit from independence from human sensory panelists and the associated requirement for quantities of safe-to-consume bitter tastants, sensory validation of novel, potentially bitter tasting compounds identified is still required. One of the main reasons for the divergence between *in silico* results and sensory perception is that chemoinformatic strategies mostly integrate data from multiple agonists targeting a given TAS2R, whereas the gustatory perception of bitterness is generated by either activation of individual specific TAS2Rs, e.g., TAS2R7,[20,21] TAS2R16,[22,23] TAS2R38,[24,25] or the complex interplay of the ∼25 TAS2Rs expressed in the human oral cavity.[12]

The implementation of cell-based *in vitro* screenings provides another strategy for the identification of novel tastants and taste modifiers.[26] Compared to sensory studies, cell-based assays can be performed at high throughput, irrespective of the toxicological safety of compounds, and can help to replace time-consuming human sensory profiling.

With further progress and insights into the taste signaling pathway of mammalian cells, native cell-based assays founded on immortal human cell lines, which endogenously express taste receptor genes from nontaste tissue, have been established. These cell-based assays represent the native transduction signaling pathways and enable the identification of agonists being active on a multi-receptor level, as well as on the native cell context, which may offer an association between the sensory perception and the cellular response to agonist−receptor activation.

For screening approaches, one of the native cell systems established for the identification of bitter tasting and bitter taste modulating compounds is based on the proton secretion by human parietal cells of the HGT-1 cell line, which is linked to the agonist-forced activation of TAS2Rs.[27−29] Since one of our recent studies demonstrated that TAS2R50 mediates an anti-inflammatory effect on IL-6 release in human gingival fibroblasts of the HGF-1 cell line induced by the bitter tasting *trans*-resveratrol (RSV),[9] we hypothesized an association of the bitter taste threshold of food constituents and their impact on the *Pg*-LPS-induced IL-6 release by HGF-1 cells. To test this hypothesis, we present a chemoinformatic approach for agonist selection combined with a native cell-based screening. In a first set of experiments, we tested whether repression of the *Pg*-LPS-induced IL-6 release by HGF-1 cells by bitter tasting compounds is specific for compounds targeting TAS2R50. Prior to these experiments, the HGF-1 cells studied were verified for the protein expression of guanine nucleotide-binding protein G(i) subunit alpha-3 (GNAI3) as an important protein for tissue and dentin regeneration in stem cells from the apical papilla (SCAPs)[30] as well as one subunit of the TAS2R signaling proteins.[31]

Based on our previous study, demonstrating RSV as an effective compound,[9] four structurally similar (sinensetin, SNT; epigallocatechin gallate, EGCG; naringin, NAR), and one structurally diverging (quinine, QHCl) TAS2R agonist were selected from the chemical bitter space (Figure 1, red circles)[32] to cover a wider range of TAS2Rs targeted. Next to the impact of these compounds on the *Pg*-LPS-induced IL-6 release in HGF-1 cells, their TAS2R50 binding potential was studied by means of molecular docking simulations. Since these results revealed no specific TAS2R50 involvement, which is in agreement with previous screening results,[18,33] the HGF-1 cell assay was conducted in an experimental setting of co-incubations, applying the abovementioned TAS2R agonists and the antagonists homoeriodictyol (HED,[34] targeting TAS2R20/31/43/50[27]) and matairesinol (MAT, demonstrated in this publication to target TAS2R4/43). As these results verified involvement of a wide range of TAS2Rs, we hypothesized the repression of LPS-induced IL-6 release in HGF-1 cells to be associated with the

https://doi.org/10.1021/acs.jafc.2c06979
J. Agric. Food Chem. 2023, 71, 5314−5325

Table 1. Structures, Names, Abbreviations, and Tested Concentration Range of the Selected Substances from the Bitter Chemical Space[32a]

Structure	Common Name	Taste threshold [μM]	HGF-1 Concentration tested [μM]; ED25 [μM]	HGT-1 Concentration tested [μM]; IPX[1] [%]
First set of experiments				
	Quinine HCl (QHCl)	8.3[45]	0.1 – 40; 23.2	10; 85.2
	Sinensetin (SNT)	56[39]	0.1 – 50; 53.1	50; 84.8
	trans-Resveratrol (RSV)	98[9]	0.1 – 250; 39.9	100; -62.4 [9]
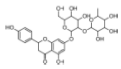	Naringin (NAR)	109[44]	0.1 – 500; 486	100; 3.22
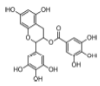	Epigallocatechin gallate (EGCG)	190[43]	0.1 – 100; 9.49	250; 0.35
Second set of experiments				
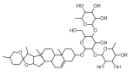	Dioscin (DIOS)	n.a.	0.01 – 1; 5.47	0.05; 11.10
	Carpinontriol B (CAB)	13[35]	0.1 – 500; 228.86	10; 13.55
	Iso-alpha acids from hops (IsoA)	21[38]	0.99 – 98.6; 8.20	96.7; -183 *
	Isosinensetin (IsoSNT)	32[39]	0.1 – 25; 4.83	25; 82.0
	Theobromine (THEO)	800[40]	0.1 – 250; 32422	300; 125
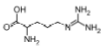	L-arginine (L-Arg)	75 000[40]	0.5 – 50000; 72026	50 000; 124

[a]Additionally, the effective dose [μM] of bitter compound needed to reach a 25% inhibition of the 10 μg/mL *Pg*-LPS-induced IL-6 release by HGF-1 cells as well as IPX [%] values[1] normalized to plate-dependent histamine effect of HGT-1 cells and the tested concentration of the respective substances in μM are given.

bitter taste quality of a food constituent, namely, its bitter taste threshold for which literature data are available. This hypothesis was tested in a second set of experiments, which included additional substances with higher structural diversity from the chemical bitter space (Figure 1, blue circles)[32] to be compared with the effect of RSV in the HGF-1 cell system: carpinontriol B (CAB),[35] dioscin (DIOS),[36,37] iso-alpha acids (IsoA),[38] isosinensetin (IsoSNT),[39] L-arginine (L-Arg),[40] and theobromine (THEO).[40] Following a model-based normalization to account for passage and plate variations, a dose−response analysis of the individual bitter taste compounds yielded the effective 25% inhibition dose concentrations (ED25) that reduced the *Pg*-LPS-evoked IL-6 release by HGF-1 cells. Finally, a linear model of the ED25 values and the bitter taste thresholds from the literature was established and compared with results obtained from the already implemented bitter response assay based on HGT-1 cells.[27−29]

MATERIALS AND METHODS

Chemicals. Lipopolysaccharides of *Porphyromonas gingivalis* (*Pg*-LPS) were acquired from InvivoGen. Triton X-100 solution was obtained from Carl Roth GmbH and the SuberBlock buffer from ThermoFisher. The IL-6 sandwich enzyme-linked immunosorbent assay (ELISA, ab178013) was bought from abcam. Sinensetin (SNT, 99.67% purity) and isosinenstin (IsoSNT, 99.26% purity) were purchased from MedChemExress. Quinine HCl (QHCl, 97% purity) was obtained from Combi-Blocks, and *trans*-resveratrol (RSV, 98% purity) was obtained from Breko GmbH. Epigallocatechin gallate (EGCG, 95% purity) as well theobromine (THEO, 98% purity) were purchased from Sigma Aldrich (Merck KGaA, Darmstadt, Germany). Bitter tasting compounds showing diverse and/or similar chemical properties from/to RSV were selected from the chemical space[32] (Figure 1). The sodium salt of homoeriodictyol (3′-methoxy-4′,5,7-trihydroxyflavanone) (HED, 94% purity), carpinontriol B (CAB, 94.2% purity) and (−)-matairesinol (MAT, 95% purity) were kindly provided by Symrise AG, synthesized, and chemically characterized as described previously.[34] The mixture of *trans-iso*-alpha acids was purified from a commercially available *iso*-alpha-acid extract (*iso*-extract 30%, Hopsteiner, Mainburg, Germany) following a protocol from the literature.[41] Analysis of the isolated mixture by quantitative ^{1}H NMR spectroscopy[42] confirmed a purity of >95%, whereas targeted HPLC−MS/MS analysis verified the expected distribution across the 3 main *trans-iso*-alpha acids (*trans*-isocohumulone 30%, *trans*-isohumulone 40%, *trans*-isoadhumulone 30%).

All other chemicals were obtained from Sigma Aldrich (Merck KGaA, Darmstadt, Germany), unless indicated otherwise.

Cell Culture. Human gingival fibroblasts (HGF-1; passage number 16) obtained from the American Type Culture Collection (ATCC 2014), human gastric tumor (HGT-1) attained from C. Laboisse (Laboratory of Pathological Anatomy, Nantes, Frances), and HEK 293 T-Gα16gust44 from ATCC were cultivated in Dulbecco's modified Eagle's medium (DMEM) high glucose (4.5 g/L D-glucose), GlutaMAX (ThermoFisher) supplemented with 10% fetal bovine serum (FBS) (Invitrogen, Vienna, Austria), 100 U mL^{-1} penicillin, and 0.1 mg mL^{-1} streptomycin at standard conditions (37 °C, 5% CO_2, and humidified atmosphere).[9]

For cell culture studies, compounds insoluble in water were predissolved in dimethyl sulfoxide (DMSO), resulting in a final test concentration of 0.1% (v/v). Appropriate controls of cell culture medium treated cells only always contained 0.1% (v/v) DMSO. For

https://doi.org/10.1021/acs.jafc.2c06979
J. Agric. Food Chem. 2023, 71, 5314−5325

inducing a pro-inflammatory IL-6 release, HGF-1 cells were treated with *Pg*-LPS in a final concentration of 10 μg/mL for 6 h.[7−9]

Cell viability for all treatments was proven by the MTT (3-(4,5-dimethyl thiazolyl-2)-2,5-diphenyltetrazolium bromide) assay as described previously for HGF-1 and HGT-1 cells.[9]

Immunofluorescence Staining of GNAI3 in HGF-1 Cells. Immunofluorescence analysis of GNAI3 was performed using 70% confluent HGF-1 cells on a cover slip. The cells were washed with PBS and fixed with 3% (v/v) formaldehyde in phosphate-buffered saline (PBS) for 20 min. Next, the fixation solution was removed, and the cells were washed with PBS. Afterward, a 30 min permeabilization step of the HGF-1 cells was carried out with 1% (v/v) Triton X-100 in SuberBlock buffer and washed with PBS again. Cells were blocked with 5% (v/v) Donkey serum and 0.5% (v/v) Triton X-100 in SuberBlock buffer for 1 h. Afterward, cells were labeled with the primary antibody, GNAI3 polyclonal antibody (# PA5-27940, InvivoGen) 1:200 (v/v), in SuberBlock buffer with 5% (v/v) Donkey serum and 0.2% (v/v) Triton X-100 overnight at +4 °C. Cells were then washed and labeled with the second antibody 1:200 (v/v) goat anti-rabbit IgG H&L (Alexa Fluor 488, Thermo Fisher Scientific) preadsorbed (ab150081, abcam) for 2 h. The cells were than washed and incubated with ActinRed 555 ReadyProbes Reagent (rhodamine phalloidin) (Invitrogen), which has a high affinity to the F-actin, following the manufacturer's protocol. Next, the cells were washed, and the nucleus was stained with NucBlue Fixed Cell ReadyProbes Reagent (DAPI) (Invitrogen) following the manufacturer's protocol. Finally, cells were washed, embedded with anti-fade fluorescence mounting medium, Aqueous, Fluoroshield (ab104135, abcam), and analyzed by confocal laser-scanning microscopy (LSM 800 KMAT, Zeiss). As control, cells without any staining with only primary antibody and only secondary antibody labeling were analyzed.

Selection of Test Compounds from the Bitter Chemical Space. For a first set of experiments (Figure 1, red circles), EGCG,[43] NAR,[44] and SNT[39] (Table 1) were selected in order to test whether these compounds, showing a structural similarity to RSV, yet targeting a wider range of TAS2Rs as compared to RSV, demonstrate a similar or different effect on the *Pg*-LPS-induced IL-6 release in HGT-1 cells compared RSV and to QHCl[45] (Table 1) as a structurally more divergent compound.

Involvement of a wider range of TAS2Rs was additionally tested by using the well-known bitter masking compounds HED[29,34] and MAT,[29] targeting TAS2R20/31/43/50 [9, 27] and TAS2R4 and 43, respectively. In a second set of experiments, we investigated a diverse subset of compounds spanning over a larger area of the chemical space[32] that target a wider range of TAS2Rs: CAB,[35] DIOS,[36,37] Iso-alphaA,[38] IsoSNT,[39] L-Arg [40]and THEO[40] (Figure 1, blue circles, Table 1).

At least six concentrations per compound with two technical and three to seven biological replicates were tested in the cell assays, covering literature taste threshold concentrations from sensory studies (Table 1).

Quantitation of IL-6 Release by HGF-1 Cells by Means of Enzyme-Linked Immunosorbent Assay (ELISA). HGF-1 cells were seeded in 96 well plates at a density of 5000 cells per well 72 h before the experiment. Prior to addition of 10 μg/mL *Pg*-LPS, the cells were pretreated for 1 h with the selected bitter substance from the chemical space (Figure 1, red circles), EGCG (100 μM), NAR (500 μM), QHCl (40 μM), and SNT (50 μM) with or without HED or MAT in a concentration ratio of 10:1.[18,20] After exposure, the cells' supernatants were harvested for the ELISA analysis after an incubation time of 6 h. In a second set of experiments, CAB, DIOS, EGCG, IsoA, IsoSNT, L-Arg, NAR, QHCl, RSV, SNT, and THEO (Figure 1, blue circles) in concentration ranges that covered their individual bitter taste threshold concentration (Table 1) were tested as described above. The supernatant was then applied to a sandwich enzyme-linked immunosorbent assay (ELISA, ab178013) to quantitate the IL-6 release of HGF-1 cells (abcam, minimal detectable dose (MDD): 1.6 pg/mL, intra-assay reproducibility CV 2.1%, inter-assay reproducibility CV 2.4%), following the manufacturer's protocol. The optical density (OD) at 450 nm was measured by a Tecan Infinite M200 PRO plate reader (Tecan, Switzerland).

Molecular Docking. Molecular docking simulations were run to deduce the potential binding pose of SNT, EGCG, QHCl, and NAR, into the 3D structure of TAS2R50, as modeled previously.[9] The ligands were prepared for the docking with the generation of stereoisomers and protonation states at pH 7 ± 0.5 with LigPrep, as implemented in the Schrödinger Small-Molecule Drug Discovery Suite Schrödinger Release 2021-4 (Schrödinger, LLC, New York, NY, 2021). Molecular descriptors AlogP, hydrogen bond acceptors (HBAs), and hydrogen bond donors (HBDs) were calculated with Schrödinger Release 2021-4 (Schrödinger). Because of the different molecular size of the investigated compounds and the uncertainness of the modeling of the extracellular loop 2 and 3 (ECL2 and 3), we cut the model from residue $Asp150^{ECL2}$ to $Arg169^{5.32}$ and from $Trp250^{6.60}$ to $Pro259^{7.33}$, respectively. Glide Standard Precision was used for docking simulations. The coordinates of $Trp88^{3.32}$ were used as centroid during the Receptor Grid Generation (Schrödinger Release 2021-4: Glide, Schrödinger). Three rotatable groups ($Ser248^{6.58}$, $Tyr85^{3.29}$ and $Tyr176^{5.39}$) were allowed to move. Docking poses underwent molecular mechanics generalized Born surface area (MM-GBSA) calculations (Schrödinger Release 2021-4: Prime, Schrödinger) (sampling method, minimize).

Analysis of ED25 Values and Establishment of a Linear Model. Normalization of uncorrected ELISA absorbance data was performed by a model-based approach using the plate and passage specific effect of the addition of a fixed concentration of RSV 100 μM to *Pg*-LPS treated cells. For each combination of passage and plate, individual linear models describing the absorbance signal reduction between *Pg*-LPS treated HGF-1 cells and similar cells treated in addition with RSV (100 μM, $n_{\text{technical replicates}} = 2$, and $n_{\text{biological replicates}} = 3-6$) were trained. Correction factors for each plate and passage were obtained from the model parameters in contrast to the global model incorporating the complete data and subsequently applied to the raw data.

Dose−response analysis of individual bitter agonists were carried out using the normalized data and extension package drc (version 3.0−1) for the statistical programming environment R and the built-in four-parameter log-logistic model functions. Dose−response models were estimated for the tested concentration ranges based on the obtained function parameters, visualized using the ggplot2 R package (version 3.3.6) and followed by revealing 25% effective inhibitory concentrations to correlate with the compounds' bitter taste threshold concentrations.

Quantitation of the Intracellular Proton Index (IPX) in HGT-1 Cells. HGT-1 cells were seeded in a density of 100,000 cells per well in 96 well plates 24 h prior to the measurement. Following cell viability analyses carried out in transparent 96 well plates, proton secretion assays for determining the intracellular proton index (IPX) were performed in black 96-well plates.

Using HGT-1 cells, the intracellular pH (pH_i) was determined by means of the pH sensitive fluorescence dye SNARF-1AM for the investigation of the proton secretion, as described before.[27,46] Briefly, HGT-1 cells were cultivated and seeded 24 h before the experiment. Cells were washed with 100 μL Krebs-Ringer-HEPES buffer (KRHB; 10 mM 4-(2-hydroxyethyl)-1-piperazineethane-sulfonic acid (HEPES), 11.7 mM D-glucose, 4.7 mM KCl, 130 mM NaCl, 1.3 mM $CaCl_2$, 1.2 mM $MgSO_4$, and 1.2 mM KH_2PO_4, adjusted to a pH of 7.4 with 5 M KOH) per well, and stained with 3 μM 1,5-carboxy-seminaphtorhodafluor acetoxymethyl ester (SNARF-1 AM) for 35 min at standard conditions. After the staining, the HGT-1 cells were washed twice with 100 μL of KRHB per well, and 100 μL of the investigated compound and the positive control histamine (1 mM) were added to the cells and incubated for at least 10 min. For substances, which are interfering with the fluorescence signal because of their own color, an additional washing step was performed after the incubation with the substance. Fluorescence was measured at 580 and 640 nm emission after excitation at 488 nm using a Flexstation 3 (Molecular Devices, Sunnyvale, CA, USA). The IPX was determined by using a pH-calibration curve (pH 7.0−8.0), calculating the intracellular H^+ concentration, followed by the calculation of a ratio between the treated and untreated cells. Data calculation was performed with a log2

https://doi.org/10.1021/acs.jafc.2c06979
J. Agric. Food Chem. 2023, 71, 5314−5325

of the ratio of treated to untreated cells, revealing the intracellular proton index (IPX), with a high secretory activity indicated by a low IPX-value. For the correlation analysis, the data were normalized to the respective histamine response.

Data Analysis. Pathway analysis for elucidation of a possible connection between TAS2R50 activation and IL6 release was performed using the pathway topology analysis tool integrated into the reactome database.[47] To analyze the connectivity, all proteins included in the interleukin-6 family signaling pathway (ID: R-HSA-6783589.6; DOI 10.3180/r-hsa-6783589.1) for species *Homo sapiens* as well as the bitter taste receptor TAS2R50 were imported into the Gene Set Analysis Function of the Reactome FIViz plugin in Cytoscape (Reactome FI Network Version 2021). Analysis was conducted using the linker genes option to integrate genes required for connection of the individual pathways. Visualization of the resulting gene set and connectivity network was performed by means of Cytoscape (version 3.9.1, cytoscape.org).

Statistical analysis was performed using the statistical programming environment R (version 4.2.0). Model assumptions were evaluated using the Shapiro−Wilk test of normality and Levene's test for homogeneity of variance across groups implemented in the R package car. Nonparametric comparison of the location parameters of multiple groups was performed by the Kruskal−Wallis rank sum test, while the procedure described by Siegel and Castellan (1988)[48] was applied for subsequent multiple comparison tests using the kruskalmc function implemented in the pgirmess package.

RESULTS

Pathway Analysis of IL-6 and TAS2R50 and the Proof via Immunofluorescence Staining. The pathway analysis revealed GNAI3 as an upstream signaling protein that links TAS2R50 and the IL-6 pathway via phosphatidylinositol 4,5-bisphosphate 3-kinase catalytic subunit alpha isoform (PIK3CA), nuclear factor NF-kappa-B (NfKB1) and AP-1 subunit, and the heterodimer Fos-Jun (Figure S1A). We, therefore, verified the protein expression of GNAI3 in the HGF-1 cells studied by immunofluorescence staining (Figure S1B). The fluorescence signal was GNAI3 specific and confirmed our pathway analysis, whereas cells treated with the secondary antibody solely did not show a specific signal (Figure S1B).

Effect of the TAS2R Agonists SNT, EGCG, QHCl, and NAR on *Pg*-LPS Induced IL-6 Release in HGF-1 Cells. In order to ensure that none of the test compounds had a detrimental effect on the viability of HGF-1 cells, an MTT-test was conducted prior to the IL-6 release experiments. The results revealed no effect on the cellular viability by any of the test compounds in any of the concentrations tested (Table S2).

First, the effect of the bitter tasting non-TAS2R50 agonists QHCl[19] and EGCG[18,49] as well as the bitter tasting NAR and SNT, for which no TAS2R activation has been tested so far, on the IL-6 release evoked by *Pg*-LPS in HGF-1 cells was tested at concentrations of 40, 50, 100, and 100 μM, respectively. Individual test concentrations were selected from preceding dose−response experiments, in which those concentrations showed the maximum effect size (Figure S2).

The resulting mean inhibitory effect sizes were $-12.6 \pm 5.92\%$ for NAR, $-45.5 \pm 4.28\%$ for SNT, $-51.0 \pm 3.42\%$ for QHCl, and $-62.1 \pm 2.37\%$ for EGCG (all $p \leq 0.05$, Figure 2A). At these concentrations, the effect of QHCl did only differ from that demonstrated for NAR, whereas no statistical difference was found when the results for QHCl were compared with those for SNT and EGCG.

Putative Binding Mode of SNT, NAR, EGCG, & QHCl to TAS2R50. To investigate the potential interaction of SNT, NAR, EGCG, and QHCl to the TAS2R50 binding site, molecular docking simulations were performed. Because of the uncertainness of ECL2 modeling and the different molecular sizes of the compounds (Table S1), the ECL2 region was removed from the model.[50−53] The ECL2 connects transmembrane helices 4 and 5 and is, except for a conserved Asn-linked glycosylation site,[54] the longest and most diverse loop among TAS2Rs.[55] It was demonstrated that docking performance could be insensitive to or even improved by excluding ECL2 from the calculations.[50−52] Indeed, the model without the ECL2 and ECL3 was proven to be able to reproduce the docking pose of RSV (Figure S3), as previously published.[9]

Among the analyzed compounds, SNT, with a docking score of −7.54 kcal/mol, is the compound predicted to best interact with TAS2R50 and is the one that most closely reproduces the RSV binding mode. On the contrary, EGCG and QHCl have low docking scores, thus confirming a lack of robust interaction of these compounds to TAS2R50 (Figure S3).

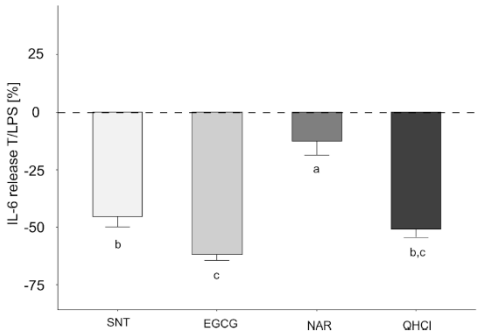

Figure 2. IL-6 release of HGF-1 cells treated with SNT 50 μM, EGCG 100 μM, NAR 100 μM, and QHCl 40 μM in a 1 h preincubation, followed by a 6 h co-incubation to *Pg*-LPS. Treatment of HGF-1 cells with 10 μg/mL *Pg*-LPS for 6 h solely revealed a mean IL-6 release of 42.62 ± 3.35 pg/mL ($n \geq 4$; t.r. = 2). Data displayed are calculated as treatment over control in percent, with the effect of *Pg*-LPS set to zero (T/LPS, %; LPS = 0%). Data are shown as mean ± SEM $n = 3-4$; t.r. = 2. Statistics: Kruskal−Wallis; $p \leq 0.05$, post hoc test: multiple comparison tests using the kruskalmc function.

Effect of SNT, EGCG, QHCl, NAR, and TAS2R Antagonists MAT and HED on the *Pg*-LPS Induced IL-6 Release in HGF-1 Cells. Prior to all experiments, effects on the viability of HGF-1 cells were excluded by MTT-tests performed (Table S2). In subsequent experiments, the antagonistic effect of MAT on TAS2R4 and TAS2R43 was demonstrated in HEK-293 T Gα16gust44 cells by means of a well-established Ca^{2+}-mobilization assay[19,22,56] (Figure S4). In these experiments, a concentration of 10 μM MAT reduced the effect evoked by aristolochic acid, targeting TAS2R43,[19] and by colchicine, targeting TAS2R4,[19] from 100% to $78.9 \pm 13.3\%$ ($p \leq 0.01$) and to $48.9 \pm 32.8\%$ ($p \leq 0.05$), respectively.

Involvement of multiple TAS2Rs in the repressive effect of bitter tasting food constituents on the *Pg*-LPS evoked IL-6 release in HGF-1 cells was also tested in co-incubation experiments with MAT and HED (Figure 3). Whereas MAT reduced the *Pg*-LPS evoked IL-6 release of SNT, NAR, and EGCG by mean percentage effect sizes of -27.1 ± 1.60, -17.8 ± 10.6, and $-27.4 \pm 1.77\%$ (all $p \leq 0.05$, Figure 3A−C), respectively, HED demonstrated a reducing effect when co-applied together with SNT ($-13.2 \pm 4.67\%$, $p \leq 0.05$, Figure 3A) and QHCl ($12.1 \pm 6.28\%$ $p \leq 0.05$, Figure 3D).

https://doi.org/10.1021/acs.jafc.2c06979
J. Agric. Food Chem. 2023, 71, 5314−5325

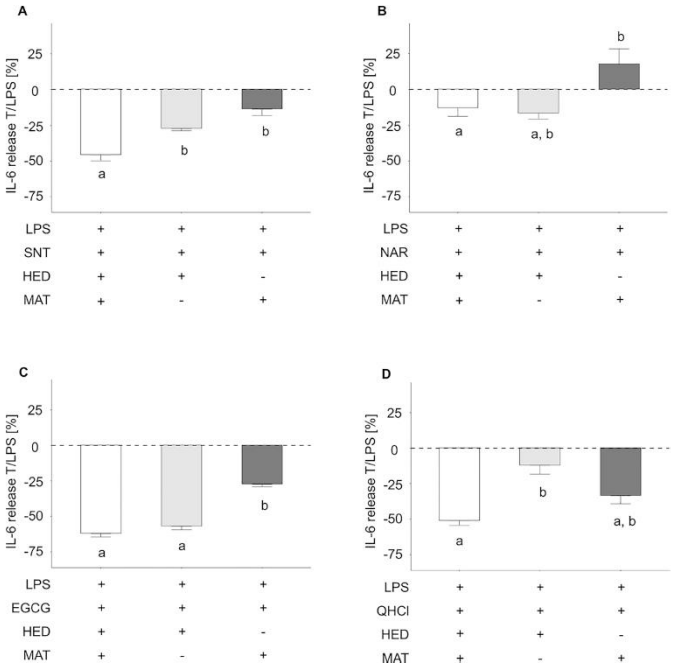

Figure 3. IL-6 release of HGF-1 cells treated with (A) SNT 50 μM, (B) NAR 500 μM, (C) EGCG 100 μM, and (D) QHCl 40 μM in a 1 h preincubation and a 6 h co-incubation with *Pg*-LPS, followed with or without HED or MAT treatment (10:1). Treatment of HGF-1 cells with 10 μg/mL *Pg*-LPS for 6 h solely revealed a mean IL-6 release of 42.62 ± 3.35 pg/mL ($n \geq 4$; t.r. = 2). Data displayed are calculated as treatment over control in percent, the effect of *Pg*-LPS set to zero (T/LPS, %; LPS = 0%). Data are shown as mean ± SEM n = 3−4; t.r. = 2. Statistics: Kruskal−Wallis; $p \leq 0.05$, post hoc test: multiple comparison tests using the kruskalmc function.

Association between the Repression of *Pg*-LPS Induced IL-6 Release in HGF-1 Cells by Compounds from the Chemical Bitter Space and Their Bitter Threshold Concentration. To test whether a repressive effect on the *Pg*-LPS induced IL-6 release by HGF-1 cells is associated with a compounds' bitter taste threshold concentration published in the literature, effects of the following test compounds from the chemical bitter space were investigated in dose response experiments: CAB, DIOS, EGCG, IsoA, IsoSNT, L-Arg, NAR, QHCl, RSV, SNT, and THEO (Figure 1). Test concentrations applied covered the individual compounds' bitter taste threshold concentration published, spanning over a total concentration range of 0.1 μM−50 mM (Figure 4, Table 1). After normalization for passage and 96-well plate effects, all test compounds except IsoSNT showed a dose-dependent repressing effect on the *Pg*-LPS induced IL-6 release (Figure 4). Next, individual data was used to calculate an effective inhibitory dose of 25% (ED_{25}) for each compound (Figure 5). The ED_{25} values for CAB (228.86 μM), DIOS (5.47 μM), EGCG (9.49 μM), IsoA (8.20 μM), IsoSNT (4.83 μM), L-Arg (72026.17 μM), NAR (485.93 μM), QHCl (23.21 μM), RSV (39.91 μM), SNT (53.06 μM), and THEO (32422.02 μM) were correlated with the respective bitter taste threshold concentration of 13 μM for CAB,[35] 190 μM for EGCG,[43] 21 μM for Iso-A,[38] 32 μM for IsoSNT[39], 75,000 μM for L-Arg,[40] 109 μM for NAR,[44] 8.3 μM for QHCl,[45] 98 μM for RSV,[9] 56 μM for SNT,[39] and 800 μM for THEO[40] published in the literature (Table 1). This linear correlation analysis according to Pearson revealed a correlation coefficient of R^2 = 0.599 (p = 0.014) was achieved. Notably, DIOS was excluded from this analysis because no taste threshold data were available in the literature.

Comparison of the Bitter Response in the HGF-1 Cell Model with the Bitter-Taste Associated Changes of the Intracellular Proton Index in HGT-1 Cells. In order to compare the linear bitter response model established for the HGF-1 cells with our previously published HGT-1 cell model,[27,29] all test compounds of the here-presented study were also tested for their impact on the intracellular proton index (IPX) in HGT-1 cells as an indicator of bitter taste quality.[27,29] Test concentrations covered the taste threshold concentrations (Table 1). After normalization of the mean IPX effect to the stimulating effect of histamine as internal quality control, mean effect sizes for CAB (13.55 ± 53.23%), DIOS (11.10 ± 35.35%), EGCG (0.35 ± 69.94%), IsoA (−183.42 ± 30.59%), IsoSNT (82.04 ± 37.84%), L-Arg (123.49 ± 156.85%), NAR (3.22 ± 44.11%), QHCl (85.17 ± 164.02%), RSV (−62.39 ± 100.96%), SNT (84.76 ± 50.58%), and THEO (125.15 ± 112.11%) were revealed. In analogy to the linear model established for the HGF-1 cells (Figure 6A), the association between the bitter threshold concentration (Table 1) and the mean IPX was investigated and revealed no significant linear relationship (R^2 = 0.153, p = 0.263).

https://doi.org/10.1021/acs.jafc.2c06979
J. Agric. Food Chem. 2023, 71, 5314−5325

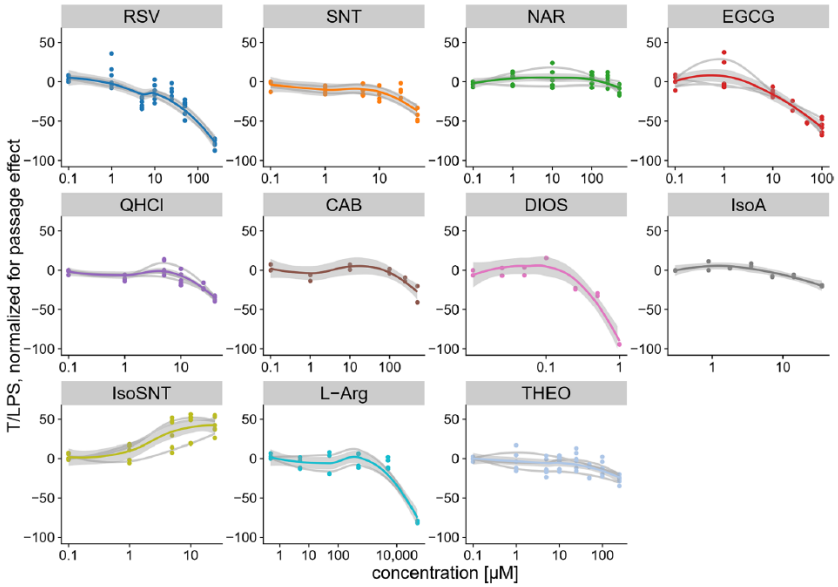

Figure 4. Dose response curves recorded for CAB, DIOS, EGCG, IsoA, IsoSNT, L-Arg, NAR, QHCl, RSV, SNT, and THEO at concentration ranges from 0.1 μM to 50 mM, covering the taste threshold values, after 1 h preincubation followed by a 6 h co-incubation with *Pg*-LPS. Treatment of HGF-1 cells with 10 μg/mL *Pg*-LPS for 6 h solely revealed a mean IL-6 release of 35.49 ± 1.53 pg/mL ($n \geq 4$; t.r. = 2). Data displayed are normalized for passage and plate effect of the cells' response to a fixed RSV 100 μM concentration (n = 3−6; t.r. = 2).

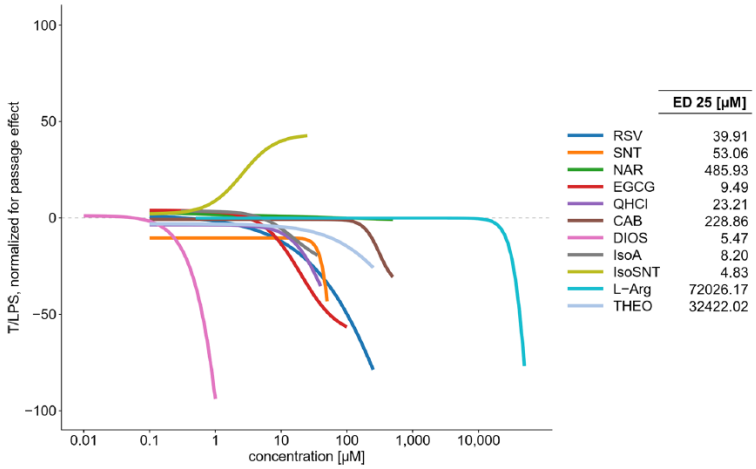

Figure 5. IL-6 release dose response of HGF-1 cells treated with CAB, DIOS, EGCG, IsoA, IsoSNT, L-Arg, NAR, QHCl, RSV, SNT, and THEO in a 1 h preincubation, followed by a 6 h co-incubation with *Pg*-LPS. Treatment of HGF-1 cells with 10 μg/mL *Pg*-LPS for 6 h solely revealed a mean IL-6 release of 35.49 ± 1.53 pg/mL ($n \geq 4$; t.r. = 2). Data displayed are normalized for passage effect and calculated as treatment over *Pg*-LPS (T/LPS, LPS = 0) (n = 3−6; t.r. = 2).

DISCUSSION

Mammalian TAS2Rs are expressed in several extra-gustatory tissues, e.g., the upper airways,[57,58] lungs,[59] gastrointestinal tract,[27,60] brain,[61] bladder,[62] and testis,[63] as well as immune competent cells, such as blood monocytes and leukocytes[64] and gingival fibroblasts.[9,10] For gingival fibroblasts, Zhou et al.[10] recently published the protein expression of guanine nucleotide-binding protein G subunit alpha 3 (GNAT3), an upstream GPCR signaling protein, and provided results that suggest an involvement of TAS2Rs in cellular downstream inflammatory responses.[10] In the here-presented work, the HGF-1 cells studied were stained positive for GNAI3, thereby confirming the

https://doi.org/10.1021/acs.jafc.2c06979
J. Agric. Food Chem. 2023, 71, 5314−5325

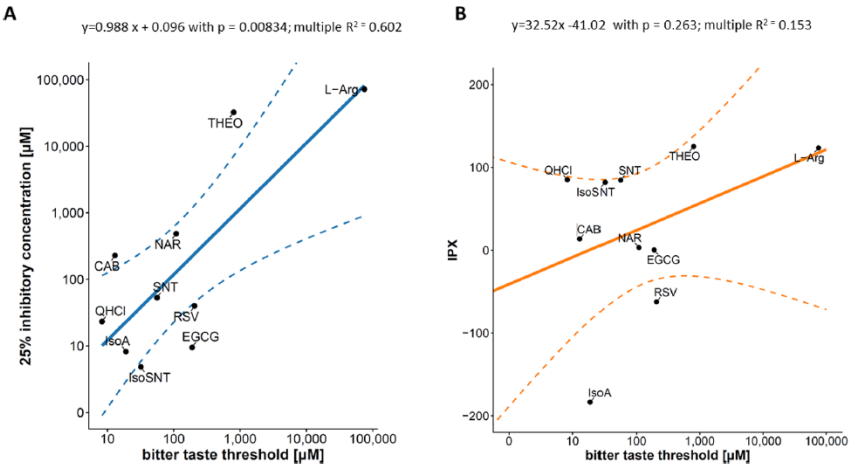

Figure 6. (A) Pearson correlation of the 25% inhibitory concentration [μM] of the selected bitter tasting compounds in HGF-1 with their respective bitter taste thresholds [μM] log transformed: $R^2 = 0.602$, $p = 0.008$. (B) Pearson correlation of IPX-values in HGT-1 cells normalized to the respective histamine control and the tested concentrations of the bitter tasting compound [μM] log transformed: $R^2 = 0.153$, $p = 0.263$.

presence of another signaling subunit in addition to GNAT3 reported by Zhou et al.[10] In recent works, it has been shown that in stem cells of the apical papilla (SCAPs), GNAI3 plays an important role in mineralization and tissue regeneration via the c-Jun N-terminal kinase (JNK) and the extracellular-signal regulated kinase (ERK) signaling.[30] For HGF cells, presenting the predominant cell type in gingival connective tissue, GNAI3 is known to promote wound healing by promoting the generation of an extracellular matrix. Moreover, in mice, it was shown that GNAI1 and GNAI3 suppress GNAI2-mediated colitis-associated tumorigenesis through negatively regulating Janus kinase (JAK) and NF-κB promoted IL-6 signaling.[65] According to existing pathway data from reactome, we deem the pathway shown in Figure S1 to be relevant for the TAS2R-induced intracellular signaling resulting in IL-6 gene transcription via NFκ-B. Moreover, the work by Zhou et al.[10] showed that heterotrimeric G-protein subunits PLCβ2 and GNAT3 are relevant in HGF-1 cells for their response to LPS. In this study, we additionally demonstrated that GNAI3, also belonging to the G-protein family, is functionally expressed in HGF-1 cells. Therefore, we consider the TAS2R-induced G-protein signaling as relevant for the cellular IL-6 response.

In the context of mammalian innate immune responses to environmental stimuli, such as metabolites derived from bacteria (e.g., LPS or quorum-sensing molecules), extra-gustatory TAS2Rs have been hypothesized to function as immune sentinels.[58,66,67] Also, more specifically, TAS2R activation in human whole blood and lung macrophages[59,68] as well as gingival fibroblasts[9,10] has been shown to antagonize LPS-induced pro-inflammatory cytokine production, suggesting a potential role of TAS2Rs in the control of inflammation.

Supported by recently published TAS2R pathway analyses[10] and our own results presented here, demonstrating TAS2R downstream signaling proteins being linked to the release of immune-modulatory, inflammatory cytokines in HGF-1 cells, we hypothesized the HGF-1 cell line expressing almost all *TAS2Rs*[10] as a novel screening tool for the identification of bitter tasting and bitter taste modulating compounds.

Since our previous study in HGF-1 cells revealed TAS2R50 to mediate the RSV-evoked reducing effect on the IL-6 release induced by *Pg*-LPS,[9] we also aimed to elucidate in the study presented here, whether this IL-6 response depends on TAS2R50 specifically or whether activation of a wide range of TAS2Rs is associated with this cellular response. To answer this question, four bitter tasting compounds (EGCG, NAR, QHCl, and SNT)[58,59,61] that are structurally similar or divergent from RSV were selected from the chemical bitter space and subjected to a bitter-sensing HGF-1 cell assay, which was paired with a chemoinformatic modeling approach.

Results from the HGF-1 cell assay revealed no clear indication for a specific involvement of TAS2R50, since all tested compounds induced a cellular response, as previously reported for RSV targeting TAS2R50.[9] The specific involvement of TAS2R50 could also be excluded by the results from docking studies, since we did not find a consensus in the binding modes of the four compounds to TAS2R50. In some cases, as for QHCL and EGCG, the docking scores were very low, whereas the response in the HGF-1 cell assay was strong, indicating no specific role of TAS2R50 in the repression of a *Pg*-LPS-induced IL-6 release by HGF-1 cells. Application of the bitter masking compounds HED,[29,34] targeting TAS2R20/31/43/50,[27] and MAT, demonstrated to target TAS2R4/43, indicate that likely more TAS2Rs than only TAS2R50 are involved in the cellular response studied. Depending on the agonist applied, co-treatment of the HGF-1 cells with one of the antagonists HED or MAT resulted in different cellular responses induced by the individual agonists EGCG, QHCl, NAR, and SNT, with each of them targeting multiple TAS2Rs (EGCG: TAS2R4/5/14/30/39/43;[18,69,70] QHCl: TAS2R4/7/10/14/31/39/40/43/46;[19] NAR: TAS2R not known yet; SNT: TAS2R not known yet). We hypothesize these results to demonstrate a complex interplay of several TAS2Rs, resulting in a net modulation of the cells' IL-6 release in response to *Pg*-LPS. This hypothesis is supported by our previously established screening model founded on the native cell line HGT-1, in which activation of TAS2Rs results in the secretion of protons.[27] In this cell model,

https://doi.org/10.1021/acs.jafc.2c06979
J. Agric. Food Chem. 2023, 71, 5314−5325

application of bitter tasting and bitter taste masking compounds results in a modulation of proton secretion, calculated as the intracellular proton index (IPX), which correlates well with the sensory bitter taste intensity.[29] However, the HGT-1 cell assay presents some limitations since results were rarely not in line with those obtained from sensory trials, e.g., when phloretin[29] or other food compounds that quench the fluorescence of membrane-bound probes[71] were tested. Also, testing of pH-sensitive compounds[72] and the requirement of high-throughput testing are restricting factors for this cell model.[73] None of these limitations applies to the HGF-1 cell assay presented here: the ELISA technique is less sensitive to quenching of the test compounds, does not rely on intracellular changes of the pH and is based on a robust technique that can easily be transformed into a high-throughput format.

In order to verify an association between a compound's ability to modulate the *Pg*-LPS-induced IL-6 release by HGF-1 cells and its bitter taste threshold concentration, a linear model was established. This model is founded on the literature of bitter taste threshold data and dose response curves of 11 bitter tasting, chemically diverse food constituents spanning over the chemical bitter space,[32] with each compound tested in at least six concentrations in three to four independent experiments with two technical replicates. For all of the bitter tasting compounds tested, a repressing effect on the *Pg*-LPS induced IL-6 release was demonstrated, except of Iso-SNT. One may speculate that this opposite effect could rely on the interaction with other TAS2Rs or the establishment of a different type of interaction with common target TAS2Rs (e.g., agonistic-antagonistic, agonistic-inverse agonistic, etc.).

Nevertheless, after normalization of the data for the plate and passage specific effects, a linear model using the ED_{25} was established. This model confirms a significant linear relationship with a Pearson correlation coefficient of 0.602 ($p = 0.008$). The same approach was applied to the HGT-1 proton secretion assay (IPX normalized to the histamine effect), revealing no significant relationship ($p = 0.263$) between the effect of the bitter tasting compounds on the IPX and the compounds' bitter taste threshold. Comparing both cell assays, the HGF-1 model was demonstrated to show a better association with the bitter taste threshold than the HGT-1 model, whereas results of the HGT-1 cell model correlated well with a compounds' bitter taste intensities.[29,46] However, for both cell models, an involvement of TAS2R-independent pathways cannot be excluded.

Generally speaking, the overall concept of using native cell lines as screening models is well-established, since the implementation of taste receptors in cell-based screening assays provides an alternative option for the identification of novel taste modifiers in addition to sensory approaches.[26] Alternative cell-based assays are founded on heterologous, reporter cell systems and used for the screening and validation of novel receptor ligands. One of the most commonly used cell line for this purpose is the human embryonic kidney cell line HEK-293 or variants thereof, which does not express bitter taste receptors natively and allows the recombinant expression of TAS2Rs[74] and promiscuous G-proteins.[75] In this cell model, agonist-induced TAS2R activation leads to an intracellular calcium mobilization, which is detected by calcium-sensitive fluorescent probes. This approach provides stable and accurate readouts in high-throughput measurements.[74] Whereas in many cases these assays correlate well with human sensory data (e.g.,[20−25]), for some compounds, deviations between in vivo and in vitro data were found (e.g.[38,76]). The apparent differences could be due to, e.g., multiple or perireceptor events, the use/existence of different receptor variants in the in vitro assay compared to the genetic background of sensory panelists, solubility issues of some compounds, or yet unknown technical issues with those TAS2Rs that have remained orphan to date. Nevertheless, TAS2R transfected HEK-293 cells are well established to study receptor binding kinetics and to identify allosteric modulators of individual TAS2Rs.[19]

Native cell-based assays are based on immortal human cell lines from nongustatory tissue, which endogenously express TAS2R receptor genes and native taste transduction signaling pathways, thereby providing the mechanistic basis for a correlation between the sensory perception and the cellular response to ligand-receptor activation. Correlations with sensory data are often strong, since bitter compounds or bitter modulators may target several TAS2Rs,[77] with the overall interaction of all targeted receptors generating the physiological response of bitter reception. In previous studies of our group, we established a cellular screening approach for high-intensity bitter compounds that is based on the TAS2R-mediated proton secretion by human parietal cells of the HGT-1 cell line.[29] However, for native cell-based models targeting the identification of bitter tasting or bitter taste modulating compounds, screening models validated for bitter taste threshold data published for a wide range of compounds from the chemical bitter space are lacking.

The term "taste threshold" was introduced in the 19th century by psychophysicists and used to denote a stimulus concentration, above which the stimulus could be detected and below which it could not. According to the ISO 13301:2018(E),[78] taste threshold evaluation studies are mainly carried out for two reasons: as measures of the sensitivity of assessors or groups of assessors to specific stimuli and as measures of the ability of substances to evoke sensory responses in assessors. In the first case, the value of the threshold is taken as a description of an assessor's performance and in the latter, as a measure of a property of the substance. For the here-presented work, published bitter taste threshold data of selected bitter tasting compounds, reported by a wide variety of panelists and captured in the chemical bitter space,[17,32] were associated with the compounds' ability to reduce the *Pg*-LPS-reduced IL-6 release by HGF-1 cells. This cell model presents an alternative native cell-based assay suitable for the identification of bitter tasting food constituents, showing a linear association between a compound's bitter taste threshold and its 25% inhibitory concentration on the IL-6 response induced by *Pg*-LPS. However, taste threshold data should always be determined by sensory studies, although cell-based assays present valuable screening approaches to identify bitter tasting and bitter taste modulating compounds. In addition, our results pinpoint a possible predictive model for the identification of bitter tasting compounds with a potential to act as anti-inflammatory substances due to their bitter taste.

Although the mechanisms and biological significance of TAS2Rs-induced anti-inflammatory effects have not been well studied in a clinical context yet, there is growing evidence for their essential role in controlling inflammatory processes, as indicated by a recently published meta-analysis of the anti-inflammatory potential of bitter tasting phytochemicals.[79]

https://doi.org/10.1021/acs.jafc.2c06979
J. Agric. Food Chem. 2023, 71, 5314−5325

■ ASSOCIATED CONTENT

Supporting Information

The Supporting Information is available free of charge at https://pubs.acs.org/doi/10.1021/acs.jafc.2c06979.

Calculated molecular descriptors of EGCG, IsoSNT, NAR, QHCl, RSV, and SNT (Table S1), HGT-1 and HGF-1 cell viability after treatment of bitter tasting test compounds (Table S2), network of TAS2R50 and IL-6 pathways by reactom as well as results from immunofluorescence analysis of GNAI3 in HGF-1 cells (Figure S1), results from dose−response experiments of SNT − sinensetin (0.1−50 μM), NAR − naringin (0.1−500 μM, EGCG − epigallocatechin gallate (0.1−100 μM), and QHCl - quinine HCl (0.1−40 μM) (Figure S2), 3D representation of the docking poses of RSV, NAR, SNT, EGCG, and QHCl into the TAS2R50 binding pocket (Figure S3), and results on the antagonistic effect of 10 μM MAT in TAS2R4 and TAS2R43 transfected HEK − 293 T-Gα16gust44 cells by co-administration with TAS2R43 agonist aristocholic acid (0.3 μM) and TAS2R4 agonist colchicine (1 mM) (Figure S4) (PDF)

■ AUTHOR INFORMATION

Corresponding Author

Veronika Somoza − *Department of Physiological Chemistry, Faculty of Chemistry, University of Vienna, Vienna 1090, Austria; Leibniz Institute for Food Systems Biology at the Technical University of Munich, Freising 85354, Germany; Chair for Nutritional Systems Biology, Technical University Munich, Freising 85354, Germany;* orcid.org/0000-0003-2456-9245; Email: v.somoza.leibniz-lsb@tum.de

Authors

Johanna Tiroch − *Department of Physiological Chemistry, Faculty of Chemistry and Vienna Doctoral School in Chemistry (DoSChem), University of Vienna, Vienna 1090, Austria*

Andreas Dunkel − *Leibniz Institute for Food Systems Biology at the Technical University of Munich, Freising 85354, Germany;* orcid.org/0000-0002-4445-6144

Sonja Sterneder − *Department of Physiological Chemistry, Faculty of Chemistry and Vienna Doctoral School in Chemistry (DoSChem), University of Vienna, Vienna 1090, Austria*

Sofie Zehentner − *Department of Physiological Chemistry, Faculty of Chemistry and Vienna Doctoral School in Chemistry (DoSChem), University of Vienna, Vienna 1090, Austria;* orcid.org/0000-0001-6462-964X

Maik Behrens − *Leibniz Institute for Food Systems Biology at the Technical University of Munich, Freising 85354, Germany;* orcid.org/0000-0003-2082-8860

Antonella Di Pizio − *Leibniz Institute for Food Systems Biology at the Technical University of Munich, Freising 85354, Germany;* orcid.org/0000-0002-8520-5165

Jakob P. Ley − *Symrise AG, Holzminden 37603, Germany;* orcid.org/0000-0001-9388-4260

Barbara Lieder − *Department of Physiological Chemistry, Faculty of Chemistry, University of Vienna, Vienna 1090, Austria;* orcid.org/0000-0002-0527-8330

Complete contact information is available at: https://pubs.acs.org/10.1021/acs.jafc.2c06979

Funding

The work was funded by Symrise AG, Holzminden/Germany, and the institutional budget of the authors' hosting institutions.

Notes

The authors declare the following competing financial interest(s): JP Ley is employed by Symrise AG, Holzminden / Germany.

■ ACKNOWLEDGMENTS

We thank the technical assistant Stefanie Hackl from the Leibniz Institute for Food Systems Biology at the Technical University of Munich for the purification and purity analysis of the iso-alpha acid. Alessandro Marchiori performed the heterologous expression experiments showing the partial inhibition of TAS2R4 and TAS2R43 by matairesinol.

■ REFERENCES

(1) Bozkurt, S. B.; Hakki, S. S.; Hakki, E. E.; Durak, Y.; Kantarci, A. Porphyromonas gingivalis Lipopolysaccharide Induces a Pro-inflammatory Human Gingival Fibroblast Phenotype. *Inflammation* **2017**, *40*, 144−153.

(2) Brewer, D. B. The fibroblast. *Proc. R. Soc. Med.* **1967**, *60*, 778−782.

(3) Komuro, T. Re-evaluation of fibroblasts and fibroblast-like cells. *Anat. Embryol.* **1990**, *182*, 103−112.

(4) Vaday, G. G.; Lider, O. Extracellular matrix moieties, cytokines, and enzymes: dynamic effects on immune cell behavior and inflammation. *J. Leukocyte Biol.* **2000**, *67*, 149−159.

(5) Ehrnhöfer-Ressler, M. M.; Fricke, K.; Pignitter, M.; Walker, J. M.; Walker, J.; Rychlik, M.; Somoza, V. Identification of 1,8-cineole, borneol, camphor, and thujone as anti-inflammatory compounds in a Salvia officinalis L. infusion using human gingival fibroblasts. *J. Agric. Food Chem.* **2013**, *61*, 3451−3459.

(6) Walker, J. M.; Maitra, A.; Walker, J.; Ehrnhoefer-Ressler, M. M.; Inui, T.; Somoza, V. Identification of *Magnolia officinalis* L. bark extract as the most potent anti-inflammatory of four plant extracts. *Am. J. Chin. Med.* **2013**, *41*, 531−544.

(7) Josino Soares, D.; Walker, J.; Pignitter, M.; Walker, J. M.; Imboeck, J. M.; Ehrnhoefer-Ressler, M. M.; Montenegro Brasil, I.; Somoza, V. Pitanga (Eugenia uniflora L.) fruit juice and two major constituents thereof exhibit anti-inflammatory properties in human gingival and oral gum epithelial cells. *Food Funct.* **2014**, *5*, 2981−2988.

(8) Schueller, K.; Hans, J.; Pfeiffer, S.; Walker, J.; Ley, J. P.; Somoza, V. Identification of Interleukin-8-Reducing Lead Compounds Based on SAR Studies on Dihydrochalcone-Related Compounds in Human Gingival Fibroblasts (HGF-1 cells) In Vitro. *Molecules* **2020**, *25*, 1382.

(9) Tiroch, J.; Sterneder, S.; Di Pizio, A.; Lieder, B.; Hoelz, K.; Holik, A. K.; Pignitter, M.; Behrens, M.; Somoza, M.; Ley, J. P.; Somoza, V. Bitter Sensing TAS2R50 Mediates the trans-Resveratrol-Induced Anti-inflammatory Effect on Interleukin 6 Release in HGF-1 Cells in Culture. *J. Agric. Food Chem.* **2021**, *69*, 13339−13349.

(10) Zhou, Z.; Xi, R.; Liu, J.; Peng, X.; Zhao, L.; Zhou, X.; Li, J.; Zheng, X.; Xu, X. TAS2R16 Activation Suppresses LPS-Induced Cytokine Expression in Human Gingival Fibroblasts. *Front. Immunol.* **2021**, *12*, 726546.

(11) Behrens, M.; Born, S.; Redel, U.; Voigt, N.; Schuh, V.; Raguse, J. D.; Meyerhof, W. Immunohistochemical detection of TAS2R38 protein in human taste cells. *PLoS One* **2012**, *7*, No. e40304.

(12) Behrens, M.; Foerster, S.; Staehler, F.; Raguse, J. D.; Meyerhof, W. Gustatory expression pattern of the human TAS2R bitter receptor gene family reveals a heterogenous population of bitter responsive taste receptor cells. *J. Neurosci.* **2007**, *27*, 12630−12640.

(13) Spaggiari, G.; Di Pizio, A.; Cozzini, P. Sweet, umami and bitter taste receptors: State of the art of in silico molecular modeling approaches. *Trends Food Sci. Technol.* **2020**, *96*, 21−29.

(14) Frank, O.; Ottinger, H.; Hofmann, T. Characterization of an Intense Bitter-Tasting 1H,4H-Quinolizinium-7-olate by Application of the Taste Dilution Analysis, a Novel Bioassay for the Screening and

Identification of Taste-Active Compounds in Foods. *J. Agric. Food Chem.* **2001**, *49*, 231−238.
(15) Dagan-Wiener, A.; Di Pizio, A.; Nissim, I.; Bahia, M. S.; Dubovski, N.; Margulis, E.; Niv, M. Y. BitterDB: taste ligands and receptors database in 2019. *Nucleic Acids Res.* **2019**, *47*, D1179−D1185.
(16) Luo, G.; Somoza, V.; Dunkel, A. https://fsbi-db.de/.
(17) Bayer, S.; Mayer, A. I.; Borgonovo, G.; Morini, G.; Di Pizio, A.; Bassoli, A. Chemoinformatics View on Bitter Taste Receptor Agonists in Food. *J. Agric. Food Chem.* **2021**, *69*, 13916−13924.
(18) Lossow, K.; Hübner, S.; Roudnitzky, N.; Slack, J. P.; Pollastro, F.; Behrens, M.; Meyerhof, W. Comprehensive Analysis of Mouse Bitter Taste Receptors Reveals Different Molecular Receptive Ranges for Orthologous Receptors in Mice and Humans. *J. Biol. Chem.* **2016**, *291*, 15358−15377.
(19) Meyerhof, W.; Batram, C.; Kuhn, C.; Brockhoff, A.; Chudoba, E.; Bufe, B.; Appendino, G.; Behrens, M. The molecular receptive ranges of human TAS2R bitter taste receptors. *Chem. Senses* **2010**, *35*, 157−170.
(20) Behrens, M.; Redel, U.; Blank, K.; Meyerhof, W. The human bitter taste receptor TAS2R7 facilitates the detection of bitter salts. *Biochem. Biophys. Res. Commun.* **2019**, *512*, 877−881.
(21) Wang, Y.; Zajac, A. L.; Lei, W.; Christensen, C. M.; Margolskee, R. F.; Bouysset, C.; Golebiowski, J.; Zhao, H.; Fiorucci, S.; Jiang, P. Metal Ions Activate the Human Taste Receptor TAS2R7. *Chem. Senses* **2019**, *44*, 339−347.
(22) Bufe, B.; Hofmann, T.; Krautwurst, D.; Raguse, J. D.; Meyerhof, W. The human TAS2R16 receptor mediates bitter taste in response to beta-glucopyranosides. *Nat. Genet.* **2002**, *32*, 397−401.
(23) Mueller, K. L.; Hoon, M. A.; Erlenbach, I.; Chandrashekar, J.; Zuker, C. S.; Ryba, N. J. P. The receptors and coding logic for bitter taste. *Nature* **2005**, *434*, 225−229.
(24) Bufe, B.; Breslin, P. A.; Kuhn, C.; Reed, D. R.; Tharp, C. D.; Slack, J. P.; Kim, U.-K.; Drayna, D.; Meyerhof, W. The molecular basis of individual differences in phenylthiocarbamide and propylthiouracil bitterness perception. *Curr. Biol.* **2005**, *15*, 322−327.
(25) Kim, U. K.; Jorgenson, E.; Coon, H.; Leppert, M.; Risch, N.; Drayna, D. Positional cloning of the human quantitative trait locus underlying taste sensitivity to phenylthiocarbamide. *Science* **2003**, *299*, 1221−1225.
(26) Riedel, K.; Sombroek, D.; Fiedler, B.; Siems, K.; Krohn, M. Human cell-based taste perception - a bittersweet job for industry. *Nat. Prod. Rep.* **2017**, *34*, 484−495.
(27) Liszt, K. I.; Ley, J. P.; Lieder, B.; Behrens, M.; Stöger, V.; Reiner, A.; Hochkogler, C. M.; Köck, E.; Marchiori, A.; Hans, J.; Widder, S.; Krammer, G.; Sanger, G. J.; Somoza, M. M.; Meyerhof, W.; Somoza, V. Caffeine induces gastric acid secretion via bitter taste signaling in gastric parietal cells. *Proc. Natl. Acad. Sci. U. S. A.* **2017**, *114*, E6260−E6269.
(28) Walker, J.; Hell, J.; Liszt, K. I.; Dresel, M.; Pignitter, M.; Hofmann, T.; Somoza, V. Identification of beer bitter acids regulating mechanisms of gastric acid secretion. *J. Agric. Food Chem.* **2012**, *60*, 1405−1412.
(29) Liszt, K. I.; Hans, J.; Ley, J. P.; Köck, E.; Somoza, V. Characterization of Bitter Compounds via Modulation of Proton Secretion in Human Gastric Parietal Cells in Culture. *J. Agric. Food Chem.* **2018**, *66*, 2295−2300.
(30) Zhang, Y.; Yuan, L.; Meng, L.; Fang, M.; Guo, S.; Wang, D.; Ma, J.; Wang, L. Guanine and nucleotide binding protein 3 promotes odonto/osteogenic differentiation of apical papilla stem cells via JNK and ERK signaling pathways. *Int. J. Mol. Med.* **2018**, *43*, 382−392.
(31) McLaughlin, S. K.; McKinnon, P. J.; Spickofsky, N.; Danho, W.; Margolskee, R. F. Molecular cloning of G proteins and phosphodiesterases from rat taste cells. *Physiol. Behav.* **1994**, *56*, 1157−1164.
(32) Dunkel, A.; Hofmann, T.; Di Pizio, A. In Silico Investigation of Bitter Hop-Derived Compounds and Their Cognate Bitter Taste Receptors. *J. Agric. Food Chem.* **2020**, *68*, 10414−10423.
(33) Behrens, M.; Brockhoff, A.; Batram, C.; Kuhn, C.; Appendino, G.; Meyerhof, W. The human bitter taste receptor hTAS2R50 is activated by the two natural bitter terpenoids andrographolide and amarogentin. *J. Agric. Food Chem.* **2009**, *57*, 9860−9866.
(34) Ley, J. P.; Krammer, G.; Reinders, G.; Gatfield, I. L.; Bertram, H. J. Evaluation of bitter masking flavanones from Herba Santa (Eriodictyon californicum (H. and A.) Torr., Hydrophyllaceae). *J. Agric. Food Chem.* **2005**, *53*, 6061−6066.
(35) Singldinger, B.; Dunkel, A.; Bahmann, D.; Bahmann, C.; Kadow, D.; Bisping, B.; Hofmann, T. New Taste-Active 3-(O-beta-d-Glucosyl)-2-oxoindole-3-acetic Acids and Diarylheptanoids in Cimiciato-Infected Hazelnuts. *J. Agric. Food Chem.* **2018**, *66*, 4660−4673.
(36) Szejtli, J.; Szente, L. Elimination of bitter, disgusting tastes of drugs and foods by cyclodextrins. *Eur. J. Pharm. Biopharm.* **2005**, *61*, 115−125.
(37) Wadhwa, J.; Puri, S. Taste Masking: A Novel Approch For Bitter And Obnoxious Drugs. *Int. J. Pharm. Prof.. Res* **2011**, *11*, 1−11.
(38) Intelmann, D.; Batram, C.; Kuhn, C.; Haseleu, G.; Meyerhof, W.; Hofmann, T. Three TAS2R Bitter Taste Receptors Mediate the Psychophysical Responses to Bitter Compounds of Hops (Humulus lupulus L.) and Beer. *Chemosens. Percept.* **2009**, *2*, 118−132.
(39) Glabasnia, A.; Dunkel, A.; Frank, O.; Hofmann, T. Decoding the Nonvolatile Sensometabolome of Orange Juice (Citrus sinensis). *J. Agric. Food Chem.* **2018**, *66*, 2354−2369.
(40) Stark, T.; Bareuther, S.; Hofmann, T. Molecular definition of the taste of roasted cocoa nibs (Theobroma cacao) by means of quantitative studies and sensory experiments. *J. Agric. Food Chem.* **2006**, *54*, 5530−5539.
(41) Intelmann, D.; Kummerlöwe, G.; Haseleu, G.; Desmer, N.; Schulze, K.; Fröhlich, R.; Frank, O.; Luy, B.; Hofmann, T. Structures of storage-induced transformation products of the beer's bitter principles, revealed by sophisticated NMR spectroscopic and LC-MS techniques. *Chemistry* **2009**, *15*, 13047−13058.
(42) Frank, O.; Kreissl, J. K.; Daschner, A.; Hofmann, T. Accurate determination of reference materials and natural isolates by means of quantitative (1)h NMR spectroscopy. *J. Agric. Food Chem.* **2014**, *62*, 2506−2515.
(43) Glabasnia, A.; Hofmann, T. Sensory-directed identification of taste-active ellagitannins in American (Quercus alba L.) and European oak wood (Quercus robur L.) and quantitative analysis in bourbon whiskey and oak-matured red wines. *J. Agric. Food Chem.* **2006**, *54*, 3380−3390.
(44) Hasegawa, S.; Berhow, M. A.; Fong, C. H., Analysis of Bitter Principles in Citrus. In *Fruit Analysis*; Linskens, H. F.; Jackson, J. F., Eds. Springer Berlin Heidelberg: Berlin, Heidelberg, 1996; pp. 59−80.
(45) Keast, R. S. J.; Roper, J. A complex relationship among chemical concentration, detection threshold, and suprathreshold intensity of bitter compounds. *Chem. Senses* **2007**, *32*, 245−253.
(46) Stoeger, V.; Liszt, K. I.; Lieder, B.; Wendelin, M.; Zopun, M.; Hans, J.; Ley, J. P.; Krammer, G. E.; Somoza, V. Identification of Bitter-Taste Intensity and Molecular Weight as Amino Acid Determinants for the Stimulating Mechanisms of Gastric Acid Secretion in Human Parietal Cells in Culture. *J. Agric. Food Chem.* **2018**, *66*, 6762−6771.
(47) Gillespie, M.; Jassal, B.; Stephan, R.; Milacic, M.; Rothfels, K.; Senff-Ribeiro, A.; Griss, J.; Sevilla, C.; Matthews, L.; Gong, C.; Deng, C.; Varusai, T.; Ragueneau, E.; Haider, Y.; May, B.; Shamovsky, V.; Weiser, J.; Brunson, T.; Sanati, N.; Beckman, L.; Shao, X.; Fabregat, A.; Sidiropoulos, K.; Murillo, J.; Viteri, G.; Cook, J.; Shorser, S.; Bader, G.; Demir, E.; Sander, C.; Haw, R.; Wu, G.; Stein, L.; Hermjakob, H.; D'Eustachio, P. The reactome pathway knowledgebase 2022. *Nucleic Acids Res.* **2022**, *50*, D687−D692.
(48) Siegel, S.; Castellan, N. J., *Non Parametric Statistics for the Behavioural Sciences*; MacGraw Hill Int.: New York: 1988.
(49) Narukawa, M.; Noga, C.; Ueno, Y.; Sato, T.; Misaka, T.; Watanabe, T. Evaluation of the bitterness of green tea catechins by a cell-based assay with the human bitter taste receptor hTAS2R39. *Biochem. Biophys. Res. Commun.* **2011**, *405*, 620−625.
(50) de Graaf, C.; Foata, N.; Engkvist, O.; Rognan, D. Molecular modeling of the second extracellular loop of G-protein coupled receptors and its implication on structure-based virtual screening. *Proteins* **2008**, *71*, 599−620.

(51) Born, S.; Levit, A.; Niv, M. Y.; Meyerhof, W.; Behrens, M. The human bitter taste receptor TAS2R10 is tailored to accommodate numerous diverse ligands. *J. Neurosci.* **2013**, *33*, 201−213.
(52) Jaiteh, M.; Rodríguez-Espigares, I.; Selent, J.; Carlsson, J. Performance of virtual screening against GPCR homology models: Impact of template selection and treatment of binding site plasticity. *PLoS Comput. Biol.* **2020**, *16*, No. e1007680.
(53) Nicoli, A.; Dunkel, A.; Giorgino, T.; de Graaf, C.; Di Pizio, A. Classification Model for the Second Extracellular Loop of Class A GPCRs. *J. Chem. Inf. Model.* **2022**, *62*, 511−522.
(54) Reichling, C.; Meyerhof, W.; Behrens, M. Functions of human bitter taste receptors depend on N-glycosylation. *J. Neurochem.* **2008**, *106*, 1138−1148.
(55) Meyerhof, W. Elucidation of mammalian bitter taste. *Rev. Physiol., Biochem. Pharmacol.* **2005**, *154*, 37−72.
(56) Behrens, M.; Brockhoff, A.; Kuhn, C.; Bufe, B.; Winnig, M.; Meyerhof, W. The human taste receptor hTAS2R14 responds to a variety of different bitter compounds. *Biochem. Biophys. Res. Commun.* **2004**, *319*, 479−485.
(57) Workman, A. D.; Palmer, J. N.; Adappa, N. D.; Cohen, N. A. The Role of Bitter and Sweet Taste Receptors in Upper Airway Immunity. *Curr. Allergy Asthma Rep.* **2015**, *15*, 72.
(58) Patel, N. N.; Workman, A. D.; Cohen, N. A. Role of Taste Receptors as Sentinels of Innate Immunity in the Upper Airway. *J. Pathog.* **2018**, *2018*, 9541987.
(59) Deshpande, D. A.; Wang, W. C. H.; McIlmoyle, E. L.; Robinett, K. S.; Schillinger, R. M.; An, S. S.; Sham, J. S.; Liggett, S. B. Bitter taste receptors on airway smooth muscle bronchodilate by localized calcium signaling and reverse obstruction. *Nat. Med.* **2010**, *16*, 1299−1304.
(60) Wu, S. V.; Rozengurt, N.; Yang, M.; Young, S. H.; Sinnett-Smith, J.; Rozengurt, E. Expression of bitter taste receptors of the T2R family in the gastrointestinal tract and enteroendocrine STC-1 cells. *Proc. Natl. Acad. Sci. U. S. A.* **2002**, *99*, 2392−2397.
(61) Singh, N.; Vrontakis, M.; Parkinson, F.; Chelikani, P. Functional bitter taste receptors are expressed in brain cells. *Biochem. Biophys. Res. Commun.* **2011**, *406*, 146−151.
(62) Deckmann, K.; Filipski, K.; Krasteva-Christ, G.; Fronius, M.; Althaus, M.; Rafiq, A.; Papadakis, T.; Renno, L.; Jurastow, I.; Wessels, L.; Wolff, M.; Schütz, B.; Weihe, E.; Chubanov, V.; Gudermann, T.; Klein, J.; Bschleipfer, T.; Kummer, W. Bitter triggers acetylcholine release from polymodal urethral chemosensory cells and bladder reflexes. *Proc. Natl. Acad. Sci. U. S. A.* **2014**, *111*, 8287−8292.
(63) Xu, J.; Cao, J.; Iguchi, N.; Riethmacher, D.; Huang, L. Functional characterization of bitter-taste receptors expressed in mammalian testis. *Mol. Hum. Reprod.* **2013**, *19*, 17−28.
(64) Malki, A.; Fiedler, J.; Fricke, K.; Ballweg, I.; Pfaffl, M. W.; Krautwurst, D. Class I odorant receptors, TAS1R and TAS2R taste receptors, are markers for subpopulations of circulating leukocytes. *J. Leukocyte Biol.* **2015**, *97*, 533−545.
(65) Li, Z. W.; Sun, B.; Gong, T.; Guo, S.; Zhang, J.; Wang, J.; Sugawara, A.; Jiang, M.; Yan, J.; Gurary, A.; Zheng, X.; Gao, B.; Xiao, S. Y.; Chen, W.; Ma, C.; Farrar, C.; Zhu, C.; Chan, O. T. M.; Xin, C.; Winnicki, A.; Winnicki, J.; Tang, M.; Park, R.; Winnicki, M.; Diener, K.; Wang, Z.; Liu, Q.; Chu, C. H.; Arter, Z. L.; Yue, P.; Alpert, L.; Hui, G. S.; Fei, P.; Turkson, J.; Yang, W.; Wu, G.; Tao, A.; Ramos, J. W.; Moisyadi, S.; Holcombe, R. F.; Jia, W.; Birnbaumer, L.; Zhou, X.; Chu, W. M. GNAI1 and GNAI3 Reduce Colitis-Associated Tumorigenesis in Mice by Blocking IL6 Signaling and Down-regulating Expression of GNAI2. *Gastroenterology* **2019**, *156*, 2297−2312.
(66) Luo, X. C.; Chen, Z. H.; Xue, J. B.; Zhao, D. X.; Lu, C.; Li, Y. H.; Li, S. M.; Du, Y. W.; Liu, Q.; Wang, P.; Liu, M.; Huang, L. Infection by the parasitic helminth Trichinella spiralis activates a Tas2r-mediated signaling pathway in intestinal tuft cells. *Proc. Natl. Acad. Sci. U. S. A.* **2019**, *116*, 5564−5569.
(67) Lee, R. J.; Chen, B.; Redding, K. M.; Margolskee, R. F.; Cohen, N. A. Mouse nasal epithelial innate immune responses to Pseudomonas aeruginosa quorum-sensing molecules require taste signaling components. *Innate Immun.* **2014**, *20*, 606−617.
(68) Grassin-Delyle, S.; Salvator, H.; Mantov, N.; Abrial, C.; Brollo, M.; Faisy, C.; Naline, E.; Couderc, L. J.; Devillier, P. Bitter Taste Receptors (TAS2Rs) in Human Lung Macrophages: Receptor Expression and Inhibitory Effects of TAS2R Agonists. *Front. Physiol.* **2019**, *10*, 1267.
(69) Soares, S.; Silva, M. S.; Garcia-Estevez, I.; Groβmann, P.; Brás, N.; Brandão, E.; Mateus, N.; de Freitas, V.; Behrens, M.; Meyerhof, W. Human Bitter Taste Receptors Are Activated by Different Classes of Polyphenols. *J. Agric. Food Chem.* **2018**, *66*, 8814−8823.
(70) Roland, W. S. U.; van Buren, L.; Gruppen, H.; Driesse, M.; Gouka, R. J.; Smit, G.; Vincken, J.-P. Bitter taste receptor activation by flavonoids and isoflavonoids: modeled structural requirements for activation of hTAS2R14 and hTAS2R39. *J. Agric. Food Chem.* **2013**, *61*, 10454−10466.
(71) Verkman, A. S. The quenching of an intramembrane fluorescent probe. A method to study the binding and permeation of phloretin through bilayers. *Biochim. Biophys. Acta, Biomembr.* **1980**, *599*, 370−379.
(72) Carmosino, M.; Procino, G.; Casavola, V.; Svelto, M.; Valenti, G. The cultured human gastric cells HGT-1 express the principal transporters involved in acid secretion. *Pfluegers Arch.* **2000**, *440*, 871−880.
(73) Beltrán, L. R.; Sterneder, S.; Hasural, A.; Paetz, S.; Hans, J.; Ley, J. P.; Somoza, V. Reducing the Bitter Taste of Pharmaceuticals Using Cell-Based Identification of Bitter-Masking Compounds. *Pharmaceuticals (Basel)* **2022**, *15*, 317.
(74) Chandrashekar, J.; Mueller, K. L.; Hoon, M. A.; Adler, E.; Feng, L.; Guo, W.; Zuker, C. S.; Ryba, N. J. P. T2Rs Function as Bitter Taste Receptors. *Cell* **2000**, *100*, 703−711.
(75) Offermanns, S.; Simon, M. I. Gα15 and Gα16 Couple a Wide Variety of Receptors to Phospholipase C. *J. Biol. Chem.* **1995**, *270*, 15175−15180.
(76) Kohl, S.; Behrens, M.; Dunkel, A.; Hofmann, T.; Meyerhof, W. Amino acids and peptides activate at least five members of the human bitter taste receptor family. *J. Agric. Food Chem.* **2013**, *61*, 53−60.
(77) Slack, J. P.; Brockhoff, A.; Batram, C.; Menzel, S.; Sonnabend, C.; Born, S.; Galindo, M. M.; Kohl, S.; Thalmann, S.; Ostopovici-Halip, L.; Simons, C. T.; Ungureanu, I.; Duineveld, K.; Bologa, C. G.; Behrens, M.; Furrer, S.; Oprea, T. I.; Meyerhof, W. Modulation of bitter taste perception by a small molecule hTAS2R antagonist. *Curr. Biol.* **2010**, *20*, 1104−1109.
(78) Stand., I. *Technical Committee ISO/TC 34. ISO 13301:2018, Sensory Analysis — Methodology — General Guidance for Measuring Odour , Flavour and Taste Detection*; Elsevier Inc. 2018 .
(79) Dragoş, D.; Petran, M.; Gradinaru, T. C.; Gilca, M. Phytochemicals and Inflammation: Is Bitter Better? *Plants* **2022**, *11*, 2991.

https://doi.org/10.1021/acs.jafc.2c06979
J. Agric. Food Chem. 2023, 71, 5314−5325

Supplemental material to

Human Gingival Fibroblasts as a Novel Cell Model Describing the Association between Bitter Taste Thresholds and Interleukin-6 Release

Johanna Tiroch[1,2], Andreas Dunkel[3], Sonja Sterneder[1,2], Sofie Zehentner[1,2], Maik Behrens[3], Antonella Di Pizio[3], Jakob P. Ley[4], Barbara Lieder[1], Veronika Somoza[1,3,5]

Tables

Table S1.

Calculated molecular descriptors of the selected compounds: molecular weight (MW), lipophilic parameter (AlogP) and hydrogen bond acceptor/donor (HBA and HBD).

Compound	MW [g/mol]	AlogP	HBA	HBD
EGCG	458.38	2.89	11	8
IsoSNT	372.38	3.79	7	0
NAR	580.55	-0.47	14	8
QHCl	324.43	2.73	3	1
RSV	228.25	3.01	3	3
SNT	372.38	3.79	7	0

Table S2.

Results of HGT-1 and HGF-1 cell viability by means of MTT shown in percent.

	Cell viability [%] of	
	HGF-1	**HGT-1**
CAB 500 µM	105.3 ± 7.6	102.9 ± 10.4
DIOS 1 µM	96.0 ± 5.5	100.9 ± 9.3
EGCG 100 µM	100.5 ± 5.4	115.9 ± 4.0 (1mM)
IsoA 35.7 ppm	100.1 ± 5.7	94.2 ± 5.5
IsoSNT 25 µM	101.3 ± 6.2	100.7 ± 6.00 (0.1 µM)
L – Arg 50000 µM	99.1 ± 4.6	Stöger et al.,2018[1]
NAR 500 µM	100.7 ± 5.9	Liszt et al., 2017[2]
QHCl 40 µM	100.5 ± 10.1	106.2 ± 6.0
RSV 250 µM	103.1 ± 10.5	100 µM Tiroch et al.,2021[3]
SNT 50 µM	102.3 ± 10.2	97.2 ± 6.8
THEO 250 µM	101.0 ± 6.1	Liszt et al., 2017[2]
MAT 50µM	100.2 ± 6.1	Liszt et al., 2017[2]
HED 50 µM	100.6 ± 3.1	Liszt et al., 2017[2]

[a] Data are indicated as mean ± SD and calculated as treatment over control (non - treated cells, set to 100 %). Calculations were made from n = 3-4 and n t.r.=3. HGF-1 cells were co-incubated with *Pg*-LPS [10 µg/mL] for 6 hr. Statistics: One way ANOVA, no significant differences compared to non – treated cells, calculation for each cell line respectively.

Figure captions

Figure S1.

(A) Pathway network of TAS2R50, and IL-6 pathway by reactom. (B) Immunofluorescence analysis of GNAI3 in HGF-1 cells. Cells were stained with: DAPI (blue) as counter stain, ActinRed (red), primary 1:200 (# PA5-27940, Invivogen) or the control (lower part) without and stained with 1:200 Alexa Fluor® 488 tag (ab150081, abcam) (green).

Figure S2.

Dose-response experiments of SNT – sinensetin (0.1 – 50 µM), NAR – naringin (0.1-500 µM, EGCG – epigallocatechin gallate (0.1 – 100 µM), QHCl - quinine HCl (0.1 – 40 µM). Data are shown as raw data points from individual passages connected by black lines, overall fit coloured line: n=3 - 4 t.r. = 2.

Figure S3.

3D representation of the docking poses of RSV, NAR, SNT, EGCG and QHCl (shown as green sticks) into the TAS2R50 binding pocket. Ligand-interacting residues are shown as grey sticks, hydrogen bonds are shown as purple dashed lines, and the π−π stacking with blue lines. Docking and MM-GBSA scores of RSV, NAR, SNT, EGCG & QHCl in complex with TAS2R50, and predicted ligand interacting residues.

Figure S4.

Antagonistic effect of 10 µM MAT in TAS2R4 and TAS2R43 transfected HEK – 293T-Gα16gust44 cells by co-administration with TAS2R43 agonist aristocholic acid (0.3 µM) and TAS2R4 agonist colchicine (1 mM). Activations caused by agonists alone were set to 100%. Statistics: T-test: * $p < 0.05$, ** $p < 0.01$;n = 2, t.r. = 2

Figure S1.

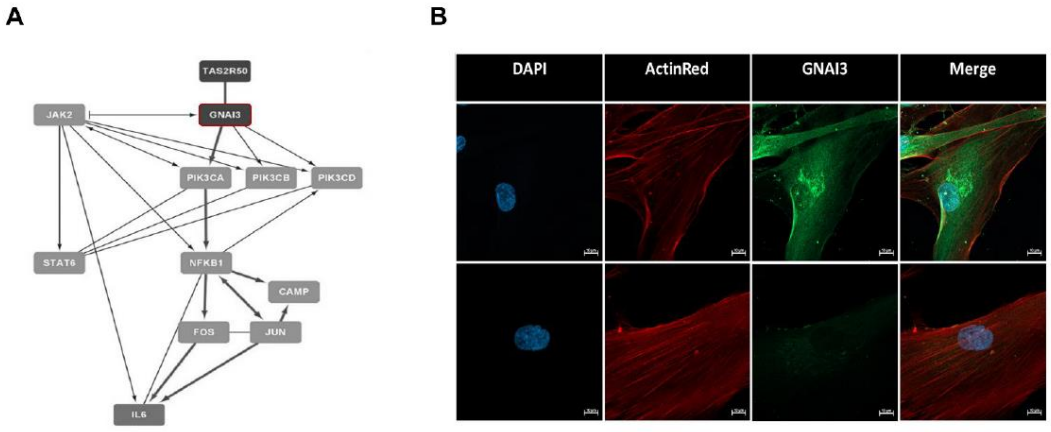
A
B
TAS2R50
JAK2
GNAI3
PIK3CA
PIK3CB
PIK3CD
STAT6
NFKB1
CAMP
FOS
JUN
IL6
DAPI
ActinRed
GNAI3
Merge

Figure S 2.

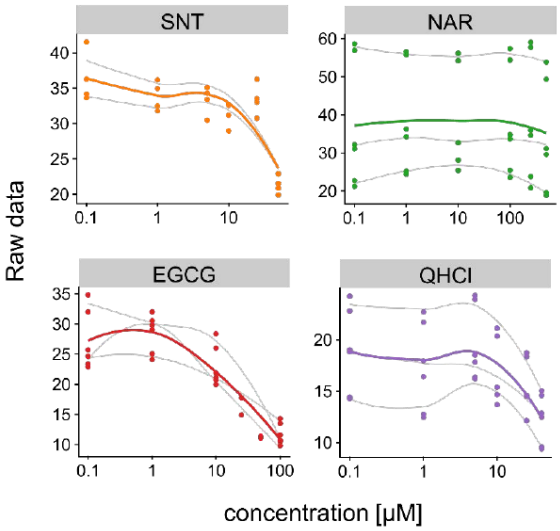

Figure S 3.

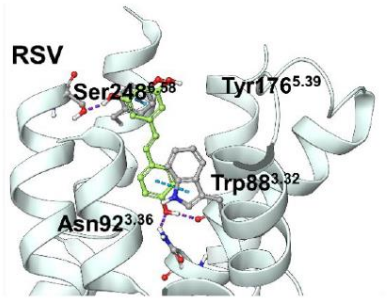

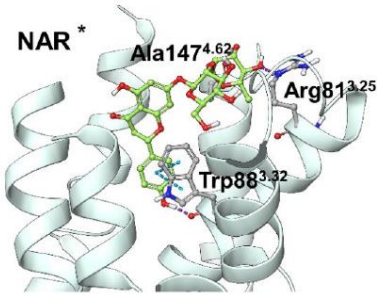

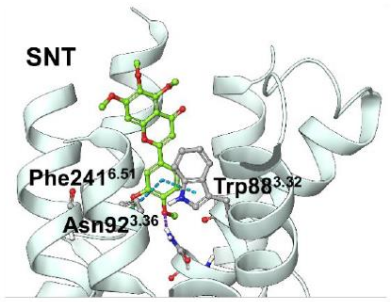

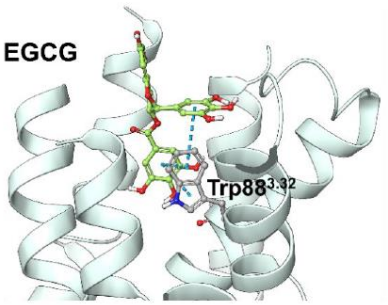

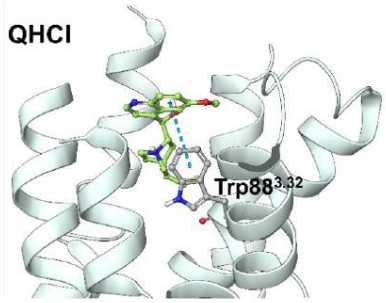

Ligand	Glide score [kcal/mol]	MM-GBSA dG Bind [kcal/mol]
RSV	-8.83	-72.21
NAR	-8.15	-89.63
SNT	-7.54	-75.03
EGCG	-5.15	-37.67
QHCl	-3.00	7.58

* At the core of the binding site, NAR could establish interactions similar to those observed for SNT and RVS. However, because of its size, NAR binding could be affected by the ECL2, though, we cannot evaluate this possibility with our model.

Figure S4.

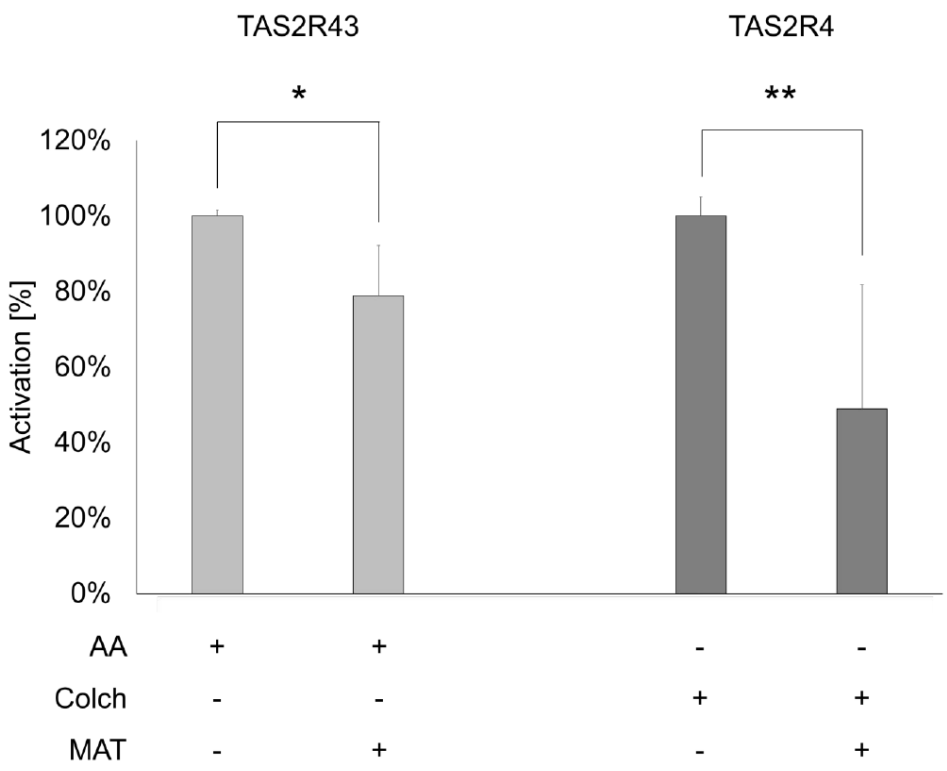

7

6 Conclusions and Perspectives

The aim of this research was to investigate whether human gingival fibroblasts (HGF-1 cells) are equipped with TAS2Rs and what role these bitter taste sensing chemoreceptors play in a bitter taste compound's evoked anti-inflammatory response by *Pg*-LPS treated HGF-1 cells. Furthermore, research was conducted to evaluate the suitability of HGF-1 cells as an alternative cellular model for identifying bitter-tasting compounds.

The first study titled "*Bitter Sensing TAS2R50 Mediates the trans-Resveratrol-Induced Anti-inflammatory Effect on Interleukin 6 Release in HGF-1 Cells in Culture*" investigated the anti-inflammatory activity of bitter tasting-substances, namely resveratrol (RSV) and rosmarinic acid (RA), and the role of bitter taste receptors (TAS2Rs) in HGF-1 cells. First, a sensory study was conducted to compare the bitterness of RSV and RA, with RSV being found more bitter. Homoeriodictyol (HED), a bitter masking compound, was used in a sensory test to confirm the general involvement of TAS2Rs. In addition, the intracellular proton index (IPX) was analysed in the RA- and RSV-treated HGT-1 human gastric cancer cell line as well-established cell model for the identification of bitter tasting and bitter taste modulating compounds to demonstrate the effect of bitterness on a cellular level. [24,25,123,124] In this model, the more bitter a substance remains the more protons are pumped out of the cells, which leads to a decreasing intracellular proton concentration. [24,25,123,124] The functional roles of RSV and RA on IPX values were confirmed, as shown in previous results. Moreover, their anti-inflammatory activity was evaluated by measuring their impact on IL-6 release induced by *Pg*-LPS in HGF-1 cells. To investigate which TAS2Rs may be involved, RSV was tested with and without the presence of the bitter masking compound HED (TAS2R20/31/43/50) [25] in HGF-1 cells using real-time quantitative PCR. The data indicated that TAS2R50 was involved, which was confirmed on a functional level by means of an siRNA knock-down approach. Furthermore, in silica computational modelling approaches suggested that RSV could bind to the hydrophobic pockets of TAS2R50.

In conclusion, the study demonstrated (1) that HGF-1 cells express TAS2Rs, and (2) that TAS2R50 plays a functional role in the anti-inflammatory activity of RSV in *Pg*-LPS treated HGF-1 cells. This finding suggests that TAS2R50 may be a promising target for the development of novel therapeutic agents for the treatment of inflammatory diseases in the oral cavity. It is worth noting that previous studies have also reported the involvement of bitter taste receptors, including TAS2Rs, in immune responses and inflammation in the oral cavity. For example, a study showed that TAS2Rs were recently detected in primary gingival epithelial cells, with the TAS2R14 recognising quorum sensing molecules from *Streptococcus mutans*, a cariogenic bacterium, and mediating an immune response via IL-6, TNF-α, CXCL-8/IL-8 release. [125]

Furthermore, a recent cross-sectional study examined the correlation between TAS2R genotypes and oral health, specifically markers for oral inflammation and unstimulated salivary flow rate. The study found that TAS2R4-rs2233998, TAS2R5-rs2227264, TAS2R50-rs1376251, and TAS2R9-rs3741845 were positively associated with a higher mean of unstimulated salivary flow rate. [126] However, an increased salivary flow rate is generally thought to be linked to higher inflammation and poor oral hygiene. [127] Additionally, the study revealed that TAS2R4-rs2234001, TAS2R4-rs2233998, and TAS2R9-rs3741845 were also associated with the number of decayed, missing, and filled teeth in the permanent teeth (DMFT-index). [126]

The conclusion of the first paper posed the question for the second study entitled "*Human Gingival Fibroblasts as a Novel Cell Model Describing the Relationship between Bitter Taste Thresholds and Pro-Inflammatory IL-6 Release*" (2). Specifically, the question was whether other plant constituents that a bitter taste have can reduce the release of IL-6 in *Pg*-LPS treated HGF-1 cells, and if there are other bitter taste receptors involved besides TAS2R50. Another main objective of this study was to investigate if there is a correlation between a compound's bitter taste threshold and its anti-inflammatory activity on the *Pg*-LPS evoked IL-6 release in HGF-1 cells.

According to a recent study by Zhou et al., HGF-1 cells do express nearly all the TAS2Rs genes identified so far. [128] In the study presented here, the TAS2R50 pathway was analysed using reactome [129], and confirmed through immunofluorescence staining. The results demonstrate the relevance of GNAI3 in the signaling of TAS2R50 and IL-6 release. Additionally, another recent study on signaling in HGF-1 cells indicated that TRPM4, rather than TRPM5, plays a critical role in the signal transduction of TAS2Rs. [128] It was also found that HGF-1 cells contain the G Protein Subunit Alpha Transducin 3 (GNAT-3) which is essential for TAS2R downstream signaling. [128]

To investigate additional substances that may potentially involve TAS2R50 in anti-inflammatory effects, further test compounds were selected from the chemical bitter space. The chemical bitter space is a 2D t-SNE plot distribution based on fingerprints, and includes a variety of bitter substances categorized into different superclasses. [2] From this dataset, a diverse set of bitter substances was selected for further analysis. Firstly, four TAS2R agonists were chosen for the study based on their structural similarities. These included epigallocatechin gallate (EGCG), naringin (NAR), and sinensetin (SNT). In addition, one TAS2R agonist with a structurally distinct composition, quinine hydrochloride (QHCl), was also selected. All selected compounds were tested for their ability to reduce the IL-6 release in *Pg*-LPS treated HGF-1 cells. Results showed that all compounds demonstrated a reducing effect on the *Pg*-LPS evoked IL-6 release. Since in the first part of this work, TAS2R50 was shown to be involved in the anti-inflammatory effect of

RSV, TAS2R50 involvement was hypothesized in this part as well. To test this receptor specificity, molecular docking studies were performed to assess the compounds' potential binding to TAS2R50. This analysis revealed a molecular interaction of Trp88$^{3.32}$ and Asn92$^{3.36}$ for SNT. NAR was excluded due to its possible interaction with the extra cellular loop. EGCG and QHCl showed a drop in the docking score compared to SNT and were missing the interaction with Asn92$^{3.36}$. This interaction might be essential for ligand recognition and activation of TAS2Rs [130]. The results suggested that other TAS2Rs might be involved because there was no correlation between the docking score and the reduction in *Pg*-LPS evoked IL-6 release caused by the bitter-tasting compounds selected.

Involvement of other TAS2Rs than TAS2R50 was also tested by co-incubation experiments using the selected bitter-tasting compounds and one of the two bitter-masking compounds, HED and matairesinol (TAS2R43/4 shown in (2) publication). The results of these experiments revealed an involvement of other TAS2Rs beside TAS2R50, as only HED, targeting TAS2R14/20/31/39/43/50 [25], was able to abolish the anti-inflammatory effect of only SNT and QHCL on the *Pg*-LPS-evoked IL-6 release in HGF-1 cells, whereas MAT was effective in all co-incubation experiments. To test the robustness of this system, seven additional substances, comprising carpinontriol B (CAB), dioscin (DIOS), iso-alpha acids (IsoA), isosinensetin (IsoSNT), L-arginine (L-Arg), RSV and theobromine (THEO), were tested in at least six different concentrations for their anti-inflammatory effect on the IL-6 release evoked by *Pg*-LPS in HGF-1 cells. The data achieved were used to calculate the 25 % inhibitory concentration on IL-6 release, which was then found to significantly correlate with the test compounds' bitter taste threshold (R^2: 0.60, $p < 0.01$). The bitter taste compounds' response revealed from this HGF-1 cell model, was compared to results from the well-established HGT-1 cell model. This model has already been well-established for the identification of bitter tasting and bitter taste modulating compounds. [23–25,59,131] Correlation analysis between the compounds' bitter taste threshold concentration and the intracellular proton index, analysed as an outcome measure of TAS2R-associated proton secretion, revealed no statistically significant association (R^2: 0.153, $p > 0.05$), making the here established HGF-1 cell model a superior approach for the identification of bitter tasting compounds.

In conclusion, this second study showed that HGF-1 cells do express several TAS2Rs genes, of which at least TAS2R50 is functionally involved in modulating the release of IL-6 by HGF-1 cells after *Pg*-LPS treatment. Quite recently, in 2021, a functional role of TAS2R16 in the *E. coli* LPS-induced cytokine expression in HGF-1 cells has been published. In this study, a TAS2R16 activation by salicin points to an anti-inflammatory role of TAS2R16 via inhibition of the NF-κB signalling cascade. [128] Furthermore, bitter taste receptors were detected recently also in gingival

epithelial cells. [125] In this study, the authors demonstrated that TAS2R14 recognises quorum sensing molecules from *Streptococcus mutans*, a cariogenic bacterium, and mediates an immune response via IL-6, TNF-α, CXCL-8/IL-8 release. [125]

An overall conclusion of this thesis is that the native cell model HGF-1 cells has been demonstrated to be a suitable native cell model for the identification and may also be used to predict bitter-tasting substances. One of the clear advantages of the HGT-1 cell model over sensory tests is that not toxicity data and only very small amounts of the compounds to be tested are needed.

Moreover, the here presented cell model might also be suitable for the identification and prediction of anti-inflammatory compounds based on their bitter taste. This perspective is of current interest and was followed by Dragos et al. in the last year 2022, who performed a meta-analysis using MoleculareTasteDB and current literature. The results showed that bitter phytochemicals act on more inflammation-related targets than non-bitter-tasting compounds. [132] Another recent review by Dong et al., also published in the year 2022, discussed the mediating effect of taste receptors, especially bitter and sweet taste receptors, on health-relevant microbiota-host interactions in the oral cavity. [133]

The here presented PhD thesis laid grounds for a novel native cell model for the identification of bitter tasting and bitter taste modulating compounds with potential anti-inflammatory activities. In the context of some bitter-tasting drugs [30] (antibiotics: chloramphenicol, erythromycin, and ofloxacin; anti-malarial drugs: quinine and chloroquine; analgesics: acetamonifen; thyrostatic agents: metimazole and propylthiouracil) [4,74] , this newfound knowledge may (1) establish a new high throughput technology to test bitter tasting substances via the HGF-1 cells and their IL-6 release, and (2) help identify new potential targets.

Additional research is necessary to confirm, on a high throughput level, the potential of the here presented HGF-1 cell line as a novel cell model for identifying bitter-tasting and bitter taste modulating compounds. In future studies, it will be essential to determine which TAS2Rs are the most critical targets, leading to an anti-inflammatory response when activated. Furthermore, it is crucial to investigate whether this is a cascade of TAS2Rs or just one pathway, which discriminates against others. Additionally, the cellular signalling pathways are not yet fully understood, particularly if other cytokines or chemokines are activated or blocked, not only in HGF-1 cells but also in other, preferably primary cell types of various tissues. These additional investigations will help to establish new targets for a healthy oral cavity, which is of particular common interest since 3.5 billion people globally are currently suffering from inflammatory oral diseases, e.g., gingivitis.

7 References

1. Ahmad, R. & Dalziel, J. E. G Protein-Coupled Receptors in Taste Physiology and Pharmacology. *Front. Pharmacol.* **11**, (2020).

2. Dunkel, A., Hofmann, T. & Di Pizio, A. In Silico Investigation of Bitter Hop-Derived Compounds and Their Cognate Bitter Taste Receptors. *J. Agric. Food Chem.* **68**, 10414–10423 (2020).

3. Kinnamon, S. C. & Finger, T. E. Recent advances in taste transduction and signaling [version 1 ; peer review : 2 approved]. *F1000Research* **8**, 1–11 (2019).

4. Kamila, T. & Agnieszka, K. *An update on extra-oral bitter taste receptors*. *Journal of Translational Medicine* vol. 19 (BioMed Central, 2021).

5. Lu, Y., Yeh, W. & Ohashi, P. S. LPS / TLR4 signal transduction pathway. *Cytokine* **42**, 145–151 (2008).

6. Soto-Barreras, U. *et al.* Stimulatory effect of Aggregatibacter actinomycetemcomitans DNA on proinflammatory cytokine expression by human gingival fibroblasts. *Arch. Oral Biol.* **82**, 127–133 (2017).

7. Behrens, M., Foerster, S., Staehler, F., Raguse, J. & Meyerhof, W. Gustatory Expression Pattern of the Human TAS2R Bitter Receptor Gene Family Reveals a Heterogenous Population of Bitter Responsive Taste Receptor Cells. **27**, 12630–12640 (2007).

8. Spaggiari, G., Di Pizio, A. & Cozzini, P. Sweet, umami and bitter taste receptors: State of the art of in silico molecular modeling approaches. *Trends Food Sci. Technol.* **96**, 21–29 (2020).

9. Wu, S. V. *et al.* Expression of bitter taste receptors of the T2R family in the gastrointestinal tract and enteroendocrine STC-1 cells. *Proc. Natl. Acad. Sci.* **99**, 2392–2397 (2002).

10. Finger, T. E. *et al.* Solitary chemoreceptor cells in the nasal cavity serve as sentinels of respiration. *Proc. Natl. Acad. Sci. U. S. A.* **100**, 8981–8986 (2003).

11. Deshpande, D. A. *et al.* Bitter taste receptors on airway smooth muscle bronchodilate by localized calcium signaling and reverse obstruction. *Nat. Med.* **16**, 1299–1304 (2010).

12. Manson, M. L. *et al.* Bitter taste receptor agonists mediate relaxation of human and

rodent vascular smooth muscle. *Eur. J. Pharmacol.* **740**, 302–311 (2014).

13. Zhai, K. *et al.* Activation of bitter taste receptors (tas2rs) relaxes detrusor smooth muscle and suppresses overactive bladder symptoms. *Oncotarget* **7**, 21156–21167 (2016).

14. Lee, S.-J., Depoortere, I. & Hatt, H. Therapeutic potential of ectopic olfactory and taste receptors. *Nat. Rev. Drug Discov.* **18**, 116–138 (2019).

15. Riedel, K., Sombroek, D., Fiedler, B., Siems, K. & Krohn, M. Human cell-based taste perception - a bittersweet job for industry. *Nat. Prod. Rep.* **34**, 484–495 (2017).

16. Running, C. A. High false positive rates in common sensory threshold tests. *Attention, Perception, Psychophys.* **77**, 692–700 (2015).

17. Dagan-Wiener, A. *et al.* Bitterdb: Taste ligands and receptors database in 2019. *Nucleic Acids Res.* **47**, D1179–D1185 (2019).

18. Luo, G., Somoza, V. & Dunkel, A. https://fsbi-db.de/. *Food Systems Biology Database (FSBI-DB), Leibniz Institute for Food Systems Biology at the Technical University of Munich, Freising, Germany* (2021).

19. Latha, R. S. & Lakshmi, P. K. Electronic tongue: An analytical gustatory tool. *J. Adv. Pharm. Technol. Res.* **3**, 3–8 (2012).

20. Podrazka, M., Báczyńska, E., Kundys, M., Jeleń, P. S. & Nery, E. W. Electronic tongue-A tool for all tastes? *Biosensors* **8**, 1–24 (2017).

21. Hochheimer, A. *et al.* Endogenous Gustatory Responses and Gene Expression Profile of Stably Proliferating Human Taste Cells Isolated From Fungiform Papillae. 359–377 (2014) doi:10.1093/chemse/bju009.

22. Ozdener, H., Spielman, A. I. & Rawson, N. E. Isolation and Culture of Human Fungiform Taste Papillae Cells 3 . Culturing of Human Fungiform Taste Papillae Cells. 2–7 (2012) doi:10.3791/3730.

23. Walker, J. *et al.* Identification of beer bitter acids regulating mechanisms of gastric acid secretion. *J. Agric. Food Chem.* **60**, 1405–1412 (2012).

24. Liszt, K. I., Hans, J., Ley, J. P., Köck, E. & Somoza, V. Characterization of Bitter Compounds via Modulation of Proton Secretion in Human Gastric Parietal Cells in Culture. *J. Agric. Food Chem.* **66**, 2295–2300 (2018).

25. Liszt, K. I. *et al.* Caffeine induces gastric acid secretion via bitter taste signaling in gastric parietal cells. *Proc. Natl. Acad. Sci. U.S.A.* **114**, E6260–E6269 (2017).

26. Bufe, B., Hofmann, T., Krautwurst, D., Raguse, J. & Meyerhof, W. The human TAS2R16 receptor mediates bitter taste in response to β-glucopyranosides. *Nat. Genet.* **32**, 397–401 (2002).

27. Meyerhof, W. *et al.* The Molecular Receptive Ranges of Human TAS2R Bitter Taste Receptors. *Chem. Senses* **35**, 157–170 (2010).

28. Ueda, T., Ugawa, S., Yamamura, H., Imaizumi, Y. & Shimada, S. Functional Interaction between T2R Taste Receptors and G-Protein α Subunits Expressed in Taste Receptor Cells. *J. Neurosci.* **23**, 7376–7380 (2003).

29. Behrens, M. *et al.* The human taste receptor hTAS2R14 responds to a variety of different bitter compounds. *Biochem. Biophys. Res. Commun.* **319**, 479–485 (2004).

30. Beltrán, L. R. *et al.* Reducing the Bitter Taste of Pharmaceuticals Using Cell-Based Identification of Bitter-Masking Compounds. *Pharmaceuticals* **15**, 317 (2022).

31. Walker, J. M. *et al.* Identification of Magnolia officinalis L. Bark Extract as the Most Potent Anti-Inflammatory of Four Plant Extracts. *Am. J. Chin. Med.* **41**, 531–544 (2013).

32. Workman, A. D., Palmer, J. N., Adappa, N. D. & Cohen, N. A. The Role of Bitter and Sweet Taste Receptors in Upper Airway Immunity. *Curr. Allergy Asthma Rep.* **15**, 72 (2015).

33. Gil, S. *et al.* Genotype-specific regulation of oral innate immunity by T2R38 taste receptor. *Mol. Immunol.* **68**, 663–670 (2015).

34. Shaw, L. *et al.* Personalized expression of bitter ‘taste’ receptors in human skin. *PLoS One* **13**, 1–18 (2018).

35. Deckmann, K. *et al.* Bitter triggers acetylcholine release from polymodal urethral chemosensory cells and bladder reflexes. *Proc. Natl. Acad. Sci.* **111**, 8287–8292 (2014).

36. Lee, R. J. *et al.* Bitter and sweet taste receptors regulate human upper respiratory innate immunity. *J. Clin. Invest.* **124**, 1393–1405 (2014).

37. Lee, R. J. & Cohen, N. A. Role of the bitter taste receptor T2R38 in upper respiratory infection and chronic rhinosinusitis. *Curr. Opin. Allergy Clin. Immunol.* **15**, 14–20 (2015).

38. Patel, N. N., Workman, A. D. & Cohen, N. A. Role of Taste Receptors as Sentinels of Innate Immunity in the Upper Airway. *J. Pathog.* **2018**, 1–8 (2018).

39. Witt, M. *Handbook of Clinical Neurology*. *Anatomy and development of the human taste system* vol. 164 (Elsevier B.V., 2019).

40. Witt, M., Rf, K. & Er, U. Embryonic and Early Fetal Development of Human Taste Buds : A Transmission Electron Microscopical Study. **523**, (1996).

41. Witt, M. Anatomy and development of the human taste system. in *Handbook of Clinical Neurology* vol. 164 147–171 (Elsevier, 2019).

42. Roper, S. D. & Chaudhari, N. Taste buds: cells, signals and synapses. *Nat. Rev. Neurosci.* **18**, 485–497 (2017).

43. Cygankiewicz, A. I. *et al.* Molecular basis of taste sense: involvement of GPCR receptors. *Crit. Rev. Food Sci. Nutr.* **54**, 771–780 (2014).

44. Calvo, S. S. & Egan, J. M. The endocrinology of taste receptors. *Nat. Rev. Endocrinol.* **11**, 213–227 (2015).

45. Behrens, M., Gunn, H. C., Ramos, P. C. M., Meyerhof, W. & Wooding, S. P. Genetic, functional, and phenotypic diversity in TAS2R38-mediated bitter taste perception. *Chem. Senses* **38**, 475–484 (2013).

46. Amerine, M. A., Roessler, E. B. & Pangborn, R. M. *Principles of Sensory Evaluation of Food*. (Elsevier, 1965). doi:10.1016/C2013-0-08103-0.

47. Caul, J. F. The Profile Method of Flavor Analysis. in 1–40 (1957). doi:10.1016/S0065-2628(08)60245-1.

48. DIN-EN-ISO. in *Sensory analysis - General guidelines for the selection, training and monitoring of selected assessors and expert sensory assessors.* German version, DIN EN ISO 8586:2014-05. (International Organization for Standardization, 2014).

49. DIN-EN-ISO. in *Sensory analysis - Methodology - Method of investigating sensitivity of taste (ISO 3972:2011 + Cor. 1:2012).* DIN-EN-ISO-3972:2013-12 (International Organization for Standardization, 2011).

50. Busch-stockfisch, M. & Höhl, K. The influence of sensory training on taste sensitivity. Effects on sweet and bitter perception over a half-year period. *Ernährungs Umschau* **62**,

208–215 (2015).

51. Kuhn, C. *et al.* Bitter taste receptors for saccharin and acesulfame K. *J. Neurosci.* **24**, 10260–10265 (2004).

52. Civille, G. V. & Carr, B. T. *Sensory Evaluation Techniques*. (CRC Press, 2015).

53. Kingdom, F. A. A. & Prins, N. *Psychophysics A Practical Introduction*. (Elsevier, 2010).

54. Morgan, M. J., Melmoth, D. & Solomon, J. A. Linking hypotheses underlying Class A and Class B methods. *Vis. Neurosci.* **30**, 197–206 (2013).

55. Nevin, J. A. Signal detection theory and operant behavior: A Review of David M. Green and John A. Swets' Signal Detection Theory and Psychophysics. 1. *J. Exp. Anal. Behav.* **12**, 475–480 (1969).

56. Jäkel, F. & Wichmann, F. A. Spatial four-alternative forced-choice method is the preferred psychophysical method for naïve observers. *J. Vis.* **6**, 1307–1322 (2006).

57. Technical Committee ISO/TC 34. ISO 13301:2018, Sensory analysis — Methodology — General guidance for measuring odour , flavour and taste detection. *Int. Stand.* (2018).

58. Lawless, H. T. & Heymann, H. Time-Intensity Methods. in 265–300 (1999). doi:10.1007/978-1-4419-7452-5_8.

59. Weiss, C. *et al.* Measurement of the intracellular ph in human stomach cells: A novel approach to evaluate the gastric acid secretory potential of coffee beverages. *J. Agric. Food Chem.* **58**, 1976–1985 (2010).

60. Carmosino, M., Procino, G., Casavola, V., Svelto, M. & Valenti, G. The cultured human gastric cells HGT-1 express the principal transporters involved in acid secretion. *Pflugers Arch. Eur. J. Physiol.* **440**, 871–880 (2000).

61. Verkman, A. S. The quenching of an intramembrane fluorescent probe. A method to study the binding and permeation of phloretin through bilayers. *Biochim. Biophys. Acta - Biomembr.* **599**, 370–379 (1980).

62. Wiener, A., Shudler, M., Levit, A. & Niv, M. Y. BitterDB : a database of bitter compounds. *Nucleic Acids Res.* **40**, D413–D419 (2012).

63. Brockhoff, A., Behrens, M., Niv, M. Y. & Meyerhof, W. Structural requirements of bitter

taste receptor activation. *Proc. Natl. Acad. Sci.* **107**, 11110–11115 (2010).

64. an der Maaten, L. & Hinto, G. Visualizing Data using t-SNE. *J. Mach. Learn. Res.* **9**, 2579–2605 (2008).

65. Bayer, S. *et al.* Chemoinformatics View on Bitter Taste Receptor Agonists in Food. *J. Agric. Food Chem.* **69**, 13916–13924 (2021).

66. Wang, Q., Liszt, K. I. & Depoortere, I. Extra-oral bitter taste receptors: New targets against obesity? *Peptides* **127**, 170284 (2020).

67. Liszt, K. I. *et al.* Human intestinal bitter taste receptors regulate innate immune responses and metabolic regulators in obesity. *J. Clin. Invest.* **132**, 1–16 (2022).

68. Nayak, A. P., Shah, S. D., Michael, J. V & Deshpande, D. A. Bitter Taste Receptors for Asthma Therapeutics. **10**, (2019).

69. Grassin-Delyle, S. *et al.* Bitter Taste Receptors (TAS2Rs) in Human Lung Macrophages: Receptor Expression and Inhibitory Effects of TAS2R Agonists. *Front. Physiol.* **10**, 1–13 (2019).

70. Malki, A. *et al.* Class I odorant receptors, TAS1R and TAS2R taste receptors, are markers for subpopulations of circulating leukocytes. *J. Leukoc. Biol.* **97**, 533–545 (2015).

71. Tran, H. T. T. T., Herz, C., Ruf, P., Stetter, R. & Lamy, E. Human T2R38 bitter taste receptor expression in resting and activated lymphocytes. *Front. Immunol.* **9**, (2018).

72. Prasad, A. S. Clinical, immunological, anti-inflammatory and antioxidant roles of zinc. *Exp. Gerontol.* **43**, 370–377 (2008).

73. Soares, S. *et al.* Human Bitter Taste Receptors Are Activated by Different Classes of Polyphenols. *J. Agric. Food Chem.* **66**, 8814–8823 (2018).

74. Clark, A. A., Liggett, S. B. & Munger, S. D. Extraoral bitter taste receptors as mediators of off-target drug effects. *FASEB J.* **26**, 4827–4831 (2012).

75. Kazius, J. *et al.* GPCR NaVa database: natural variants in human G protein-coupled receptors. *Hum. Mutat.* **29**, 39–44 (2008).

76. Behrens, M. & Lang, T. Extra-Oral Taste Receptors—Function, Disease, and Perspectives. *Front. Nutr.* **9**, 1–7 (2022).

77. Beaglehole, R., Habib, B., Crail, J. & Mackay, J. *The oral health atlas: mapping a neglected global health issue.* (2009).

78. FDI, W. D. F. The Challenge of Oral Disease – A call for global action. The Oral Health Atlas. **2nd ed.**, (2015).

79. Peres, M. A. *et al.* Oral diseases: a global public health challenge. *Lancet* **394**, 249–260 (2019).

80. Wade, W. G. The oral microbiome in health and disease. *Pharmacol. Res.* **69**, 137–143 (2013).

81. Dentino, A., Lee, S., Mailhot, J. & Hefti, A. F. Principles of periodontology. *Periodontol. 2000* **61**, 16–53 (2013).

82. Darveau, R. P. Periodontitis: a polymicrobial disruption of host homeostasis. *Nat. Rev. Microbiol.* **8**, 481–490 (2010).

83. Socransky, S. S., Haffajee, A. D., Cugini, M. A., Smith, C. & Kent, R. L. Microbial complexes in subgingival plaque. *J. Clin. Periodontol.* **25**, 134–144 (1998).

84. Coventry, J., Griffiths, G., Scully, C. & Tonetti, M. ABC of oral health: Periodontal disease. *BMJ* **321**, 36–39 (2000).

85. Graves, D. Tissue Destruction. *Periodontology* **79**, 1585–1591 (2008).

86. Singh, A. *et al.* The Capsule of Porphyromonas gingivalis Leads to a Reduction in the Host Inflammatory Response , Evasion of Phagocytosis , and Increase in Virulence □ †. *Infect. Immun.* **79**, 4533–4542 (2011).

87. Alberts, B., Alexander, Johnson Lewis, J., Martin, R., Roberts, K. & Walter, P. Molecular Biology of the Cell. in (Garland Science, 2002).

88. Neumann, J. *et al.* Chronic Inflammation Under the Microscope. *Micros. Today* **24**, 38–45 (2016).

89. Ogawa, T., Asai, Y., Makimura, Y. & Tamai, R. Chemical structure and immunobiological activity of Porphyromonas gingivalis lipid A. *Front. Biosci.* **12**, 3795–3812 (2007).

90. Poltorak, A. *et al.* Defective LPS Signaling in C3H/HeJ and C57BL/10ScCr Mice: Mutations in Tlr4 Gene. *Science (80-.).* **282**, 2085–2088 (1998).

91. Tobias, P. S., Soldau, K. & Ulevitch, R. J. Isolation of a lipopolysaccharide- binding acute phase reactant from rabbit serum. *J Exp Med* **164**, 777–793 (1986).

92. Wright, S. D., Tobias, P. S., Ulevitch, R. J. & Ramos, R. A. Lipopolysaccharide (LPS) binding protein opsonizes LPS-bearing particles for recognition by a novel receptor on macrophages. *J. Exp. Med.* **170**, 1231–1241 (1989).

93. Neill, L. A. J. O. & Bowie, A. G. The family of five: TIR-domain- containing adaptors in Toll-like receptor signalling. *Nat. Rev. Immunol.* **7**, 353–364 (2007).

94. Liu, T., Zhang, L., Joo, D. & Sun, S. NF-κB signaling in inflammation. *Signal Transduct. Target. Ther.* **2**, 17023 (2017).

95. Tanaka, T., Narazaki, M. & Kishimoto, T. IL-6 in Inflammation, Immunity, and Disease. *Cold Spring Harb. Perspect. Biol.* **6**, a016295–a016295 (2014).

96. Kishimoto, T. & Ishizaka, K. Regulation of Antibody Response in Vitro : X . Biphasic Effect of Cyclic AMP on the Secondary anti-Hapten Antibody Response to anti-Immunoglobulin and Enhancing Soluble Factor Tadamitsu Kishimoto and Kimishige Ishizaka Why The JI ? Submit online . • Rapid. *J. Immunol.* **116**, 534–541 (1976).

97. Zilberstein, A., Ruggieri, R., H.Korn, J. & Revel, M. Structure and expression of cDNA and genes for human interferon-beta-2 a distinct.pdf. *EMBO J.* **5**, 2529–2537 (1986).

98. HAEGEMAN, G. *et al.* Structural analysis of the sequence coding for an inducible 26-kDa protein in human fibroblasts. *Eur. J. Biochem.* **159**, 625–632 (1986).

99. Jones, S. A., Scheller, J. & Rose-John, S. Therapeutic strategies for the clinical blockade of IL-6/gp130 signaling. *J. Clin. Invest.* **121**, 3375–3383 (2011).

100. Garbers, C., Aparicio-Siegmund, S. & Rose-John, S. The IL-6/gp130/STAT3 signaling axis: Recent advances towards specific inhibition. *Curr. Opin. Immunol.* **34**, 75–82 (2015).

101. Rose-John, S. & Heinrich, P. C. Soluble receptors for cytokines and growth factors: generation and biological function. *Biochem. J.* **300**, 281–290 (1994).

102. Irwin, C. R. & Myrillas, T. The role of IL-6 in the pathogenesis of periodontal disease.pdf. *Oral Dis.* **4**, 43–47 (1998).

103. Hunter, C. A. & Jones, S. A. IL-6 as a keystone cytokine in health and disease. *Nat.*

Immunol. **16**, 448–457 (2015).

104. Kurtis, B., Develioglu, H., Taner, I. L., Balos, K. & Tekin, I. Ö. IL-6 levels in gingival crevicular fluid (GCF) from patients with non-insulin dependent diabetes mellitus (NIDDM), adult periodontitis and healthy subjects. *J. Oral Sci.* **41**, 163–167 (1999).

105. Ehrnhöfer-Ressler, M. M. *et al.* Identification of 1,8-cineole, borneol, camphor, and thujone as anti-inflammatory compounds in a salvia officinalis L. Infusion using human gingival fibroblasts. *J. Agric. Food Chem.* **61**, 3451–3459 (2013).

106. Josino Soares, D. *et al.* Pitanga (Eugenia uniflora L.) fruit juice and two major constituents thereof exhibit anti-inflammatory properties in human gingival and oral gum epithelial cells. *Food Funct.* **5**, 2981–2988 (2014).

107. Walker, J. *et al.* Identification of an anti-inflammatory potential of: Eriodictyon angustifolium compounds in human gingival fibroblasts. *Food Funct.* **7**, 3046–3055 (2016).

108. Schueller, K. *et al.* Identification of Interleukin-8-Reducing Lead Compounds Based on SAR Studies on Dihydrochalcone-Related Compounds in Human Gingival Fibroblasts (HGF-1 cells) In Vitro. *Molecules* **25**, 1382 (2020).

109. Abercrombie, M. The Fibroblast. in *J Clin Pathol Suppl (R Coll Pathol)* vol. 12 1–6 (1978).

110. Bautista-Hernández, L. A., Gómez-Olivares, J. L., Buentello-Volante, B. & Bautista-de Lucio, V. M. Fibroblasts: the unknown sentinels eliciting immune responses against microorganisms. *Eur. J. Microbiol. Immunol.* **7**, 151–157 (2017).

111. HASSELL, T. M. Tissues and cells of the periodontium. *Periodontol. 2000* **3**, 9–38 (1993).

112. Okada, H. & Murakami, S. Cytokine expression in periodontal health and disease. *Crit. Rev. Oral Biol. Med.* **9**, 248–266 (1998).

113. Prabhu, A., Michalowicz, B. S. & Mathur, A. Detection of Local and Systemic Cytokines in Adult Periodontitis. *J. Periodontol.* **67**, 515–522 (1996).

114. Yamazaki, K. *et al.* Cytokine messenger RNA expression in chronic inflammatory periodontal disease. *Oral Microbiol. Immunol.* **12**, 281–287 (1997).

115. Hayashi, C., Gudino, C. V., Gibson, F. C. & Genco, C. A. REVIEW: Pathogen-induced inflammation at sites distant from oral infection: bacterial persistence and induction of

cell-specific innate immune inflammatory pathways. *Mol. Oral Microbiol.* **25**, 305–316 (2010).

116. Chaussain-Miller, C., Fiorett, F., Goldberg, M. & Menashi, S. The Role of Matrix Metalloproteinases (MMPs) in Human Caries. *J Dent Res* **85**, 22–32 (2006).

117. Kobayashi, Y. The role of chemokines in neutrophil biology. *Front. Biosci.* **13**, 2400–2407 (2008).

118. Hajishengallis, G. New developments in neutrophil biology and periodontitis. *Periodontol. 2000* **82**, 78–92 (2020).

119. Wang, P.-L. & Ohura, K. Porphyromonas gingivalis L ipopolysaccharide S ignaling in G ingival F ibroblasts –CD14 and T oll-like R eceptors. *Crit. Rev. Oral Biol. Med.* **13**, 132–142 (2002).

120. Dongari-Bagtzoglou, A. I. & Ebersole, J. L. Increased Presence of Interleukin-6 (IL-6) and IL-8 Secreting Fibroblast Subpopulations in Adult Periodontitis. *J. Periodontol.* **69**, 899–910 (1998).

121. Dongari-Bagtzoglou, A. I. & Ebersole, J. L. Production of inflammatory mediators and cytokines by human gingival fibroblasts following bacterial challenge. *J. Periodontal Res.* **31**, 90–98 (1996).

122. Okada, N. *et al.* Interleukin-6 production in human fibroblasts derived from periodontal tissues is differentially regulated by cytokines and a glucocorticoid. *J. Periodontal Res.* **32**, 559–569 (1997).

123. Liszt, K. I., Eder, R., Wendelin, S. & Somoza, V. Identification of Catechin, Syringic Acid, and Procyanidin B2 in Wine as Stimulants of Gastric Acid Secretion. *J. Agric. Food Chem.* **63**, 7775–7783 (2015).

124. Sterneder, S. *et al.* Astringent Gallic Acid in Red Wine Regulates Mechanisms of Gastric Acid Secretion via Activation of Bitter Taste Sensing Receptor TAS2R4. *J. Agric. Food Chem.* **69**, 10550–10561 (2021).

125. Reddy, M. *et al.* Bitter taste receptor T2R14 detects quorum sensing molecules from cariogenic Streptococcus mutans and mediates innate immune responses in gingival epithelial cells. *FASEB J.* **35**, 1–18 (2021).

126. Kaur, K. *et al.* A Cross-Sectional Study of Bitter-Taste Receptor Genotypes, Oral Health,

and Markers of Oral Inflammation. *Oral* **1**, 122–138 (2021).

127. Idrees, M., Nassani, M. & Kujan, O. Assessing the association between unstimulated whole salivary flow rate (UWSFR) and oral health status among healthy adult subjects : A cross-sectional study. *Med Oral Patol Oral Cir Bucal* **23**, e384-390 (2018).

128. Zhou, Z. *et al.* TAS2R16 Activation Suppresses LPS-Induced Cytokine Expression in Human Gingival Fibroblasts. *Front. Immunol.* **12**, 1–13 (2021).

129. Gillespie, M. *et al.* The reactome pathway knowledgebase 2022. **50**, 687–692 (2022).

130. Di Pizio, A. *et al.* Comparing Class A GPCRs to bitter taste receptors. in *Methods in Cell Biology* vol. 132 401–427 (Elsevier Ltd, 2016).

131. Stoeger, V. *et al.* Identification of Bitter-Taste Intensity and Molecular Weight as Amino Acid Determinants for the Stimulating Mechanisms of Gastric Acid Secretion in Human Parietal Cells in Culture. *J. Agric. Food Chem.* **66**, 6762–6771 (2018).

132. Dragoș, D., Petran, M., Gradinaru, T.-C. & Gilca, M. Phytochemicals and Inflammation: Is Bitter Better? *Plants* **11**, 2991 (2022).

133. Dong, H. *et al.* Oral Microbiota-Host Interaction Mediated by Taste Receptors. *Front. Cell. Infect. Microbiol.* **12**, 1–12 (2022).

Appendix

8 Abstract

The main objective of this dissertation was to investigate whether there is a functional role of chemoreceptors sensing bitter tasting compounds, named bitter taste receptors (TAS2Rs), in cellular immune responses. The research specifically aimed to examine whether and how bitter tasting compounds modulate the response of immune-competent human gingival fibroblasts to a pro-inflammatory stimulus via TAS2Rs. Specifically, a functional role of TAS2Rs in reducing a stimulus-evoked release of the pro-inflammatory cytokine IL-6 in immortalized human gingival fibroblasts of the HGF-1 cell line was hypothesized. Proof for this hypothesis could lay grounds for using HGF-1 cells as an alternative model to identify bitter tasting and bitter taste modulating compounds.

The first study hypothesized a TAS2R-mediated anti-inflammatory activity of the two bitter tasting compounds, resveratrol (RSV) and rosmarinic acid (RA), in HGF-1 cells treated with lipopolysaccharides from *Porphyromonas gingivalis* (*Pg*-LPS) as pro-inflammatory stimulus that induces a release of the pro-inflammatory cytokine interleukin-6 (IL-6). The results revealed a more potent ameliorating effect of the *Pg*-LPS induced IL-6 release and transcription, as quantitated by ELISA and qRT-PCR, respectively, for RSV, of which the bitterness in a two-alternative-forced-choice test (2-AFC) was also ranked higher by sensory panelists than that of RA. Mechanistically, the functional role of one of the TAS2Rs, namely TAS2R50, in the RSV-evoked anti-inflammatory effect was identified by means of a HGF-1 cell-based TAS2R50-targeted siRNA knock-down experiment, and by an *in silico* molecular docking approach which demonstrated a potential binding of RSV to the hydrophobic pockets of TAS2R50.

The second study aimed to investigate whether other bitter tasting plant constituents, that are widely distributed over the structurally divers chemical bitter space and target a variety of all human TAS2Rs identified so far, could also reduce the *Pg*-LPS induced release of IL-6 in HGF-1 cells, and if, in addition to TAS2R50, other TAS2Rs as well mediate this anti-inflammatory response. In an initial step, cellular TAS2R50 signalling pathways were analysed using reactome and immunofluorescence staining, revealing an essential role for the signalling protein GNAI3. On a functional level, dose-response analyses were performed for each bitter tasting compound, resulting in a linear association (R^2: 0.60, $p < 0.01$) between the compound's concentration to inhibit 25 % of the *Pg*-LPS-evoked IL-6 release, quantitated by means of ELISA, and the compound's bitter taste threshold reported in the literature.

In conclusion, the HGF-1 cell model established may serve as a novel native cell model suitable for the identification of bitter tasting compounds. Moreover, the results demonstrated provide important insights into the role of bitter taste receptors in inflammation, suggesting them as new targets for anti-inflammatory therapies.

9 Zusammenfassung

Ziel dieser Arbeit war es, zu untersuchen, ob Chemorezeptoren, die bitter schmeckenden Verbindungen erkennen, sogenannte Bittergeschmacksrezeptoren (TAS2Rs), eine funktionelle Rolle bei zellulären Immunreaktionen spielen. Konkret sollte untersucht werden, ob und wie bitter schmeckende Verbindungen die Reaktion immunkompetenter menschlicher Zahnfleischfibroblasten auf einen entzündungsfördernden Stimulus über TAS2Rs modulieren. Konkret wurde eine funktionelle Rolle der TAS2Rs bei der Verringerung der durch einen Stimulus ausgelösten Freisetzung des pro-inflammatorischen Zytokins IL-6 in immortalisierten menschlichen Zahnfleischfibroblasten der HGF-1-Zelllinie postuliert. Der Nachweis dieser Hypothese könnte eine Grundlage für die Verwendung von HGF-1-Zellen als alternatives Modell zur Identifizierung von bitter schmeckenden und den Bittergeschmack modulierenden Verbindungen bilden.

In der ersten Studie wurde eine TAS2R-vermittelte entzündungshemmende Wirkung von den bitter schmeckenden Verbindungen Resveratrol (RSV) und Rosmarinsäure (RA) in HGF-1-Zellen untersucht, die mit Lipopolysacchariden von *Porphyromonas gingivalis* (*Pg*-LPS) als pro-inflammatorischem Stimulus behandelt wurden. *Pg*-LPS induziert eine Freisetzung des pro-inflammatorischen Zytokins Interleukin-6 (IL-6). Die Ergebnisse zeigten eine stärkere Verringerung der durch *Pg*-LPS induzierten IL-6-Freisetzung und Transkription, quantifiziert durch ELISA bzw. qRT-PCR, für RSV, dessen Bitterkeit in einem Zwei-Alternativen-Forced-Choice-Test (2-AFC) von sensorischen Panelisten ebenfalls höher eingestuft wurde als die von RA. Auf mechanistischer Ebene wurde die funktionelle Rolle eines der TAS2Rs, nämlich TAS2R50, bei der durch RSV hervorgerufenen entzündungshemmenden Reaktion durch ein auf HGF-1-Zellen basierendes TAS2R50-gezieltes siRNA-Knock-down-Experiment und durch einen In-silico-Molekular-Docking-Ansatz identifiziert, der eine potenzielle Bindung von RSV an die hydrophoben Taschen von TAS2R50 zeigte.

In der zweiten Studie sollte untersucht werden, ob andere bitter schmeckende Pflanzeninhaltsstoffe, die weit über den strukturell vielfältigen chemischen Bitterraum verteilt sind und auf eine Vielzahl aller bisher identifizierten human TAS2Rs abzielen, ebenfalls die *Pg*-LPS-induzierte Freisetzung von IL-6 in HGF-1-Zellen reduzieren können und ob neben TAS2R50 auch andere TAS2Rs diese entzündungshemmende Reaktion vermitteln. In einem ersten Schritt wurden die zellulären TAS2R50-Signalwege mit Hilfe von Reaktome und Immunfluoreszenzfärbungen analysiert, wobei sich eine wesentliche Rolle für das Signalprotein GNAI3 herausstellte. Auf funktioneller Ebene wurden für jede bitter schmeckende Verbindung Dosis-Wirkungs-Analysen durchgeführt, die einen linearen Zusammenhang (R^2: 0,60, $p < 0,01$) zwischen der Konzentration der Verbindung zur Hemmung von 25 % der durch *Pg*-LPS ausgelösten IL-6-Freisetzung,

die mittels ELISA quantifiziert wurde, und der in der Literatur angegebenen Bitterkeitsschwelle der Verbindung ergaben.

Zusammenfassend lässt sich sagen, dass das etablierte HGF-1-Zellmodell als neuartiges natives Zellmodell für die Identifizierung von bitter schmeckenden Verbindungen dienen kann. Darüber hinaus bieten die Ergebnisse wichtige Einblicke in die Rolle der Bittergeschmacksrezeptoren bei Entzündungen und deuten darauf hin, dass diese Chemorezeptoren neue Ziele für entzündungshemmende Medikamente darstellen können.

10 Scientific Career

Publications

2022	Tiroch, J. et al. Human Gingival Fibroblasts as a Novel Cell Model Describing the Association between Bitter Taste Thresholds and Interleukin-6 Release. J. Agric. Food Chem. (2023).
2021	Tiroch, J. et al. Bitter Sensing TAS2R50 Mediates the trans-Resveratrol-Induced Anti-inflammatory Effect on Interleukin 6 Release in HGF-1 Cells in Culture. J. Agric. Food Chem. (2021).
2021	De Corte, D. et al. Microbes mediating the sulfur cycle in the Atlantic Ocean and their link to chemolithoautotrophy. Environ. Microbiol. 00, 1–16 (2021).
2020	Fruehwirth, S. et al. In vitro digestion of grape seed oil inhibits phospholipid-regulating effects of oxidized lipids. Biomolecules 10, (2020).

Symposia

10/2021	**1. DoSChem Retreat – Panel B** “The anti-inflammatory effect of trans-resveratrol in HGF-1 cells is mediated by the human bitter taste sensing receptor TAS2R50”
09/2021	**ECRO XXXI Meeting - ECRO 2021 - 50th Anniversary of ECRO** “The anti-inflammatory effect of trans-resveratrol (RSV) in human gingival cells in culture is mediated by the bitter taste sensing receptor TAS2R50”
05/2021	**XVI Weurman Flavour Research Symposium** “The anti-inflammatory effect of trans-resveratrol (RSV) in HGF-1 cells is mediated by the human bitter taste sensing receptor TAS2R50”

Award

10/2021	1. DoSChem Retreat – Panel B **Best Poster Award**